SOURCE AND RECEIVER ARRAYS

by

Andrew Pap

Report compiled for Amoco Research as the knowledge base for an Expert System

Amoco Canada, 1983

88263ACC0008-p

TABLE OF CONTENTS

Page

I. Introduction 1

II. Properties of Signal and Noise in the Time Domain 5

A. The Nyquist Frequency 5
B. Temporal Aliasing 8

III. Properties of Signal and Coherent Noise in the Spatial Domain 13

A. Apparent Velocity and Wavelength 18
B. Spatial Nyquist Frequency and Wavelength 23
C. Spatial Aliasing in the Time-Distance Domain 24

1. The Nyquist Velocity for a Given Frequency 25
2. The Maximum Dip or Moveout Per Trace 25
3. Aliased Dips in the Time-Distance Domain 32
4. Why is Spatial Aliasing Undesirable? 32
5. The Recognition of Aliasing in the t-x Domain . . . 37
6. The Removal of Aliasing in Processing 38
7. The Computation of Aliased Velocities (Dips) 38
8. The Maximum Non-Aliased Frequency 39
9. The Properties of Aliased Velocities 39

D. The Properties of Signal and Noise in the f-k Domain . . 40

1. The Appearance of Seismic Events in the f-k Plain . 41
2. Spatial Aliasing in the f-k Domain 44

a. Spatial Nyquist Velocity 44
b. The Minimum Allowable Velocity 47
c. The Maximum Spatial Sample Interval 47
d. The Maximum Non-Aliased Frequency 48
e. Wraparound 50
f. The Computation of Aliased Frequencies 51
g. The Effect of Statics on Aliasing 56
h. ________________________________ . . . .
i. The Advantages of f-k Representation of Data . 57

IV. Source and Receiver Arrays 62

A. Arrays as Temporal and Spatial Frequency Filters 62
B. Types of Arrays 64

1. Linear Arrays 65

a. Definitions 65
b. The Output of Linear Arrays 65
c. Basic Properties of Linear Arrays 70
d. The Performance of Linear Arrays 76
e. The Effect of Number of Elements (n) on Attenuation 79
f. The Fundamental Limitations of Linear Arrays . 79
g. Arrays as Antialias Filters 80

Page

h. The Effect of Linear Arrays on the Reflected Signal 83
The First Notch Frequency 85
The Effect of Group Length on First Notch Frequency 88
The Effect of Offset on First Notch Frequency . 89
The Effect of Dip on First Notch Frequency . . 93
The Maximum Acceptable Group Length 93
The Attenuation of CDP Trace 107
i. The Maximum Acceptable Elevation Change Across a Group 114

2. Linearly Tapered Arrays 118

a. Methods to Increase Reject Band Attenuation . . 118
b. The Implementation of Tapered Arrays in the Field 122
c. The Response of Two or More Subarrays 132
d. The Properties of Combined Subarray Responses . 133
e. Practical Considerations in Tapered Array Design 138

3. Non-Linearly Tapered Arrays (Weighted Arrays) . . . 139

a. Savit Array 142
b. Chebyshev Array: 142
Parameter Selection 143

C. Practical Limitations of Arrays 150

V. The Design of Source and Receiver Arrays 156

A. Field Tests Necessary for Array Design 158
B. Array Design in the Time-Distance Domain 160

1. Coherent Noise Attenuation 160

a. Steps in Linear Array Design 160
b. Tapered Receiver Arrays 170
c. Combination of Linear Source and Receiver Arrays 171

2. Reflected Signal Attenuation 172

C. Array Design in the f-k Domain 179

1. Coherent Noise Attenuation 179
2. Reflected Signal Attenuation 185

D. Complementary Field Tests for Array Design 186

1. Residual Wave Test 186
2. Residual Wave Test Simulation (RWAV) 187
3. Multifold Arrays as Spatial Filters of Noise 192
4. Expanding Spread 195

I. Introduction

The term array, as used in seismic, applies to a group of receivers or combination of receivers and sources laid out in a pattern designed to enhance the useful seismic data.

Arrays have three objectives:

1) To improve the S/N of data by multiplicity: the random noise cancellation is proportional to $\sqrt{n}$, where "n" is the number of independent observations (e.g., receivers).

2) To prevent spatial aliasing of the recorded data.

3) To attenuate coherent noise. Coherent noise is most commonly defined as any unwanted linear event on the seismic record. However, signal and coherent noise are a matter of definition. Figure 1 and 2 show a variety of events which may be recorded: airwaves, ground roll, direct waves, refractions, multiples, diffractions, and reflections. Since in reflection exploration the main interest is the primary reflections, all other events are considered noise. In refraction work, reflections interfering with the refraction arrivals are undesirable, hence are considered noise.

   Therefore, based on their desirability, the recorded seismic waves may be classified into two groups:

CONTRIBUTIONS TO A RECORDED TRACE

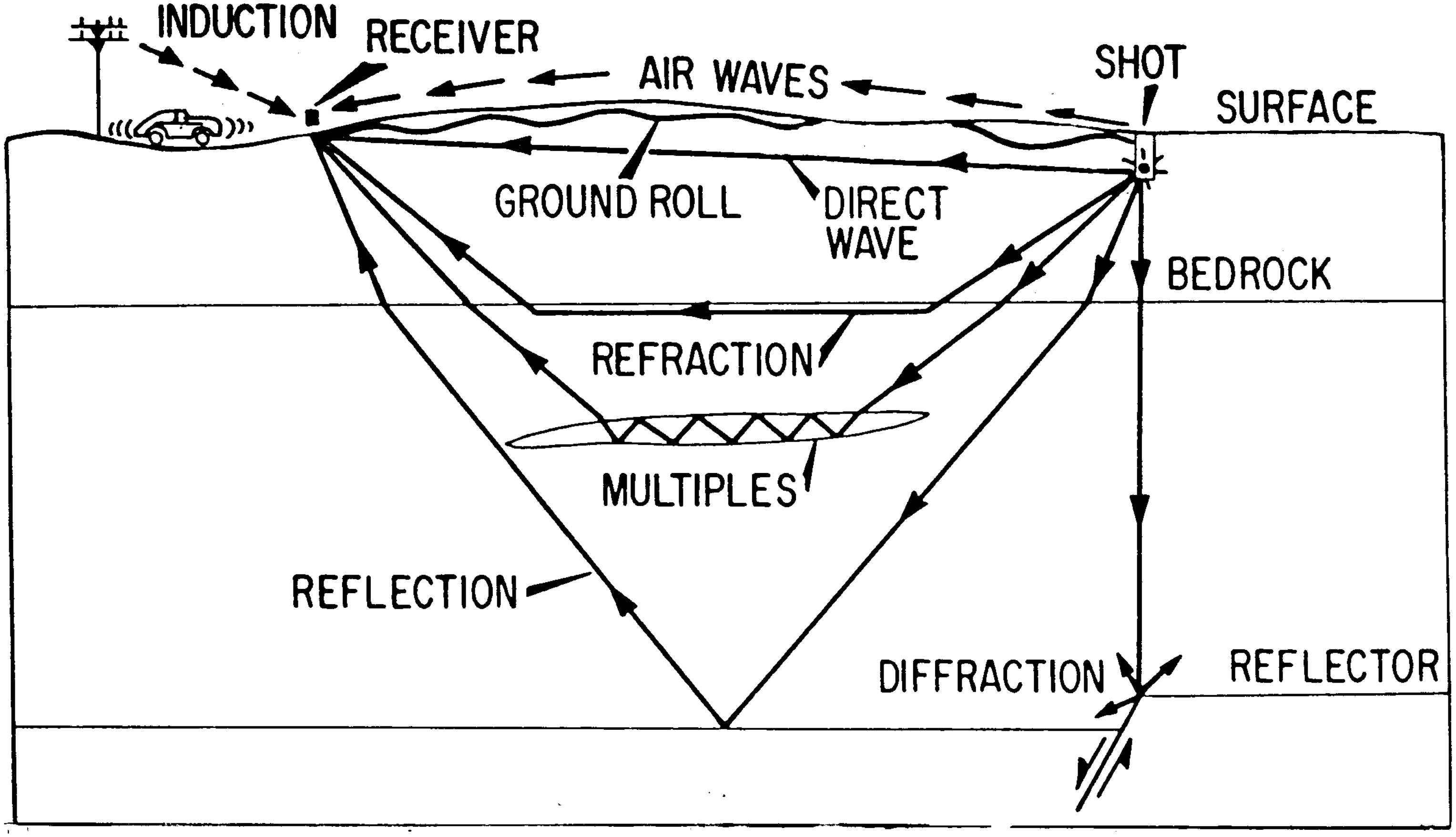

FIGURE 1 A selection of some events which may be recorded by a geophone. In exploration for hydrocarbons, we are generally interested only in the primary reflections from relatively deep horizons.

(2)

Contributions to a record

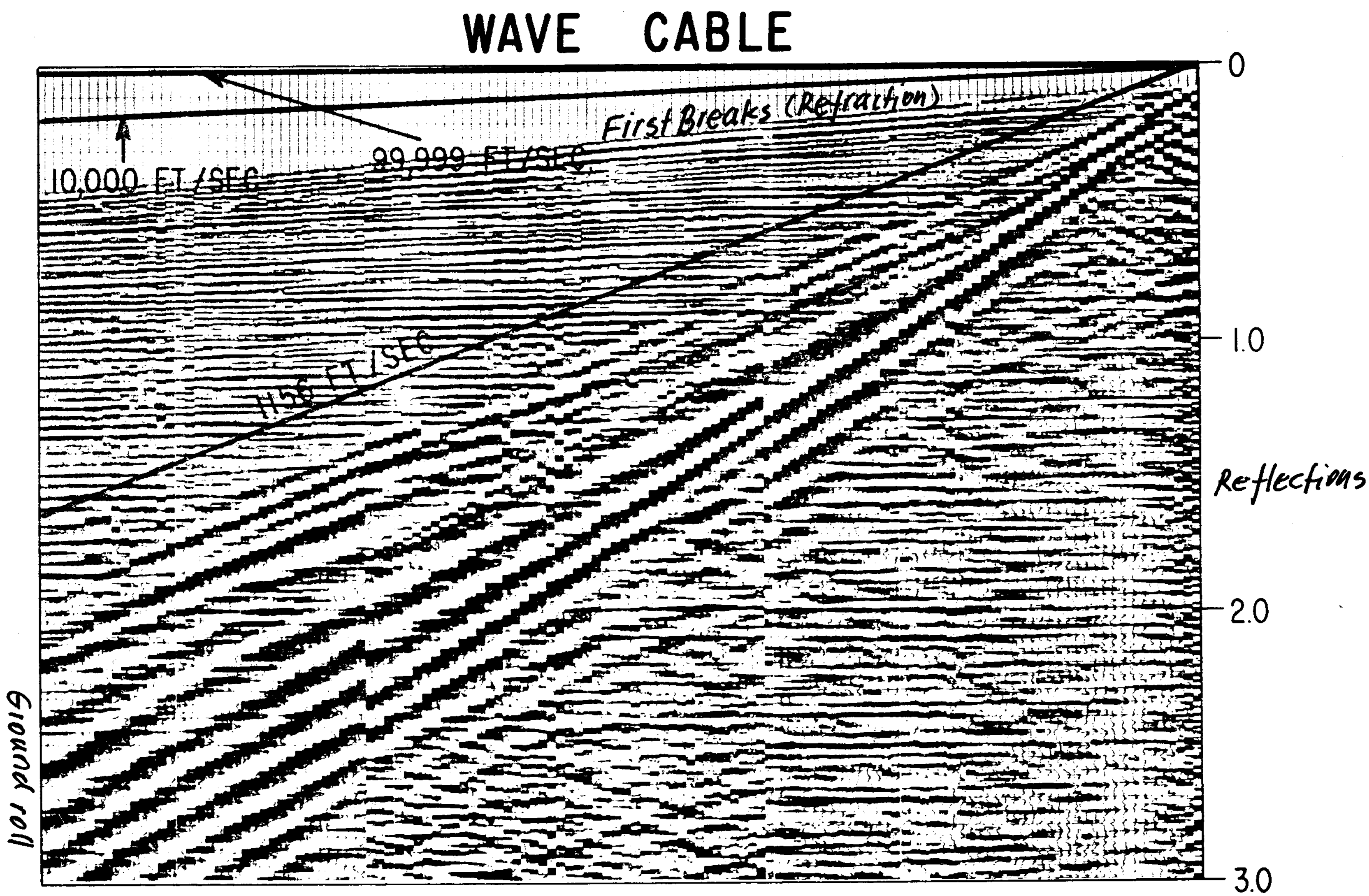

Figure 2

a. Always Undesirable:

(1) Near surface generated linear events: ground roll, airwaves, trapped waves, reverberating first arrival refractions, and side swipes from surface discontinuities.

(2) Linear events of deeper origin: reflected refractions and side swipes from buried geological structures.

(3) Non-linear events: short and long period multiples and converted waves.

b. Desirable or undesirable depending on the exploration method used and type of target:

(1) Refractions: noise for reflection work and signal for refraction surveys.

(2) Diffractions: noise for mapping targets below origin of diffraction, signal for locating faults.

(3) Primary reflections: noise for refraction surveys, signal for reflection work.

II. Properties of Signal and Coherent Noise in the Time Domain

A seismic trace is an analog signal representing ground motion as the function of time. The amplitude of the trace is proportional to the ground displacement.

In digital recording the amplitude is stored as the function of time by regularly sampling the trace and recording the measured amplitude values. The spacing of the samples is the sample interval (Figure 3). The seismic trace contains a wide band of frequencies of various amplitudes, hence can be represented by the sum of its frequency components (Fourier components). Each frequency component is described by a sine wave of certain amplitude and period (Figure 4).

Sampling theory states, that two non-zero samples per period can uniquely define any frequency plus all its harmonics. Therefore, a certain sample rate defines a maximum frequency which can be uniquely defined. The maximum frequency is called the "Nyquist frequency".

A. The Nyquist Frequency

$$f_N = \frac{1}{2\Delta t} \text{ Hz}$$

where Δt = sample interval (in msec).

A SEISMIC TRACE IS REPRESENTED BY DISCRETE SAMPLES

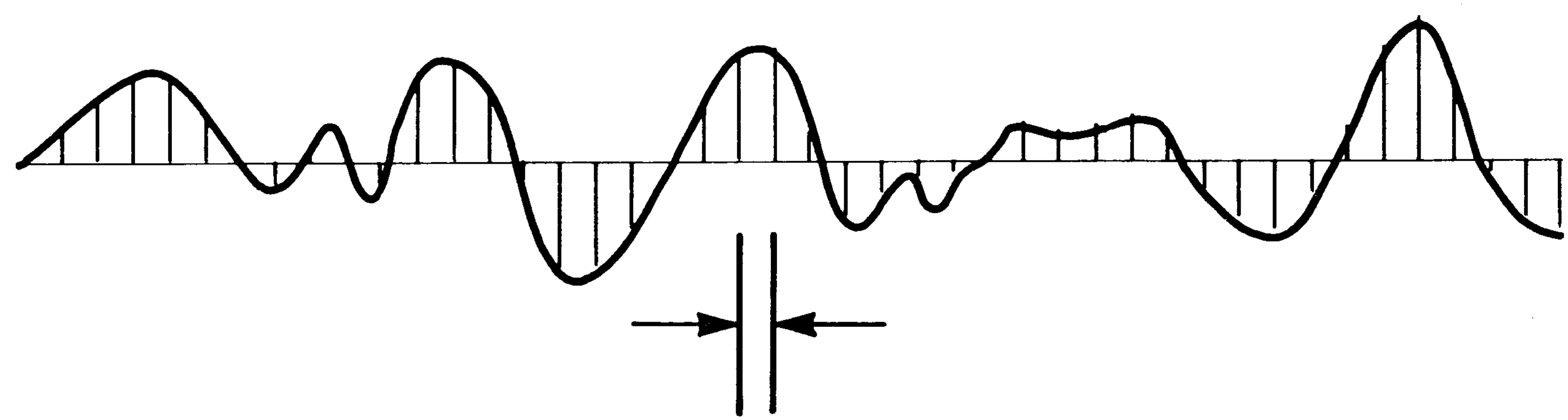

Figure 3

A FREQUENCY CAN BE DESCRIBED BY THE PERIOD OF ITS SAMPLES

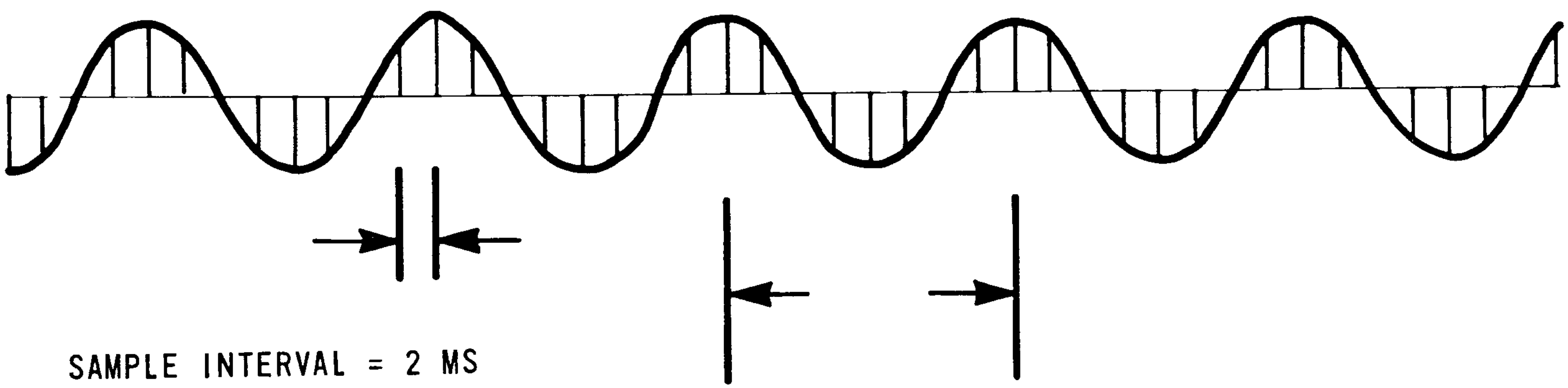

$$\text{FREQUENCY} = \frac{1}{\text{PERIOD}} = 62.5 \text{ Hz}$$

Figure 4

(7)

B. Temporal Aliasing

The maximum retrievable frequency by a sampler is the Nyquist frequency. Frequencies higher than Nyquist will appear as lower frequencies (Figure 5). Their value is a mirror image on the Nyquist, as shown on the lower graph of Figure 5. Frequencies above the Nyquist frequency is sometimes called "aliasing" or "foldover" frequencies.

The analog signal entering the multiplexer (sampler) contains frequencies higher than the Nyquist (e.g., frequencies greater than 250 Hz for 2 ms sample rate). The aliased frequencies must be attenuated before sampling or their folded equivalent will be sampled and added to the true frequencies equivalent to the folded frequency, hence the final amplitude spectrum of the signal is distorted as shown on Figure 6.

The purpose of the antialias filter is to ensure that frequencies higher than the Nyquist are attenuated by at least 70 db before the analog signal is digitized by the multiplexer. The usual requirements for the antialias filter are:

1. Slope = 70 db/octave.

2. Nyquist frequency amplitude is attenuated by 70 db.

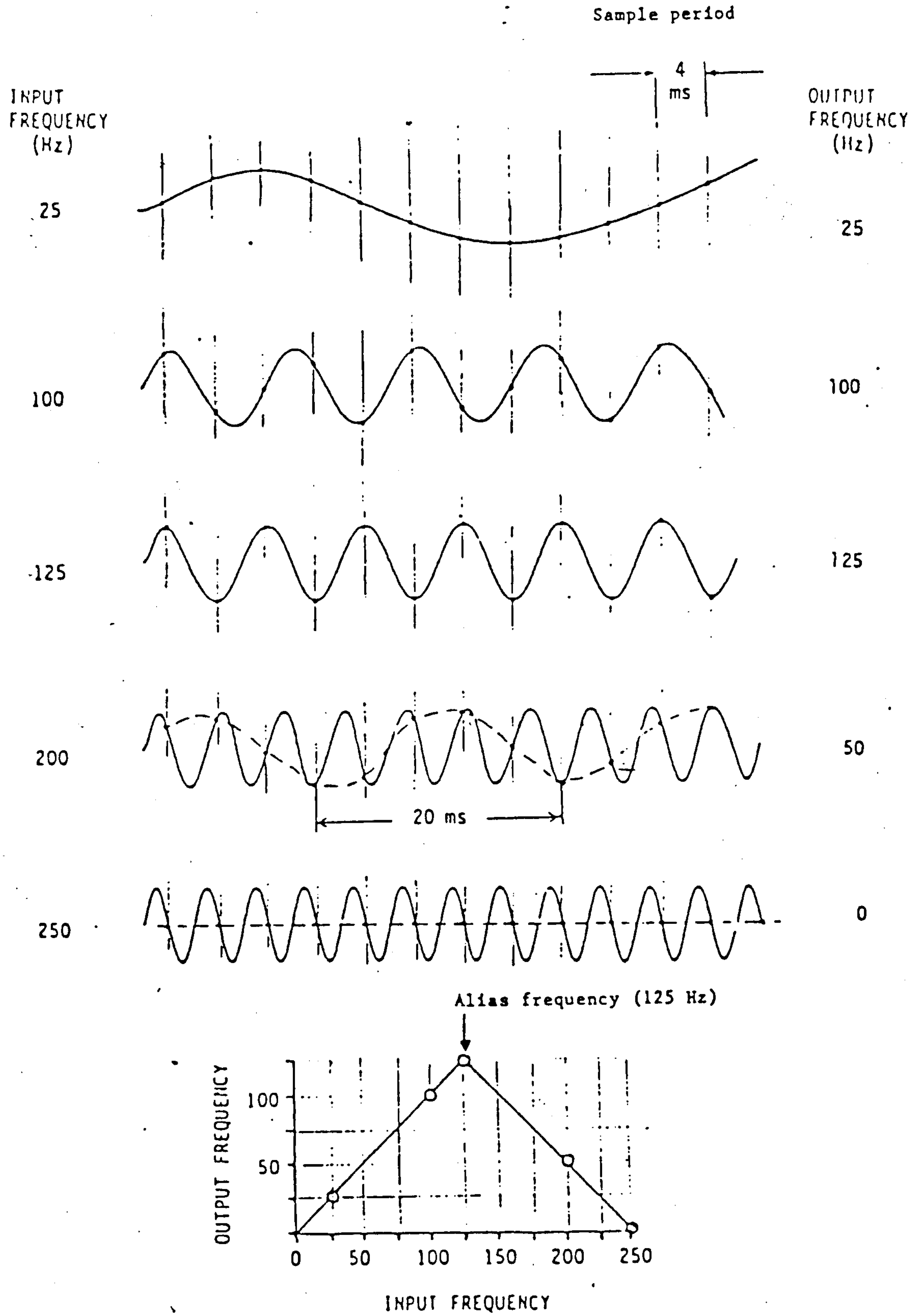

Figure 5 - The Concept of Aliasing

Temporal Aliasing in the Amplitude Spectrum

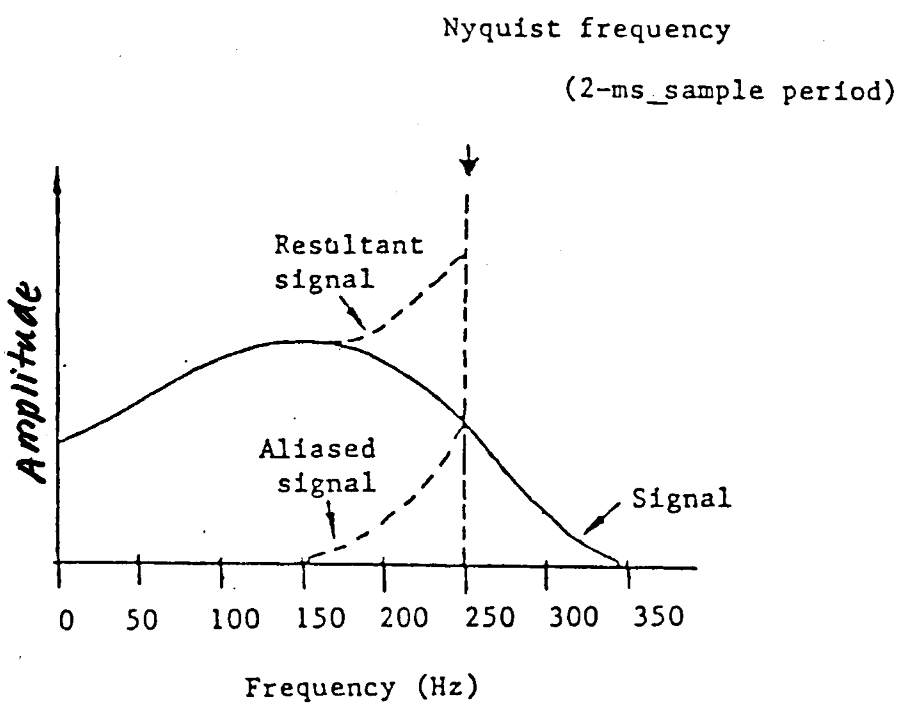

Figure 6

There are two important facts to remember about temporal aliasing:

a. Aliased temporal frequencies cannot be recovered by any means.

b. Two samples per period will only fully reconstruct the frequency and amplitude. The phase of the output waves is distorted. The amount of distortion depends on the position of the sample points as illustrated on Figure 7.

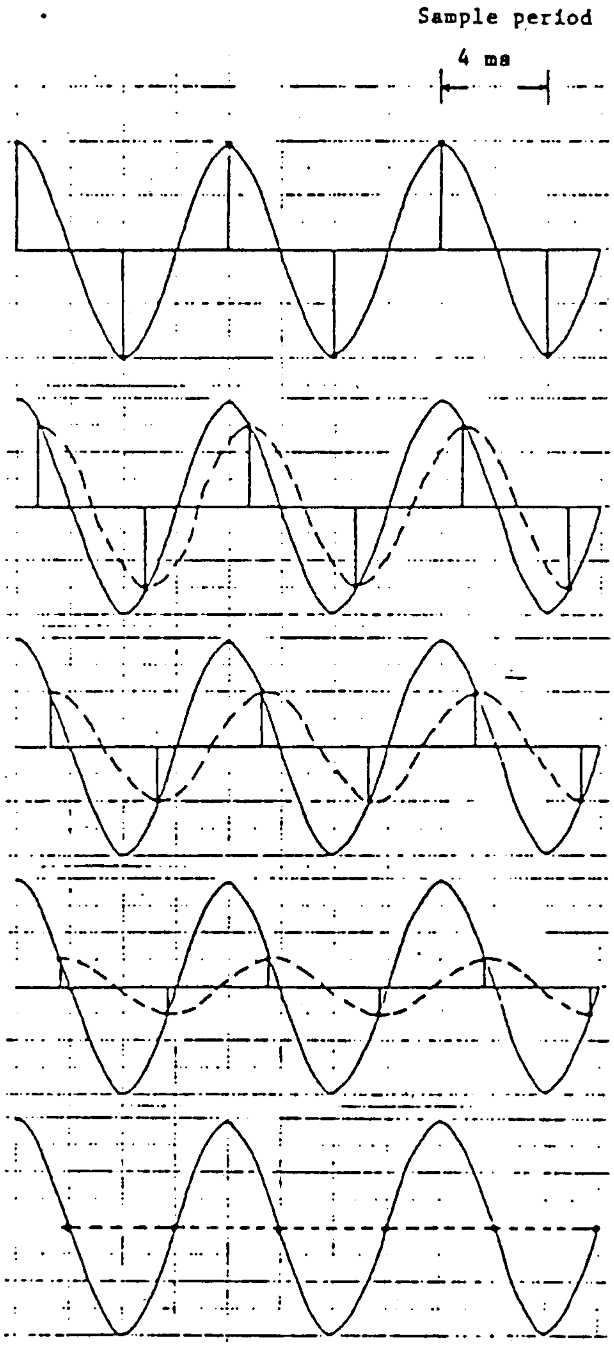

INPUT			OUTPUT		
Freq.	Amp.	Phase	Freq.	Amp.	Phase
125 Hz.	1	0 ms	125 Hz.	1	0 ms
125	1	0	125	0.75	0.8
125	1	0	125	0.50	1.2
125	1	0	125	0.25	1.6
125	1	0	0	0	-

Figure 7 Effect of the Minimum Two Samples per Period on Amplitude and Phase of the Reconstructed Wave

III. Properties of Signal and Coherent Noise in the Spatial Domain

If the seismic disturbance reaching the surface is only sampled by one receiver, its recorded amplitude, frequency, and phase are the true values. The signal does not have spatial properties, regardless of the direction of propagation (Figure 8).

However, single trace recording is seldom used. The seismic disturbance is recorded by a number of groups (usually 96-240) distributed evenly in a linear or spatial pattern. Each group consists of a number of receivers laid out in some pattern.

Therefore, the disturbance is sampled by the receivers spatially in a plane represented by the surface.

The spatially sampled wavefield (signal plus coherent noise) has a number of simple properties which must be understood for the effective use of arrays.

Seismic waves are described by their amplitude, velocity, frequency, and wavelength. These terms, except amplitude are related by:

$$V = f\lambda \tag{1}$$

where V = velocity (feet/sec or m/sec)
f = temporal frequency (Hz)
λ = wavelength (feet/cycle or m/cycle)

Two additional terms are also used:

The period: T (sec/cycle)

The spatial frequency: k (cycle/feet)

"T" and "k" are related to the basic terms by:

$$T = \frac{1}{f} \tag{2}$$

$$k = \frac{1}{\lambda} \tag{3}$$

The seismic data is usually displayed in the time-distance (t-x) plane. An event in the t-x plane is described by a locus of wavelets. The velocity of an event is the slope of the event.

Spatial Signal Independence of Direction of Propagation For Single Receiver

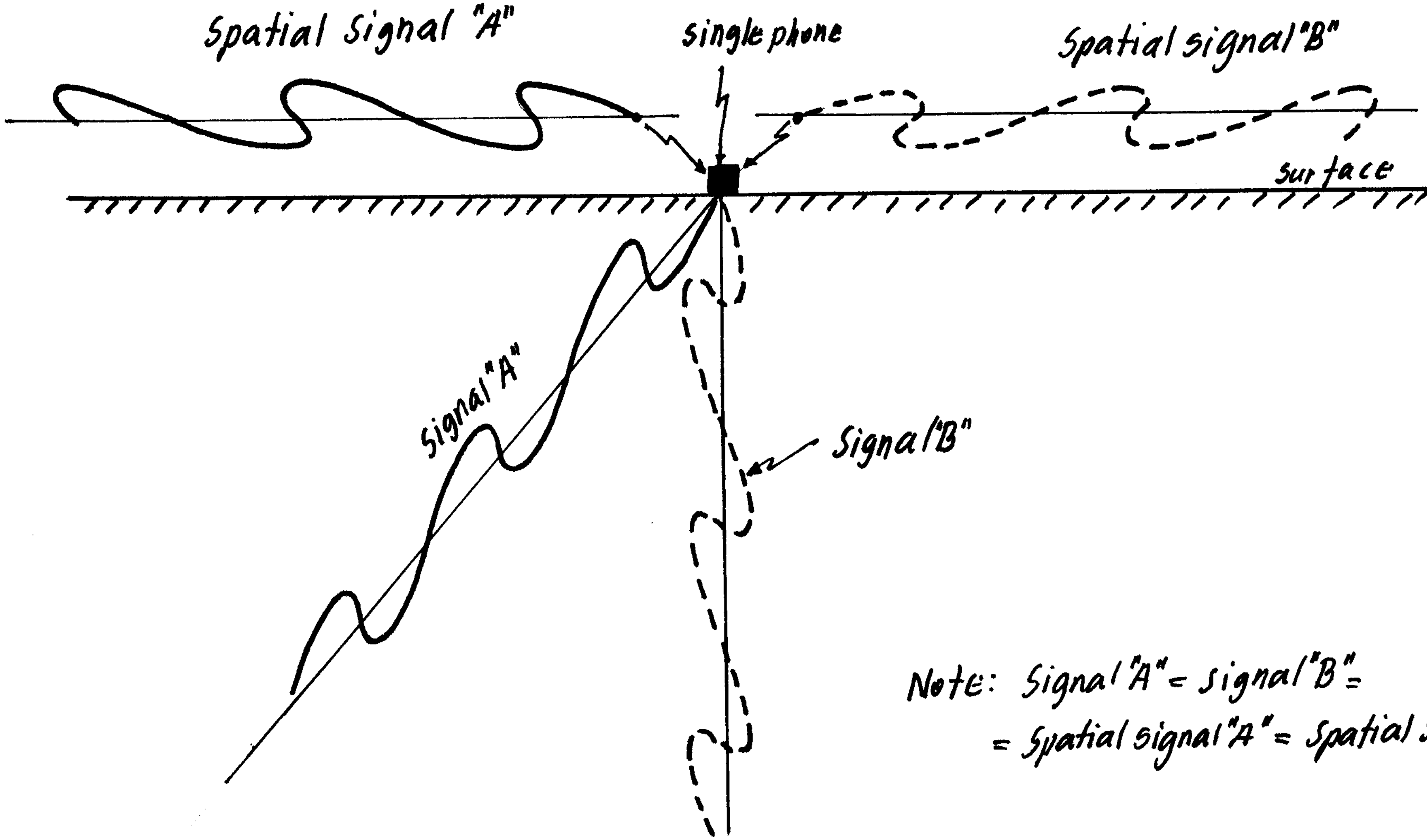

Note: Signal "A" = signal "B" =
= Spatial signal "A" = Spatial Signal "B"

Figure 8

By combining equations 1 and 2:

$$V = \frac{\lambda}{T} \qquad (4)$$

If equation (4) is used to determine the velocity, then the spatial period (wavelength) and temporal period must be measured.

The seismic data may also be displayed in the f-k plane (or frequency plane):

From equations (1) and (3)

$$V = \frac{f}{k} \qquad (5)$$

In the frequency plane the temporal frequency is the ordinate and the spatial frequency is the abscissa. The velocity of an event is the slope of the event. The relationship between the time-distance plane and frequency plane are summarized on Figure 9.

All seismic events have a velocity when sampled by the receivers on the surface. This velocity, defined as the "apparent velocity" is a spatial property and should not be confused with the vertical or geological velocity. The apparent velocity ranges from a very low value to infinity depending on the slope of the event, or the angle of arrival.

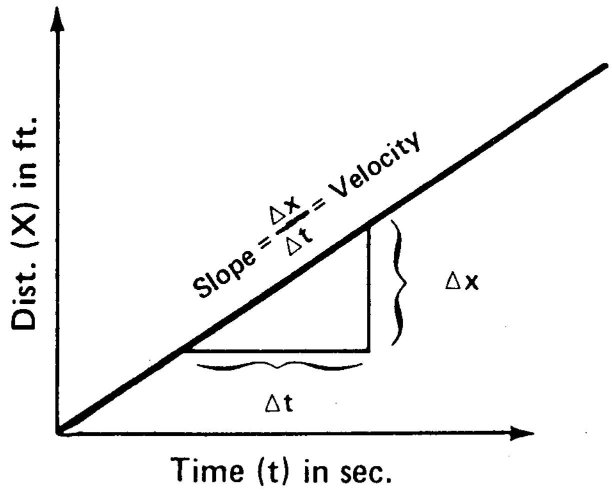

t - x Plane

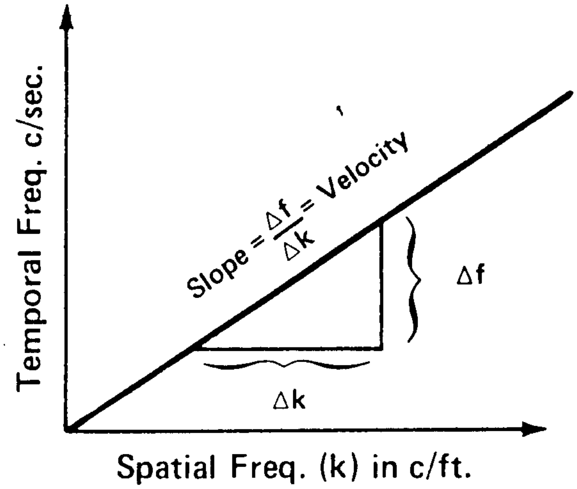

f - k Plane

$$V = f\lambda$$

$$V = \underbrace{\lambda / T}_{t\text{ - }x\text{ plane}} = \underbrace{f/K}_{f\text{ - }k\text{ plane}}$$

where	V	=	Velocity (ft/sec.)
	λ	=	Wave length (ft/cycle)
	T	=	period (sec/cycle)
	f	=	temp. freq. (cycle/sec)
	k	=	spatial freq. (cycle/ft)

Figure 9

A. Apparent Velocity and Wavelength

Figures 10-12 explain the concept of apparent velocity and apparent wavelength.

Figure 10 illustrates the distribution of a particle subsurface in the presence of a horizontally travelling sinusoidal event. The disturbance is sampled on the surface by nine receivers.

The apparent velocity is defined as the propagation of the disturbance along the surface as seen by the receivers.

The apparent wavelength = $\frac{Vapp}{f}$

In the case of horizontally travelling disturbances (e.g., ground roll) the apparent velocity and wavelength are the same as in the subsurface, hence apparent wavelength and velocity are equal to the true wavelength and velocity.

As the angle of emergence decreases (Figure 11, wide angle reflections), the apparent wavelength increases:

$$\lambda app = \frac{\lambda}{\cos\theta} \qquad (6)$$

Where θ = the angle of incidence.

HORIZONTALLY PROPOGATING WAVE

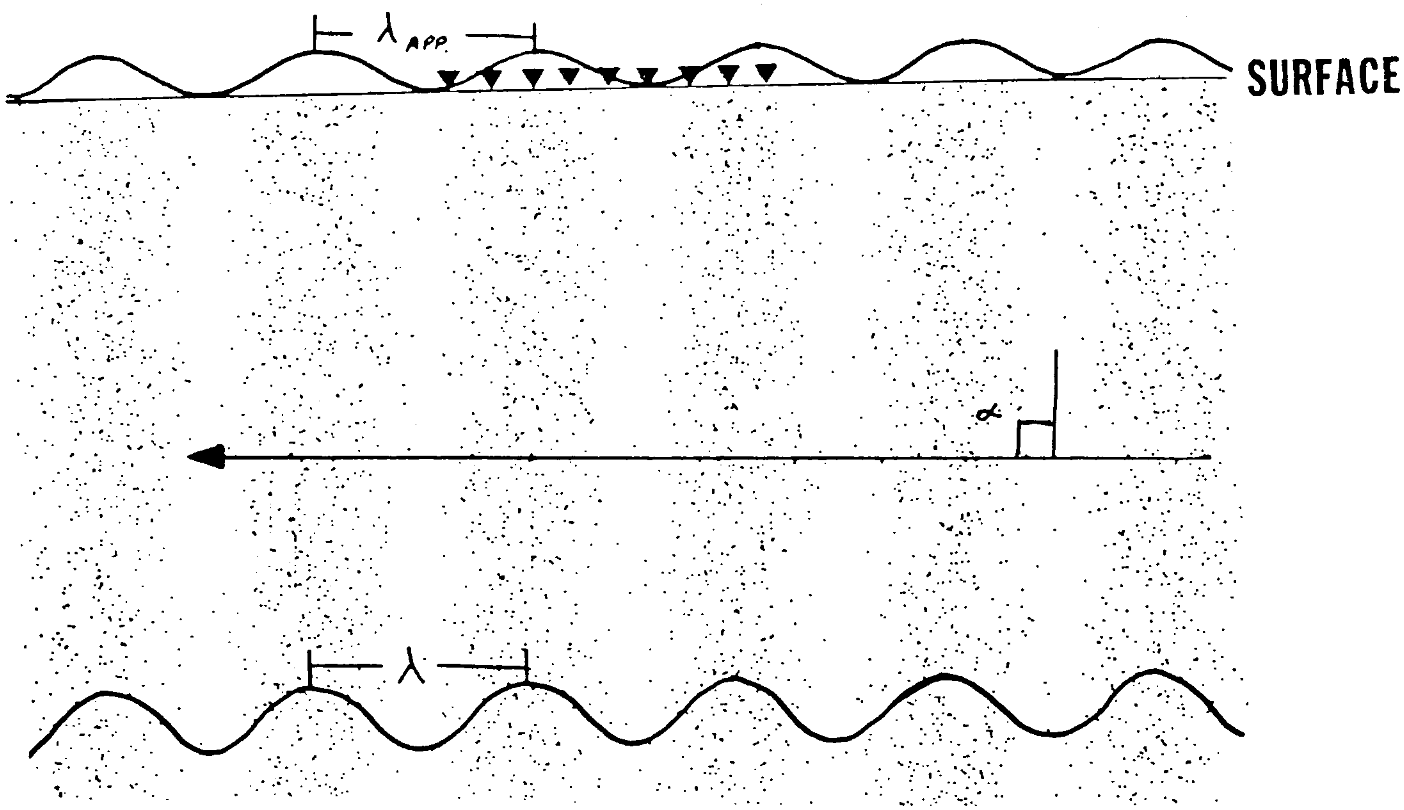

FIGURE 10 A mono-frequency sinusoidal signal along the direct ray path. The apparent wavelength (measured at the surface) is the same as the true wavelength.

WIDE ANGLE REFLECTION

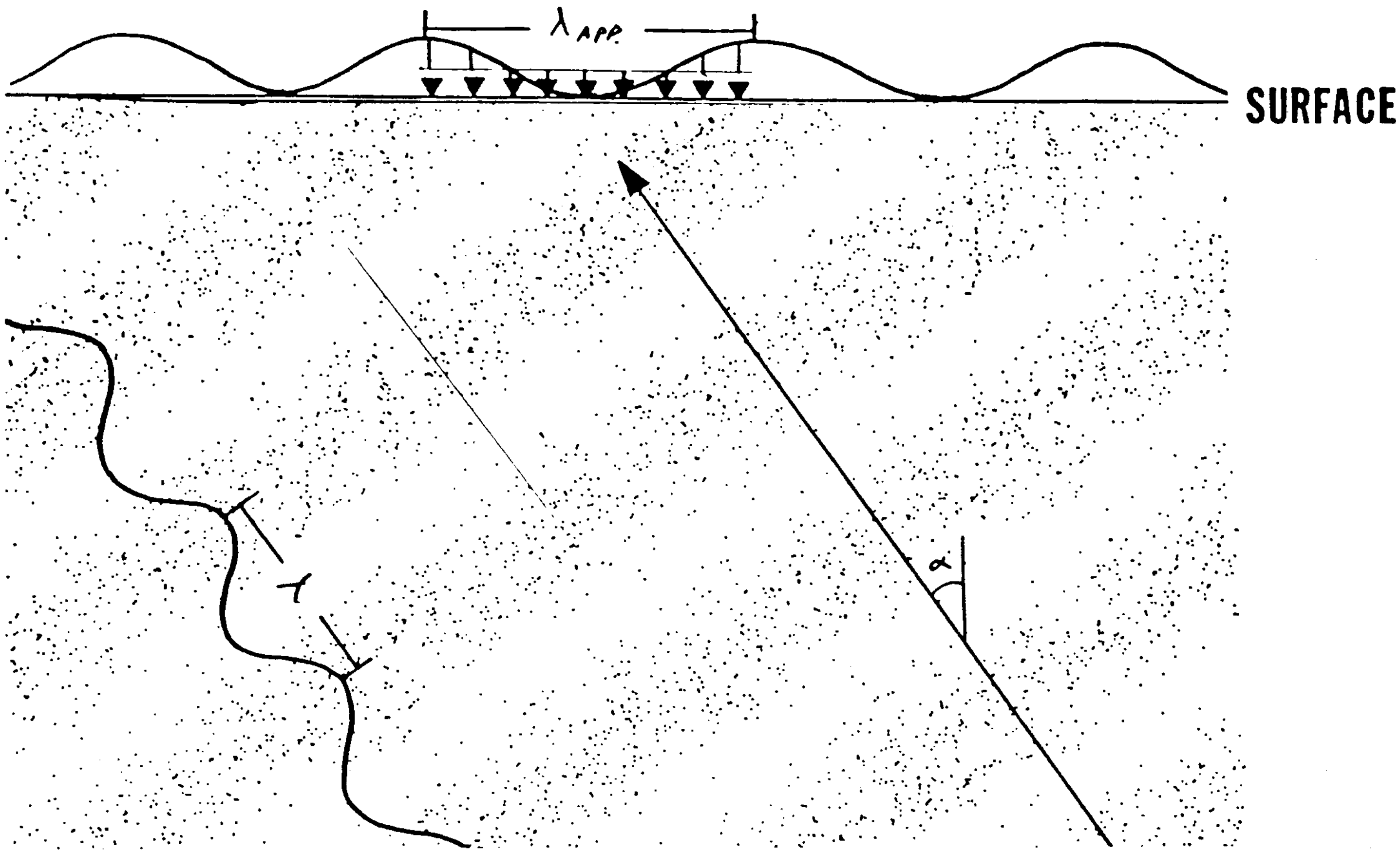

FIGURE 11 Angle of emergence is about 30°. Apparent wavelength is $1/\cos(30^{\circ})$ or about 1 1/2 times the true wavelength.

APPROACHING NORMAL INCIDENCE REFLECTION

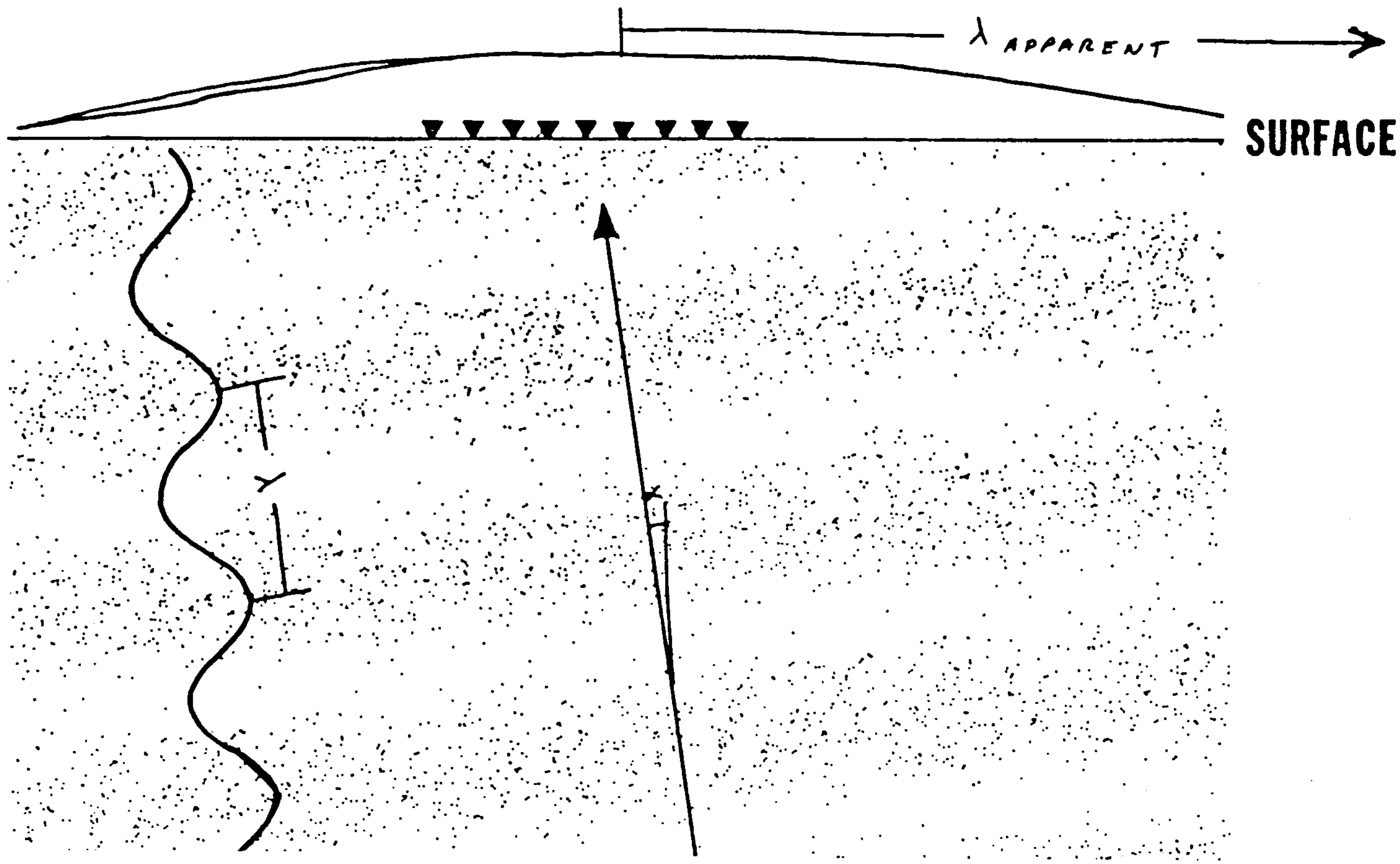

FIGURE 1.2 Angle of emergence approaches zero, apparent wavelength approaches infinity, and wavenumber approaches zero. Normalized output of the array is same as amplitude of the disturbance.

Since,

$$Vapp = \frac{\lambda app}{f}$$

$$Vapp = \frac{\lambda}{f \cos\theta} \qquad (7)$$

Therefore, the apparent velocity also increases. As the angle of emergence approaches zero (near normal incidence, near trace reflection from a flat horizon) the apparent wavelength and apparent velocity approach infinity (Figure 12).

It is important to remember, that a spatial array samples the apparent wavelength (or apparent spatial frequency) and not the true wavelength of a propagating disturbance.

Therefore, the apparent wavelength, apparent velocity and spatial frequency are present due to and related to multiple receiver recording.

Spatial Aliasing

The sampling theory discussed in the time domain representation of the signal also applies in the spatial domain: a minimum of two samples per apparent spatial wavelength are necessary to reconstruct the "spatial signal".

A "spatial signal" is any event on the seismic section and is sampled by two samplers: the groups and the receivers in a group. Hence in seismic recording there are two sample rates:

1. The group interval (trace spacing).

2. The spacing of receivers in a group.

Since the group interval is always larger than the receiver spacing in a group, the group interval is more critical to spatial sampling than the geophone spacing. However, it will be shown, that the geophone array of a group can effectively be used as a spatial antialias filter.

B. Spatial Nyquist Frequency and Wavelength

If the group interval is "Δx":

1. Spatial Nyquist wavelength (the longest allowable apparent wavelength on a section) = $2\Delta x$.

2. The spatial Nyquist frequency (the highest allowable "k" on the seismic section or field record):

$$k_N = \frac{1}{2\Delta x} \qquad (8)$$

Spatial frequencies higher than "k_N" will be aliased.

C. Spatial Aliasing in the Time-Distance Domain

As shown on Figures 10-12, the apparent spatial wavelength for a flat event approaches infinity (k=0), hence the signal cannot be spatially aliased. As the dip of an event on the seismic section increases (apparent velocity decreases), its spatial wavelength decreases and may become shorter than the Nyquist wavelength and "k" exceeds "k_N". The "dip is spatially aliased".

The dip on a section, which is equivalent to the inverse of the apparent velocity may also be expressed as a certain moveout per trace:

$$dip = \frac{1}{Vapp} = \frac{\Delta t}{\Delta x} \qquad (9)$$

where Δt = moveout per trace in sec.
Δx = group interval in feet or meters.

Using the equations

$$k_N = \frac{1}{2\Delta x} \quad \text{and} \quad k = \frac{f}{Vapp}$$

there is a minimum velocity corresponding to "k_N":

(1) <u>The minimum allowable velocity to avoid spatial aliasing for a given frequency data (also known as the Nyquist velocity for a given f)</u>

$$(Vapp)min = \frac{f}{k_N} = \frac{f}{\frac{1}{2\Delta x}} = 2f\Delta x$$

$$(Vapp)min = 2f\Delta x \qquad (10)$$

(2) <u>The maximum allowable dip, or the maximum allowable moveout per trace</u>:

$$\text{Max dip} = \frac{1}{(Vapp)min} = \frac{\Delta tmax}{\Delta x} = \frac{1}{2f\Delta x}$$

$$\Delta tmax = \frac{1}{2f} \qquad (11)$$

"$\Delta tmax$" corresponds to the Nyquist spatial frequency, "k_N" and depends only on the temporal frequency of data. The concept of spatial aliasing in the time-distance domain is illustrated by the synthetic examples on Figures 13-18. The temporal frequency of the data is 30 Hz.

$$\Delta tmax = \frac{1}{2x30} = 16.67 \text{ ms/trace}$$

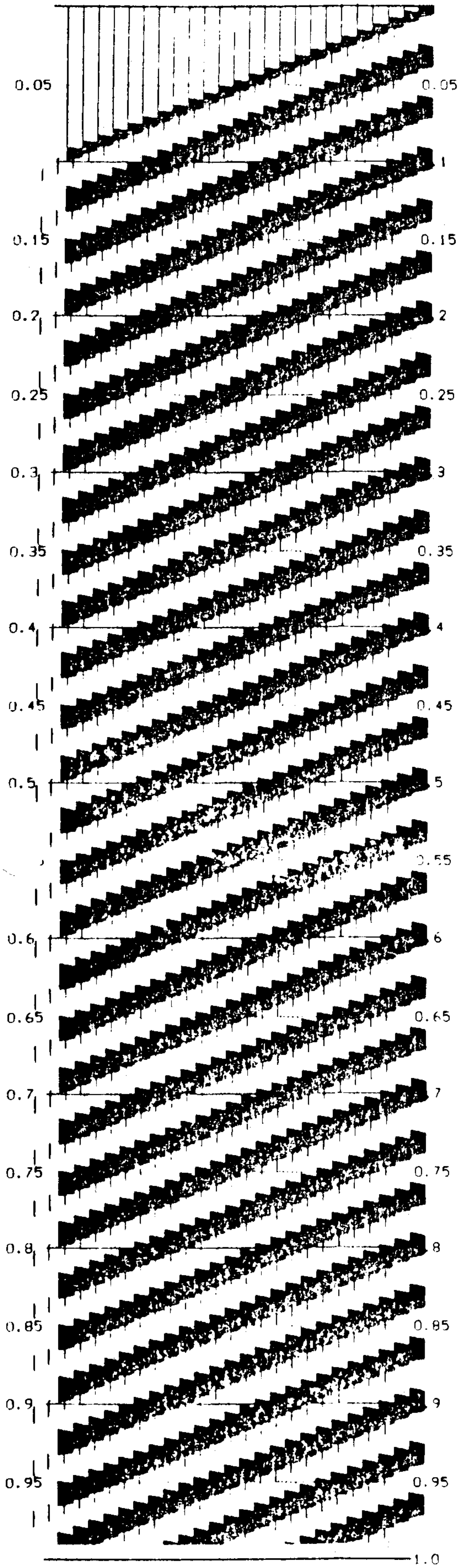

AMOCO

CHIMBLØ

LINE DIRECTIØN

FREQ PANEL: 30 HZ; DIP=4MS/TRACE

INPUT REEL HEADER INFØRMATIØN

REEL NUMBER	TVX765
DATE CREATED	10/12/78
NUMBER SAMPLE/TRACE	992
SAMPLE RATE IN MILLS	1
PRØCESSØR	CHIMBLØ
LINE NUMBER	CHIMBLØ
JØB NUMBER	CHIMBLØ
SECTIØN NUMBER	
PRØCESSING STEP	

PRØCESSING SEQUENCE

MERG
UTØP*(LINE HEADER ØNLY
ARCH
ARCH
REST(REPEAT BY PANEL)
REST(EXTERNAL STATICS)
PLØT**

****** FILMING PARAMETERS ******

PERCENT GAIN	100	
HØRIZØNTAL SCALE	10.	TR/IN
VERTICAL SCALE	10.	IN/SEC
FILMING DIRECTIØN	R/L	
PERCENT BAR	0	
PØLARITY	BLACK+VE	

Figure 13

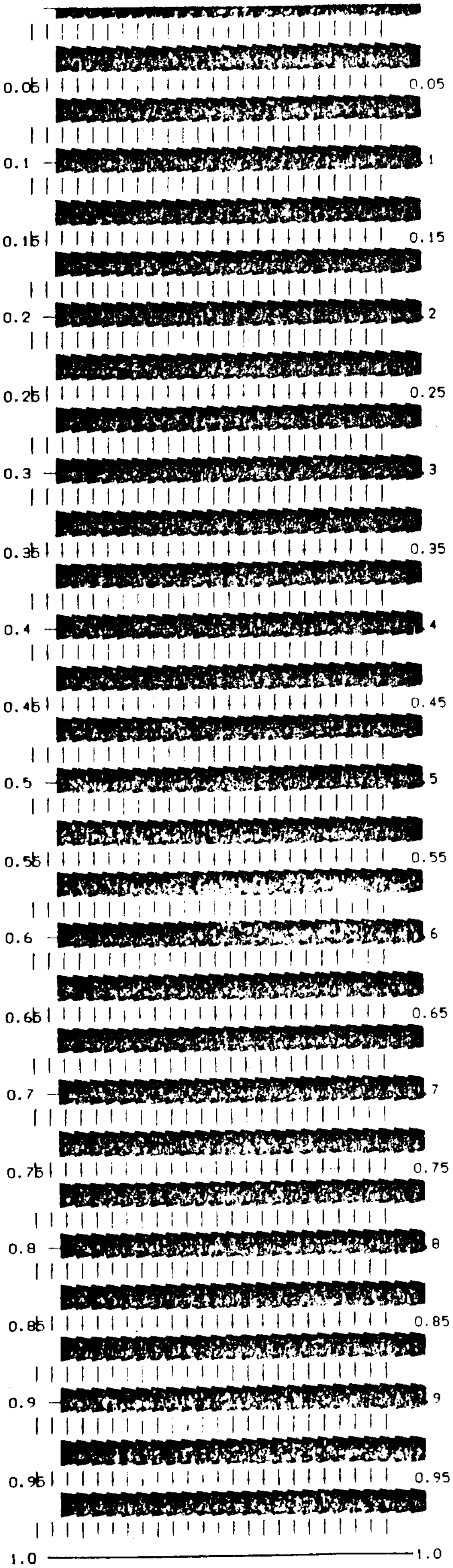

AMOCO

CHIMBLØ

LINE DIRECTIØN

FREQ PANEL: 30 HZ; NØ DIP

INPUT REEL HEADER INFØRMATIØN

REEL NUMBER	TSE719
DATE CREATED	10/12/78
NUMBER SAMPLE/TRACE	992
SAMPLE RATE IN MILLS	1
PRØCESSØR	CHIMBLØ
LINE NUMBER	CHIMBLØ
JØB NUMBER	CHIMBLØ
SECTIØN NUMBER	
PRØCESSING STEP	

PRØCESSING SEQUENCE

MERG
UTØP*(LINE HEADER ØNLY
ARCH
ARCH
REST(REPEAT BY PANEL)
PLØT**

****** FILMING PARAMETERS ******

PERCENT GAIN	100
HØRIZØNTAL SCALE	10. TR/IN
VERTICAL SCALE	10. IN/SEC
FILMING DIRECTIØN	R/L
PERCENT BAR	0
PØLARITY	BLACK+VE

Figure 14

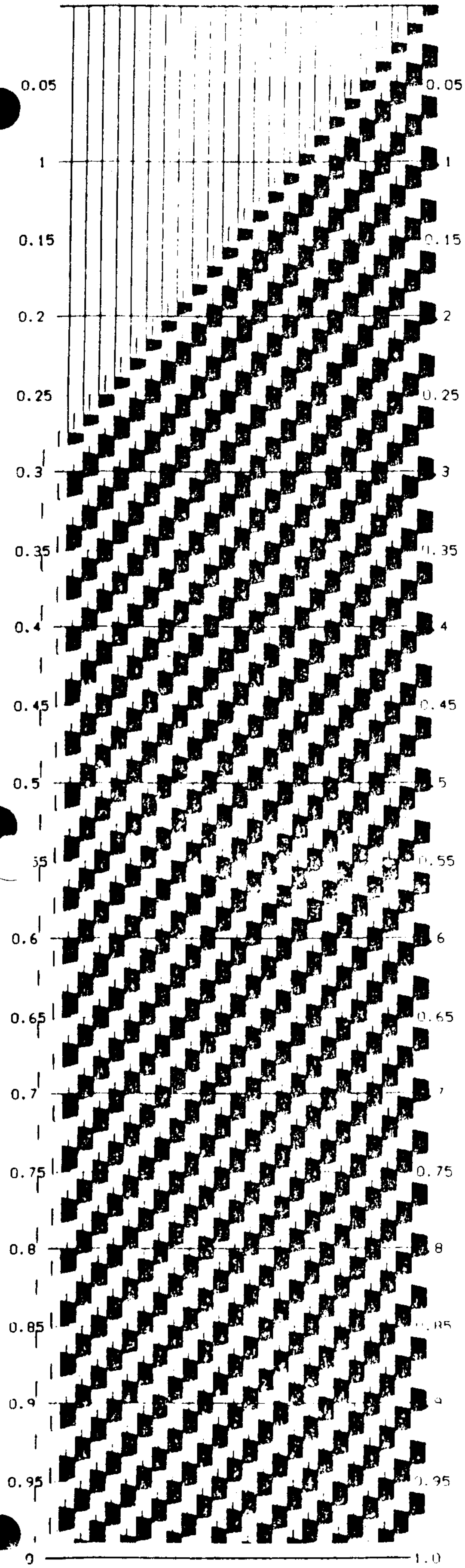

AMOCO

CHIMBLØ

LINE DIRECTIØN

FREQ PANEL: 30 HZ; DIP=12MS/TRACE

INPUT REEL HEADER INFØRMATIØN

REEL NUMBER	TSE017
DATE CREATED	10/12/78
NUMBER SAMPLE/TRACE	992
SAMPLE RATE IN MILLS	1
PRØCESSØR	CHIMBLØ
LINE NUMBER	CHIMBLØ
JØB NUMBER	CHIMBLØ
SECTIØN NUMBER	
PRØCESSING STEP	

PRØCESSING SEQUENCE

MERG
UTØP*(LINE HEADER ØNLY
ARCH
ARCH
REST(REPEAT BY PANEL)
REST(EXTERNAL STATICS)
PLØT**

****** FILMING PARAMETERS ******

PERCENT GAIN	100
HØRIZØNTAL SCALE 10.	TR/IN
VERTICAL SCALE 10.	IN/SEC
FILMING DIRECTIØN	R/L
PERCENT BAR	0
PØLARITY	BLACK+VE

Figure 15

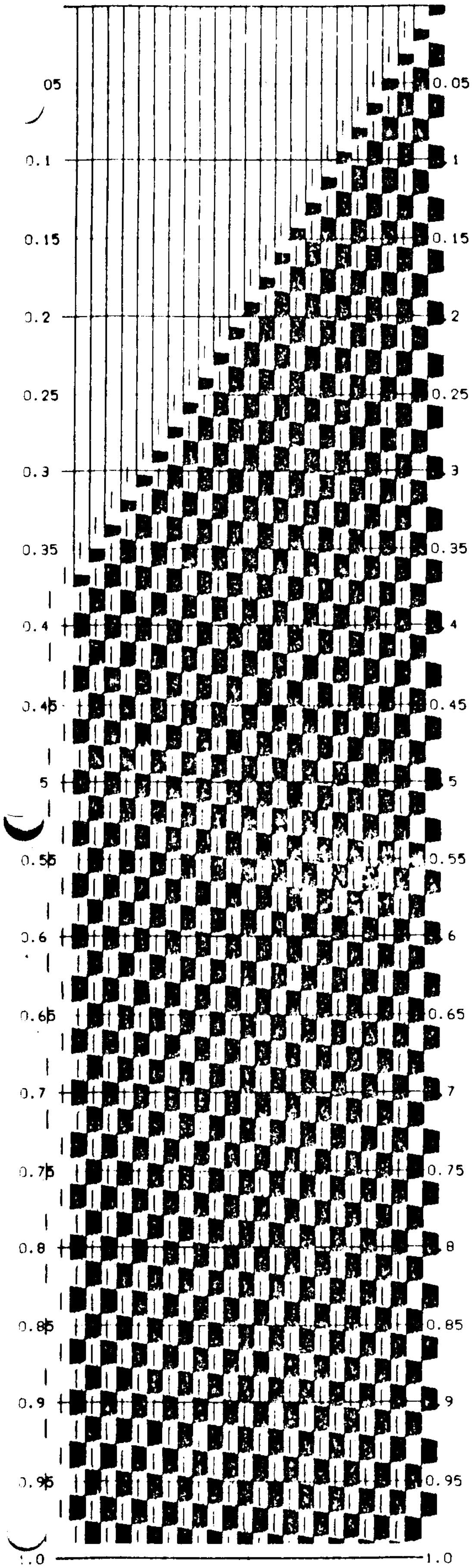

AMOCO

CHIMBL0

LINE DIRECTI0N

FREQ PANEL: 30 HZ; DIP=16MS/TRACE

INPUT REEL HEADER INF0RMATI0N

REEL NUMBER	TRE535
DATE CREATED	10/16/78
NUMBER SAMPLE/TRACE	992
SAMPLE RATE IN MILLS	1
PR0CESS0R	CHIMBL0
LINE NUMBER	CHIMBL0
J0B NUMBER	CHIMBL0
SECTI0N NUMBER	
PR0CESSING STEP	

PR0CESSING SEQUENCE

MERG
UT0P*(LINE HEADER 0NLY
ARCH
ARCH
REST(REPEAT BY PANEL)
REST(EXTERNAL STATICS)
GASP(MAA,100%, WIND 0-1000 MS)
TR T0 TR EQUALIZATI0N)
PL0T*

****** FILMING PARAMETERS ******

PERCENT GAIN	100	
H0RIZ0NTAL SCALE	10.	TR/IN
VERTICAL SCALE	10.	IN/SEC
FILMING DIRECTI0N		R/L
PERCENT BAR		0
P0LARITY		BLACK+VE

Figure *16*

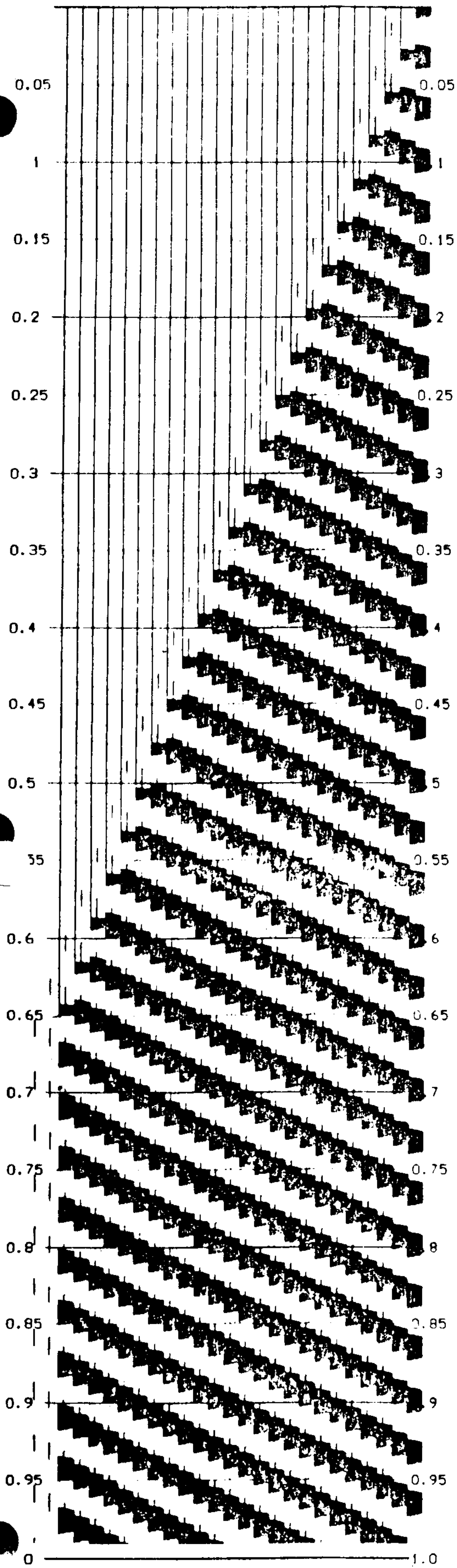

(30)

AMOCO

CHIMBLØ

LINE DIRECTIØN

FREQ PANEL: 30 HZ; DIP=28MS/TRACE

INPUT REEL HEADER INFØRMATIØN

REEL NUMBER	TR0741
DATE CREATED	10/16/78
NUMBER SAMPLE/TRACE	992
SAMPLE RATE IN MILLS	1
PRØCESSØR	CHIMBLØ
LINE NUMBER	CHIMBLØ
JØB NUMBER	CHIMBLØ
SECTIØN NUMBER	
PRØCESSING STEP	

PRØCESSING SEQUENCE

MERG
UTØP*(LINE HEADER ØNLY
ARCH
ARCH
REST(REPEAT BY PANEL)
REST(EXTERNAL STATICS)
GASP(MAA,100%, WIND 0-1000 MS)
TR TØ TR EQUALIZATIØN)
PLØT*

****** FILMING PARAMETERS ******

PERCENT GAIN	100	
HØRIZØNTAL SCALE	10.	TR/IN
VERTICAL SCALE	10.	IN/SEC
FILMING DIRECTIØN		R/L
PERCENT BAR		0
PØLARITY		BLACK+VE

Figure 7

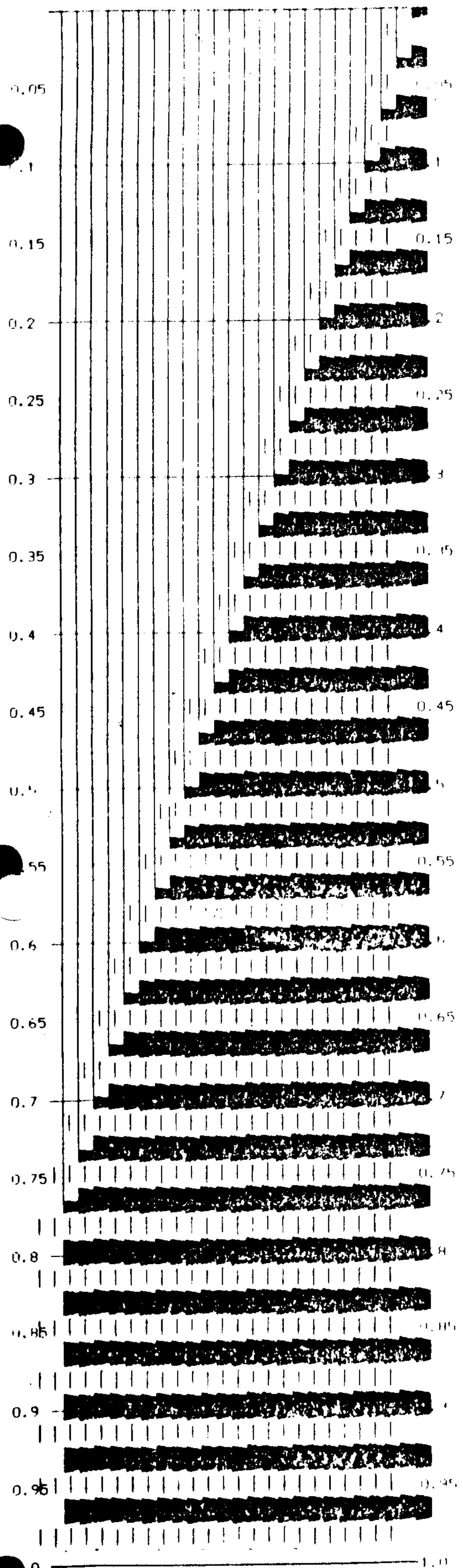

AMOCO

CHIMBL0

LINE DIRECTI0N

FREQ PANEL: 30 HZ; DIP=33MS/TRACE

INPUT REEL HEADER INF0RMATI0N

REEL NUMBER	TTC823
DATE CREATED	10/16/78
NUMBER SAMPLE/TRACE	992
SAMPLE RATE IN MILLS	1
PR0CESS0R	CHIMBL0
LINE NUMBER	CHIMBL0
J0B NUMBER	CHIMBL0
SECTI0N NUMBER	
PR0CESSING STEP	

PR0CESSING SEQUENCE

MERG
UT0P•(LINE HEADER ONLY
ARCH
ARCH
REST(REPEAT BY PANEL)
REST(EXTERNAL STATICS)
GASP(MAA, 100%, WIND 0-1000 MS)
TR TO TR EQUALIZATI0N)
PL0T•

•••••• FILMING PARAMETERS ••••••

PERCENT GAIN		100
H0RIZONTAL SCALE	10.	TR/IN
VERTICAL SCALE	10.	IN/SEC
FILMING DIRECTI0N		R/L
PERCENT BAR		0
P0LARITY		BLACK+VE

Figure 18

3. For dips greater than 16.67 ms/trace, spatial aliasing occurs. The dip is increased from 0-33 ms/trace. As the spatial Nyquist is approached (Figure 15) a second dip appears and at the Nyquist (Figure 16) two sets of distinct dips appear. The second set of dips is due to spatial aliasing and <u>are called aliased dips</u>. As the dip is further increased (Figure 17) only the aliased dips are visible and note that the rate of aliased dip is decreasing until at a moveout/trace equal to twice the Nyquist, flat dips appear (Figure 18).

   The characteristics of aliased dips in the time-distance domain:

   a. Aliased dips always appear as lower than true dips.

   b. Aliased dips are always opposite of the true dips.

4. <u>Why is Spatial Aliasing Undesirable?</u>

   Reasons:

   a. Due to the two sets of conflicting dips often evident on spatially aliased data:

(1) Migration is unreliable (aliased dips are also migrated).

(2) Stacking velocity determination is unreliable.

(3) Automatic static programs become unreliable.

b. The true coherent noise velocities are unrecognizable. Figure 19 shows aliased ground roll. The phase velocities necessary for array design are masked by the aliased dips (velocities).

c. Aliasing reduces the efficiency of f-k filtering (as will be shown).

d. f-k plots are difficult to analyze.

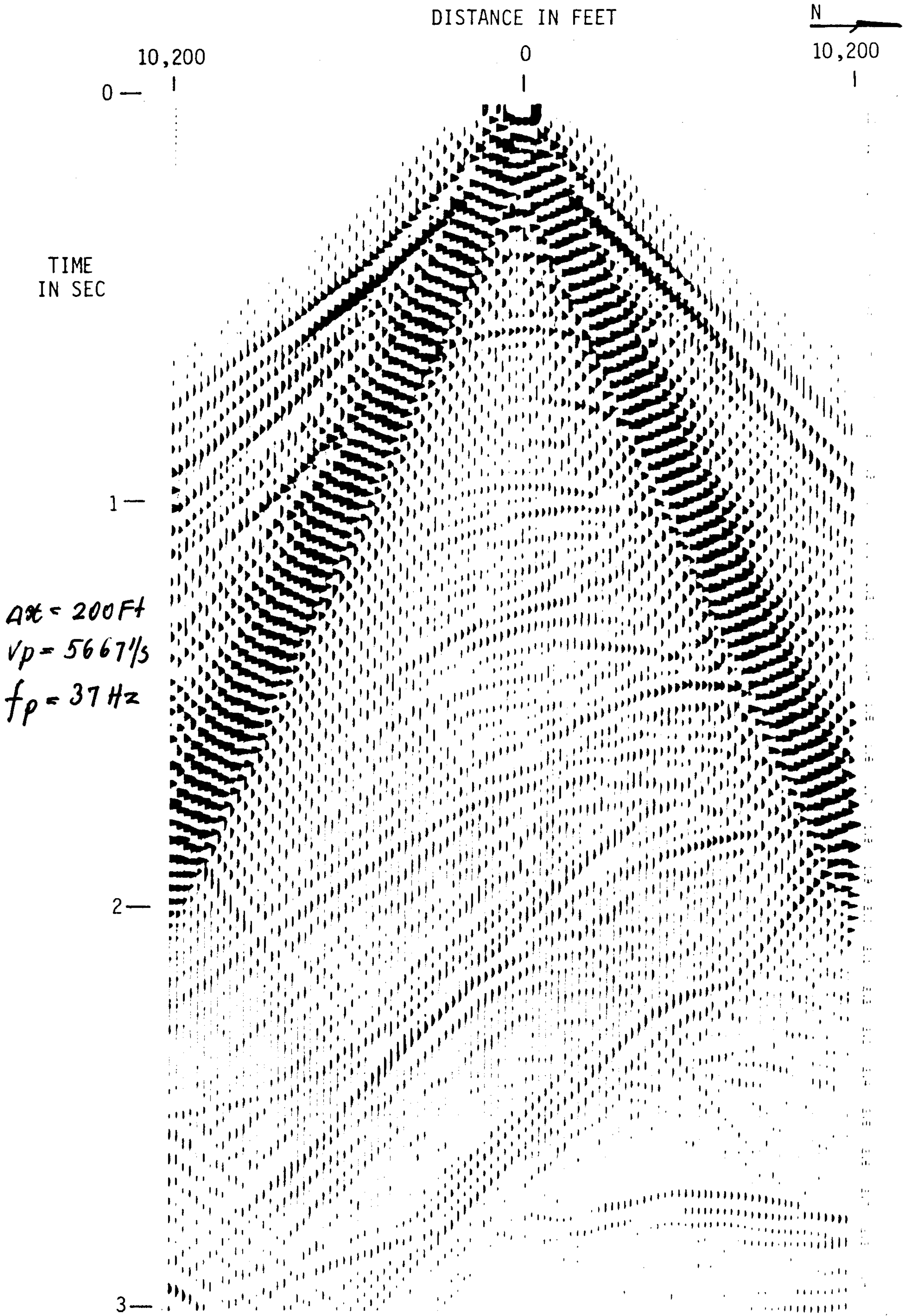

FIG. 19 Aliased Ground Roll.

Hidden Aliasing

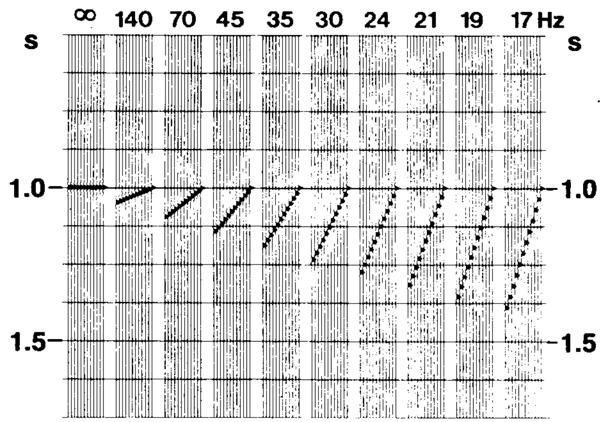

Figure 20a Broadband (5 to 80 Hz) dipping events. The data are adequately sampled in time (4-msec interval). For each dipping event, frequencies higher than those labelled above the dip segments are spatially aliased.

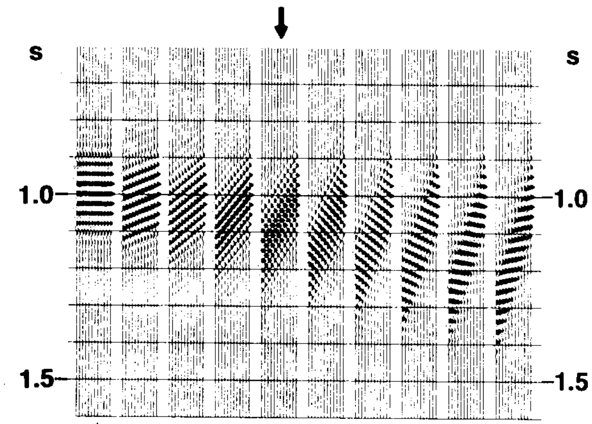

Figure 20b Narrow bandpass filtering of the dipping events in Figure 2 (passband is 35-40 Hz). Events to the right of the arrow are spatially aliased. That is, the dips that the human observer (and computer) would interpret differ from the true dips as seen in Figure 20a

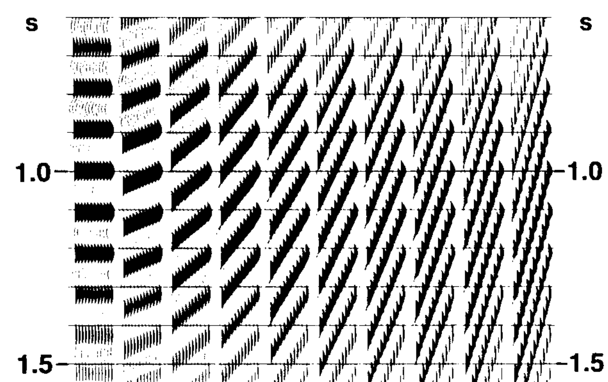

Figure 20c Narrow bandpass filtering of the dipping events in Figure (passband is 8.75-10 Hz). No frequencies within this passband are aliased, even for the most steeply dipping events. There is no difficulty in inferring the true dips of all the events.

Figure 20

The Effect of Aliasing on Migration

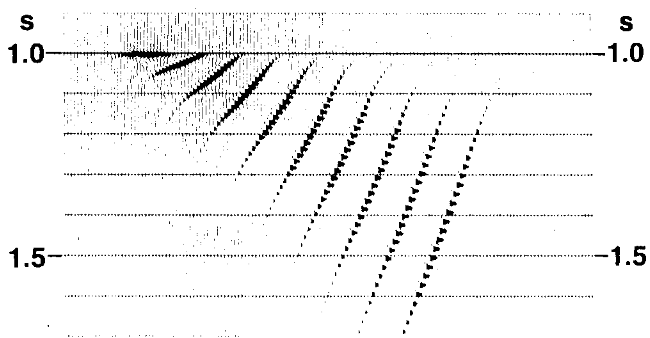

Figure 21a Synthetic zero-offset section created from dipping reflector segments. With the 48-m trace spacing, much of the frequency content in the steeper events is aliased.

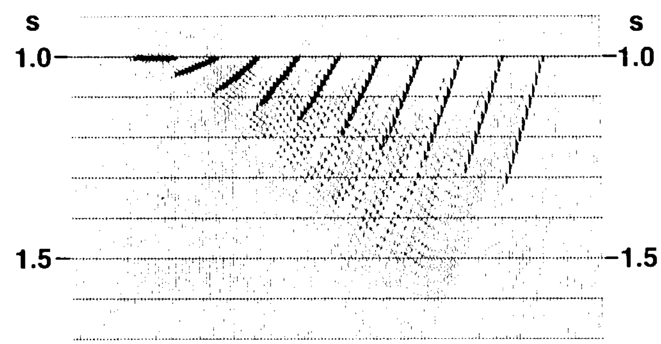

Figure 21b Frequency domain migration of the data in Figure 21a The aliased frequencies have migrated to the wrong positions, creating "migration noise" and causing a loss of the higher frequencies in the more steeply dipping events.

Figure 21

5. Is Spatial Aliasing Always Identifiable In The Time-Distance Domain?

It has been shown, that on the seismic record (or section) for a given dip spatial aliasing is the function of frequency. Since the recorded seismic data is broadband, some of the higher frequencies may be aliased. Whether a dipping event is visually aliased on the section, depends on the predominant frequency of the data: If the predominant frequency is not aliased, the dips do not appear aliased, yet aliasing may occur at higher frequencies. This is illustrated on Figures 20 and 21. Figure 20a shows a broadband event with increasing dip. Spatial aliasing is not evident. However, the narrow band pass filtering on Figures 20b and c show, that spatial aliasing does exist at higher frequencies. Figures 21a and b shows the effect of aliasing on migration: aliased frequencies are migrated to the wrong position causing the loss of high frequencies in the most steeply dipping events and also causing migration noise.

6. The Removal of Aliasing in Processing

Is it possible to remove spatial aliasing in processing?

Yes, but only if "buried" aliasing is present (the predominant frequency is not aliased). The method consists of creating extra traces to reduce spatial sampling by interpolation programs based on multi trace cross correlation. If the data is severely aliased as shown on Figure 19, the cross correlation program cannot produce non aliased extra traces.

7. The Computation of Aliased Velocities (Dips)

If the apparent velocity of an event is known and it is aliased, the equivalent aliased velocity (or dip) may easily be estimated from the simple equation:

$$Va = V \frac{f\Delta x}{f\Delta x - V} \qquad (12)$$

Where

Va = aliased velocity
V = apparent velocity of event (or measured velocity)
f = predominant frequency of event
Δx = group interval

Equation (12) is only applicable if the signal is aliased. The signal is aliased only if $2f\Delta x > V$. The term "$2f\Delta x$" is the Nyquist velocity for a given "f" and "Δx" as shown by equation (10).

It is important to know, if any of the frequencies contained in a dipping event of apparent velocity "V" and recorded by a group interval "Δx" are aliased.

8. The Maximum Non-Aliased Frequency

$$fmax = \frac{V}{2\Delta x} \tag{13}$$

Frequencies higher than fmax are aliased. From the aliased velocity, the unaliased equivalent velocity (V) is determined by:

$$V = \frac{f\Delta x}{Va + f\Delta x} \tag{14}$$

9. The Properties of Aliased Velocities

a. The aliased velocity is negative (dip is opposite to unaliased velocity).

b. The aliased velocity is always higher (the dip is less) than the unaliased velocity.

c. Temporal frequency of aliased data is unchanged.

D. The Properties of Signal and Noise in the f-k Domain

The seismic data may also be displayed in the f-k plane. In the frequency plane the temporal frequency is the ordinate and the spatial frequency is the abscissa.

The limits of the plane are:

1) The temporal Nyquist on the "f" axis (temporal frequencies higher than Nyquist cannot be recorded).

2) The negative and positive spatial Nyquist on the "k" axis (spatial frequencies higher than Nyquist cannot be recorded, only their aliased equivalent).

At the origin of the f-k plane, both the temporal and spatial frequencies are zero.

All of the seismic data is displayed in these two quadrants by fast Fourier transform of the recorded t-x data. Other quadrants also exist and a very small portion of the seismic energy disperses into these quadrants. For an accurate inverse transform (back into the t-x domain) these quadrants are necessary. However, from the practical point of view two quadrants are sufficient.

1. The Appearance of Seismic Events in the f-k Plane

Figure 22 summarizes the most commonly occurring seismic events in the f-k plain. The various spatial frequencies represent dips (apparent velocities):

a. Velocity in f-k plain = slope

$$V = \frac{\Delta f}{\Delta k} \quad \text{or} \quad V = \frac{f}{k}$$

b. Steep slope = high velocity
Low angle slope = low velocity.

c. Band limited flat reflection: the apparent velocity of a flat event is infinity, hence its k=0. Therefore, the signal is "bunched" around the vertical axis.

The Appearance of Seismic Events in the F-K Plain

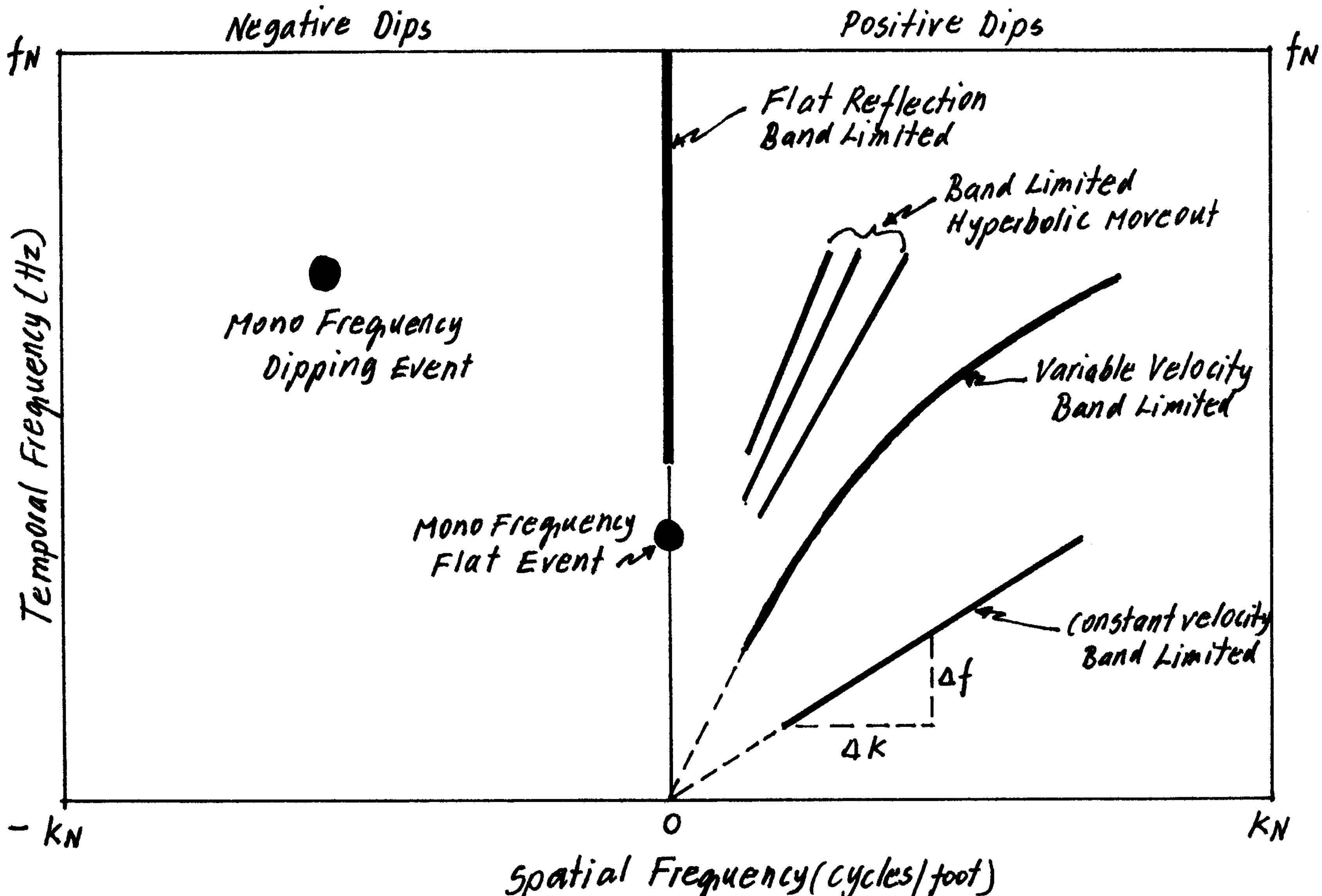

Figure 22

d. A mono frequency flat event or series of flat events is a "dot" (or very small area) on the vertical axis.

e. A mono frequency dipping event or reverberatory event (e.g., Figure 14) is a "dot" off the vertical axis. Its velocity:

$$V = \frac{f}{k}$$

f. A constant velocity band limited events (e.g., non dispersive ground roll, airwaves, reflected refractions, refraction arrivals, and their reverberation, dipping reflections) occupy a straight line, the slope being the velocity of the event. Linear reverberations always stack up at the position of primary.

g. Variable velocity band limited events (e.g., dispersive ground roll, higher Rayleigh modes, and trapped modes) are curved lines (or bands). The apparent velocity at any one point is the slope of the tangent line. Due to dispersion, the apparent velocity increases with a decrease in frequency.

h. Reflections uncorrected for NMO (hyperbolic moveout) appear as a series of straight lines, since the asymptotic limit of the hyperbola dominates the spectrum. The separation or notching, or spread in the k direction occurs since the reflection hyperbola contains some contribution at all dips less than the asymptotic dip of the hyperbola. Figures 22a and b better illustrate the problem.

2. Spatial Aliasing in the f-k Domain

The seismic wavefield only occupies the two main quadrants and (Figure 23) any signal outside of these quadrants is "folded back" into these quadrants, said to be "aliased" or "wrapped around". Before discussing the principle of aliasing a number of concepts need to be defined.

a. Spatial Nyquist Velocity (V_N)

It is the minimum allowable velocity (without aliasing) for a dipping event containing all frequencies up to the temporal Nyquist and spatially sampled at Δx intervals (event "A" on Figure 23).

$$V_N = \frac{f_N}{k_N}$$

Hyperbolic Event on F-K Plot

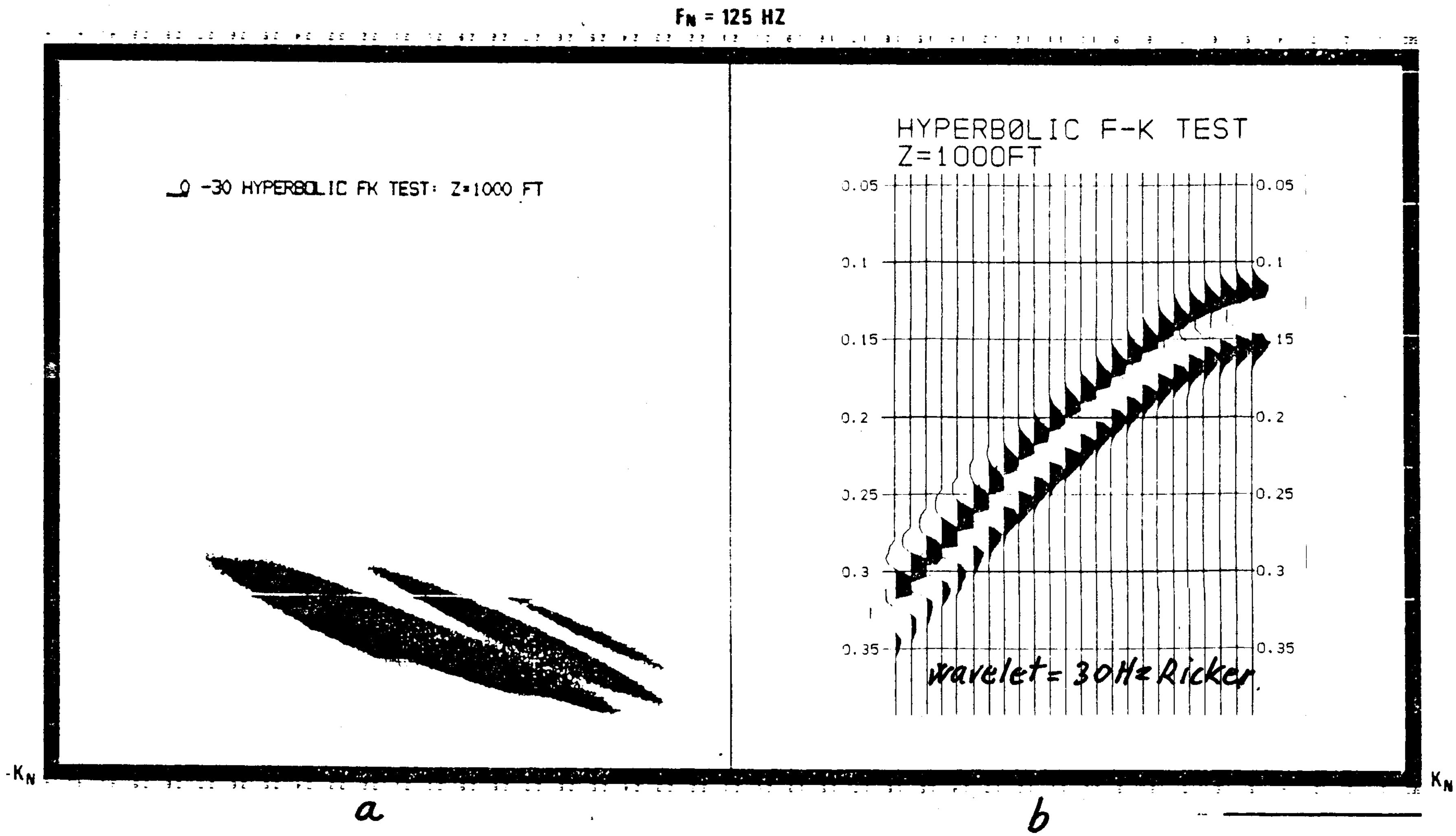

Figure 22 a, b

Spatial Nyquist Velocity (V_N) and Min. Allowable Velocity For "f_1" and "Δx":

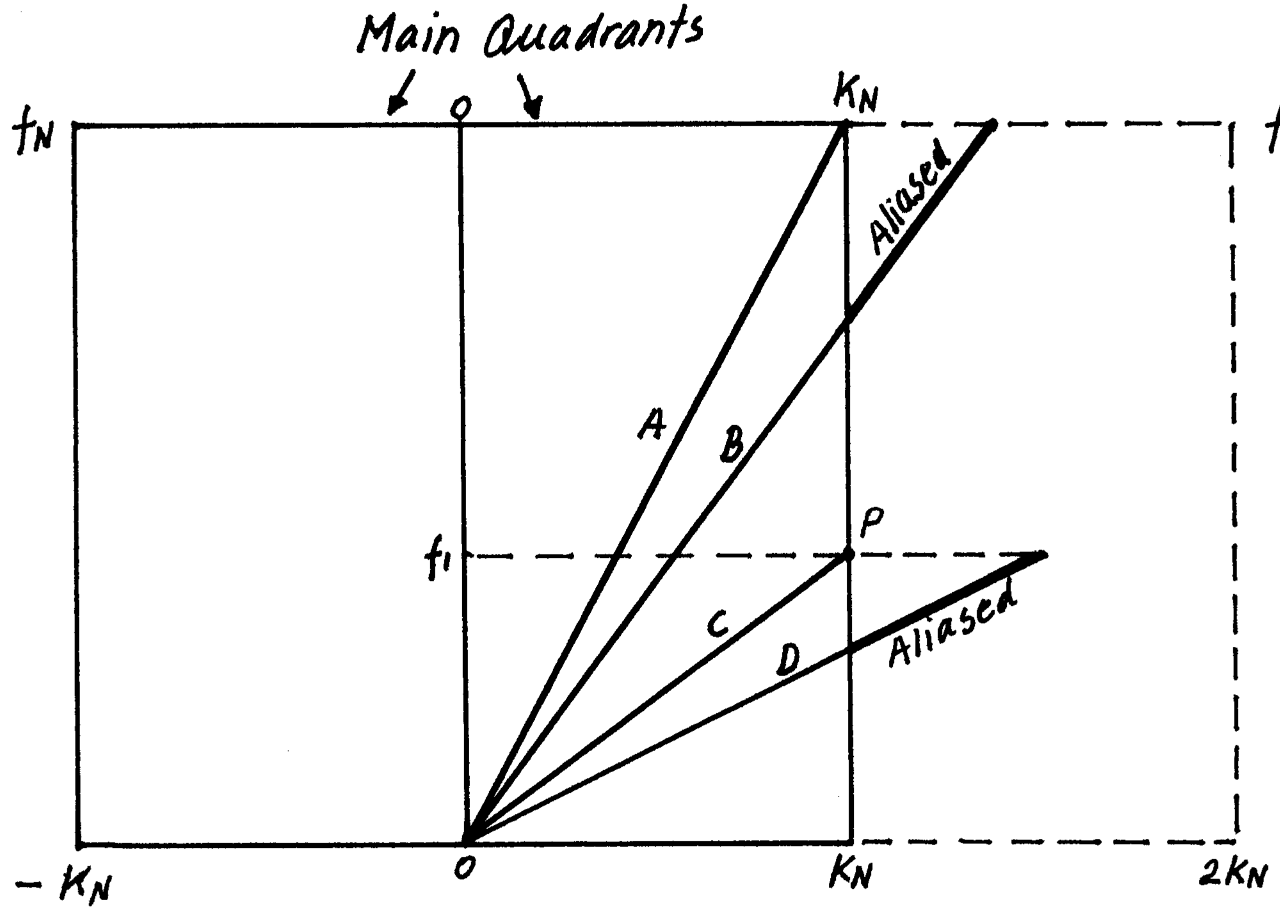

$f_n = \frac{1}{2\Delta t}$

$K_N = \frac{1}{2\Delta x}$

Δt = temporal sample rate

Δx = spatial sample rate (group interval)

A = Spatial Nyquist Velocity

C = Min. allowable velocity for a given "f_1" and "Δx"

Figure 23

Since

$$f_N = \frac{1}{2\Delta t} \quad \text{and} \quad k_N = \frac{1}{2\Delta x} \qquad V_n = \frac{\Delta x}{\Delta t}$$

where Δt = temporal sample interval

Velocities lower than V_N are aliased (event "B" on Figure 23).

b. <u>The Minimum Allowable Velocity</u> (to avoid spatial aliasing) for a band limited event ($0<f\leq f_1$). Event "C" on Figure 23.

$$V\text{min} = \frac{f_1}{k_N} = \frac{f_1}{\frac{1}{2\Delta x}} = 2f_1\Delta x$$

"Vmin" is also known as the Nyquist velocity for "f_1". Velocities lower than "Vmin" are aliased (line"D").

c. <u>The Maximum Spatial Sample Interval</u> (group interval = Δxmax) to avoid spatial aliasing for a band limited event ($0\leq f\leq f_1$) of velocity "V": Curve "C" on Figure 23 may be used to illustrate the computation procedure. The intersection of velocity "V" and the horizontal line through the max frequency

"f_1" (point P) defines the maximum allowable spatial frequency kmax.

$$kmax = \frac{1}{2\Delta xmax} = \frac{fmax}{V}$$

Therefore,

$$\Delta xmax = \frac{V}{2fmax} \tag{15}$$

d. <u>The Maximum Non-Aliased Frequency</u> for an event of velocity "V" sampled by "Δx".

$$fmax = \frac{V}{2\Delta x}$$ same as equation (13)

Spatial aliasing in the f-k domain is a complex phenomenon and it is difficult to understand.
Figure 24 summarizes the basic principles. Suppose the primary event of velocity "V" contains all temporal frequencies to the Nyquist and all spatial frequencies up th "$7k_N$". All the spatial frequencies above "k_N" are aliased or folded back into the main quadrants. The mono frequency event at "A" is aliased. Where is the aliased equivalent (A') in the main quadrant?

Spatial Aliasing (Wraparound) in the F-K Plain.

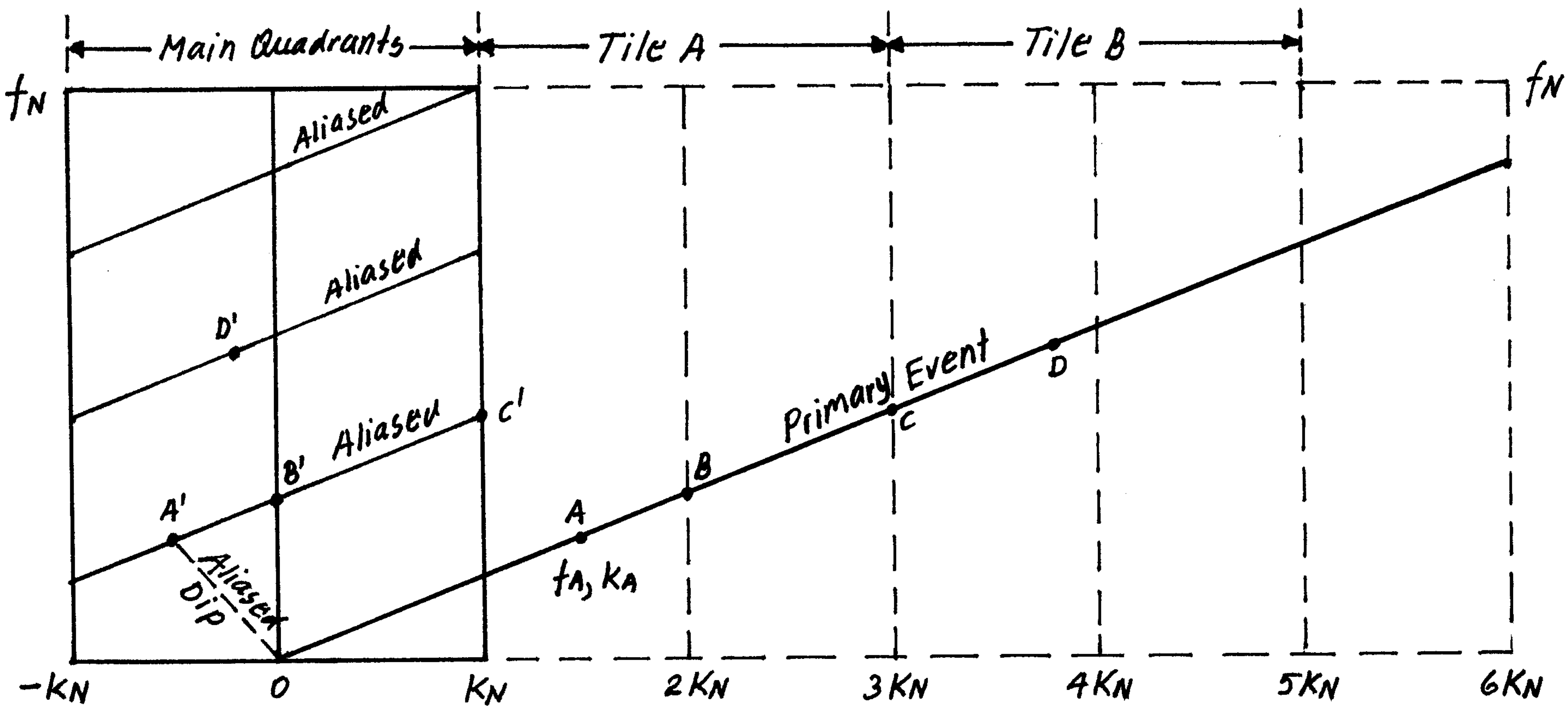

Figure 24

K_A is folded back about "$-k_N$" (a signal at k_N also appears at $-k_N$), its distance from $-k_N$ is the same as the distance of "A" from "k_N" that is frequencies higher than k_N will masquerade as lower frequencies, similarly to temporal aliasing.

Therefore the aliased spatial frequency:

$$k_{A'} = k_A - 2k_N \tag{16}$$

The aliased velocity is negative and higher (the dip is lower) than the primary dip (as shown by Figures 13-18). "B" is folded back to B'. At B' the dip is flat as shown on Figure 18 and it is said that a complete "foldover" occurred. "C" is folded back to C' and the process is repeated for higher spatial frequencies.

e. <u>Wraparound</u>

Since the primary event is the sum of distinct frequencies such as A, B, C (the sum of its Fourier components), the aliased equivalent is a series of straight lines parallel to the primary event. The process is also known as "wraparound".

Wraparound may also be visualized by dividing the f-k space into a series of "tiles" as shown on Figure 24.

The position of aliased spatial frequencies is found by simply stacking tiles A, B, C, etc., on top of the main quadrants.

f. <u>The Computation of Aliased Frequencies</u>

The aliased spatial frequency for each component of the primary event shown on Figure 24 is predictable.

If Primary is in tile A, ($k_N \leq kp \leq 3k_N$):

$$k_A = kp - 2k_N$$

If Primary is in tile B, ($3k_N \leq kp \; 5k_N$):

$$k_A = kp - 4k_N$$

If Primary is in the "n"-th tile, [$(2n-1)k_N \leq kp \leq (2n+1)k_N$]

$$k_A = kp - 2nk_N \qquad (17)$$

Where,

$$k_A = \frac{f}{V_A} \quad ; \quad k_N = \frac{1}{2\Delta x} \quad ; \quad kp = \frac{f}{Vp}$$

$$\frac{f}{V_A} = \frac{f}{Vp} - \frac{1}{\Delta x}$$

$$V_A = Vp \frac{f\Delta x}{f\Delta x - Vp} \qquad \text{which is equation (12)}$$

Similarly if the aliased velocity is measured on the section, the primary velocity is predictable: from equation 12.

$$Vp = V_A \frac{f\Delta x}{f\Delta x + V_A} \tag{18}$$

For the "n"-th tile

$$Va = Vp \frac{f\Delta x}{f\Delta x - nVp} \tag{19}$$

$$Vp = Va \frac{f\Delta x}{f\Delta x + nVa} \tag{20}$$

Equations 12, 18-20 may also be expressed as the function of kp, ka, and k_N.

Equation (12):

$$V_A = \frac{f}{kp - 2k_N} \tag{21}$$

Equation (18):

$$Vp = \frac{f}{k_A + 2k_N} \tag{22}$$

Equation (19):

$$Va = \frac{f}{kp - 2nk_N} \tag{23}$$

Equation (20):

$$Vp = \frac{f}{ka + 2nk_N} \qquad (24)$$

It has been emphasized, that the aliased dip is always less than the primary dip, its spatial frequency is lower hence the aliased velocity is higher than the velocity of the primary event. Furthermore, as stated in equations 18-24 the aliased velocities are predictable from the f-k plots.

However, the velocity from f-k plots is computed by:

$$V = \frac{\Delta f}{\Delta k}$$

and Figure 24 shows it very clearly that the aliased velocity of a band limited event is exactly the same as that of the primary. This is a paradox. The predictability of aliased dips (or velocities) was deducted by folding the individual temporal and spatial frequency pair points. This conclusion is true and can be applied to the seismic section. The visual aliased dip is the result of the predominant frequency being aliased. Therefore, if the predominant temporal frequency and its velocity is measured, the aliased visual dip is predictable.

The reason for the apparent paradox is not known.

The facts are:

1) The aliased dip (or velocity) seen on the t-x display is not recognizable on the f-k plot.

2) The sum of all the apparent aliased velocities in a complete wraparound (from $-k_N$ to $+k_N$) is the velocity of the primary event.

3) The visual aliased dip seen on the t-x display is predictable from the predominant frequency and velocity of the primary event and vice versa (Figure 25).

Visual Aliased Dips of Predominant Frequency (f_p).

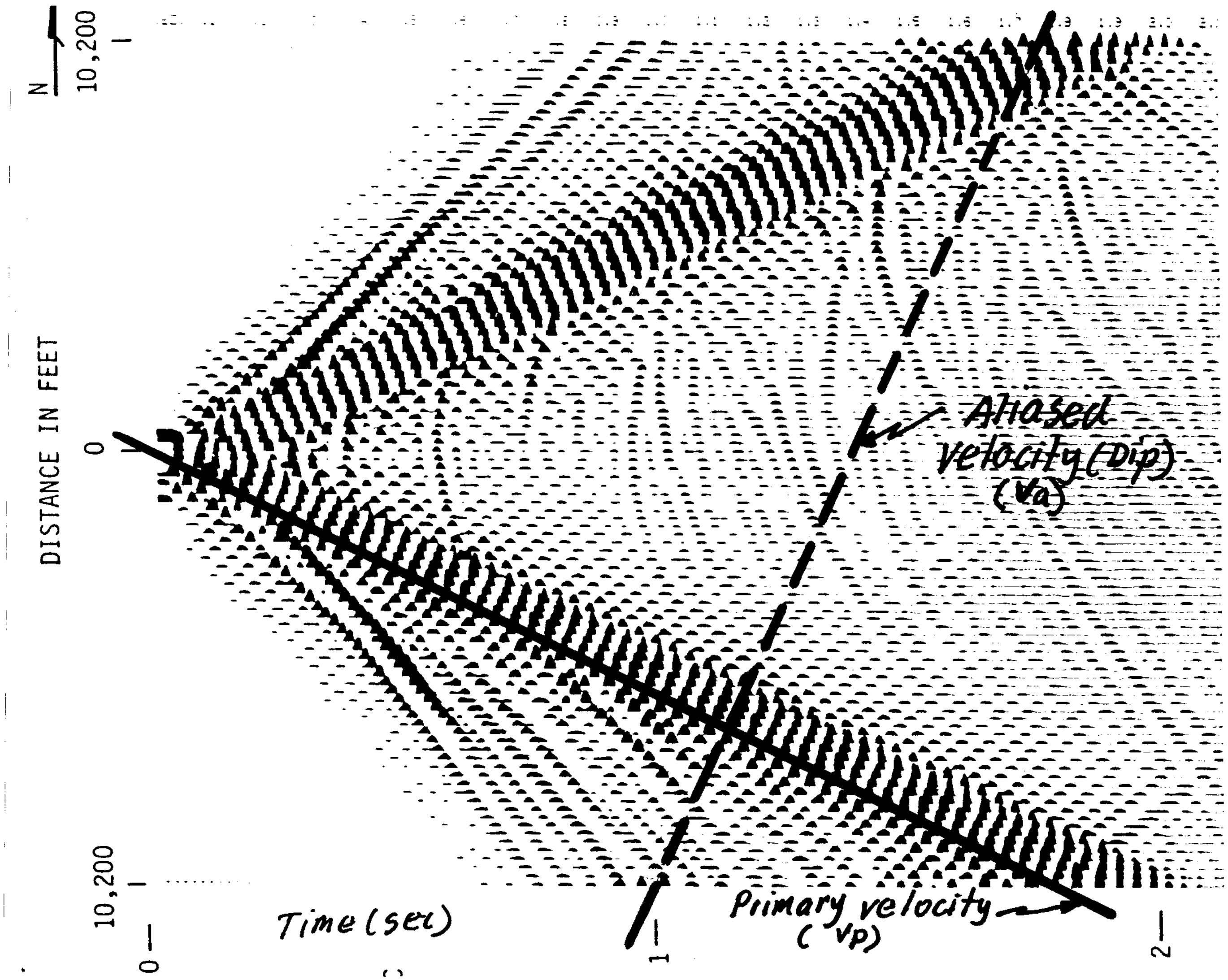

$\Delta x = 200$ Ft
$V_p = 5667'/s$
$f_p = 37$ Hz

Computed Aliased Vel.:

$$V_a = V_p \frac{f \Delta x}{f \Delta x - V_p} = 24{,}200'/s$$

Observed Aliased Vel.:

$V_a = 25{,}500'/s$

Figure 25

g. The Effect of Statics on Aliasing

Trace to trace static variations introduce sharp changes in the apparent velocities, hence a high frequency modulation on the spatial wavelength. The amplitude of modulation depends on the magnitude of static errors. These higher frequency components may introduce aliasing into the otherwise unaliased data. The larger the static error, the more aliasing (smearing) will occur. This is illustrated on Figures 26-28 where at 50 percent statics (the random static movement is 50 percent of the predominant period) will smear the signal all across the f-k plain.

Static variations belong to the family of "edge effects". Other edge effects causing aliasing (smearing) are:

1) Dead traces.

2) Discontinuity in slope of data (split spread).

3) Window selection without proper taper.

i. <u>The Advantages of f-k Representation of Data Over t-x Display</u>

In spite of all the difficulties encountered with the interpretation of f-k plots, there are two significant advantages:

The Effect of Statics on Spatial Aliasing

0 % Statics

Record

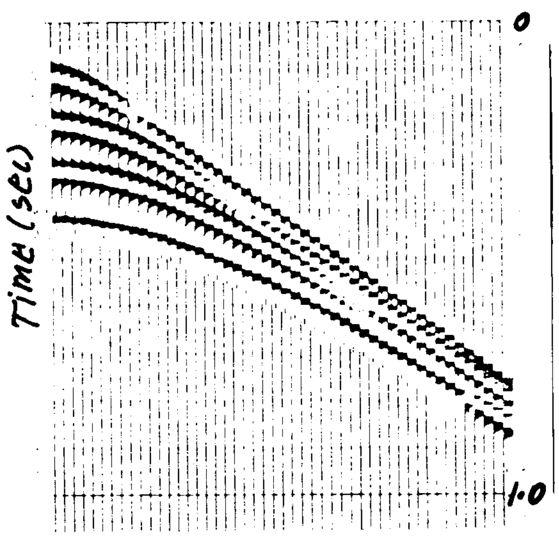

$\Delta x = 75$ Ft

$x = 3525$ Ft

$\bar{V} = 5000$ Ft/sec

F-K Plot

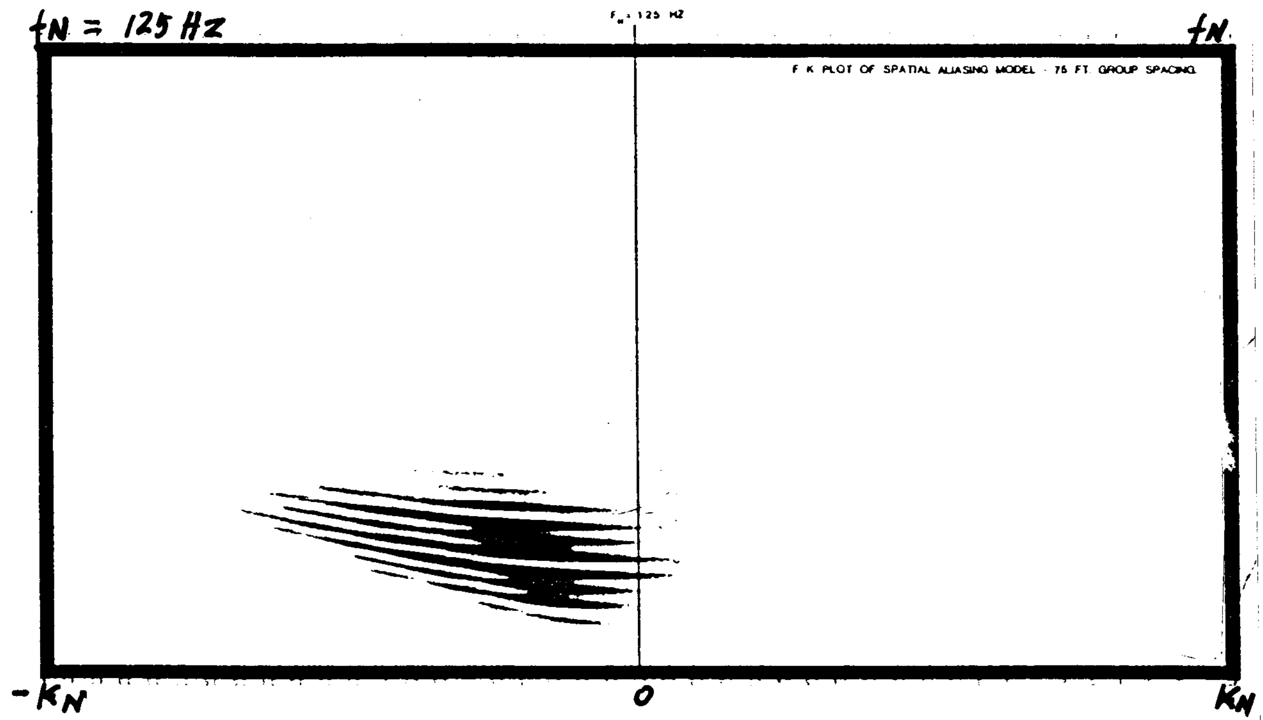

Figure 26

The Effect of Statics on Spatial Aliasing

10% statics

Record

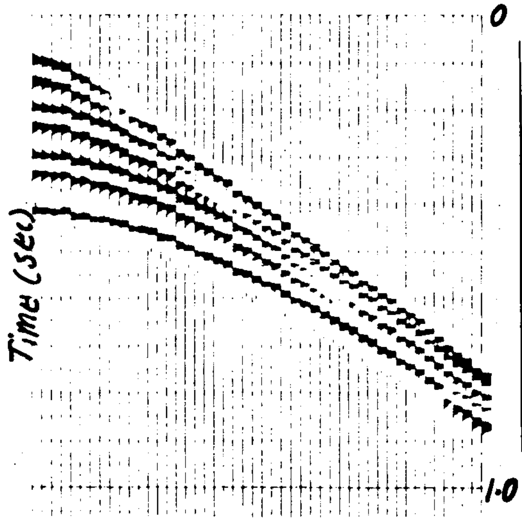

F- K Plot

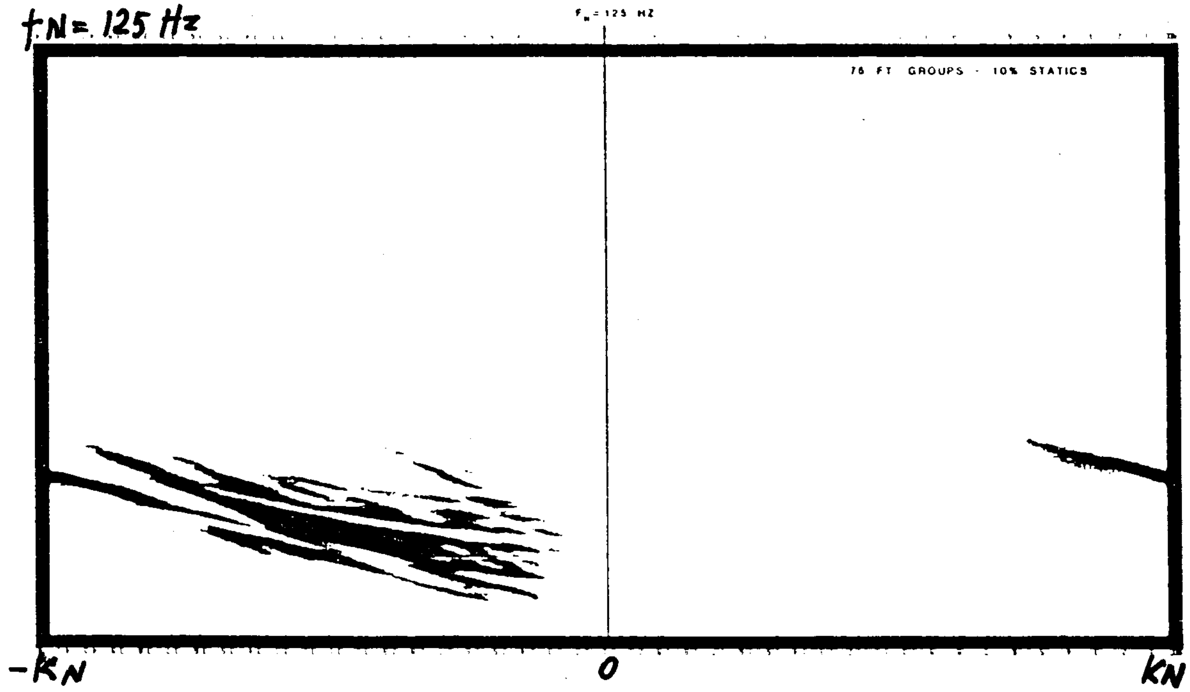

$\Delta x = 75$ Ft
$x = 3525$ Ft
$\bar{V} = 5000$ Ft/sec
Dominant period = 33ms ($fp \approx 30$Hz)
10% statics $\approx$ 4ms

Figure 27

The Effect of Statics on Spatial Aliasing

50% Statics

Record

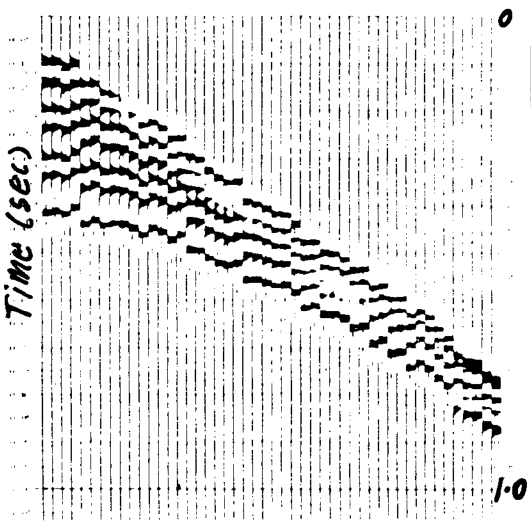

F-K Plot

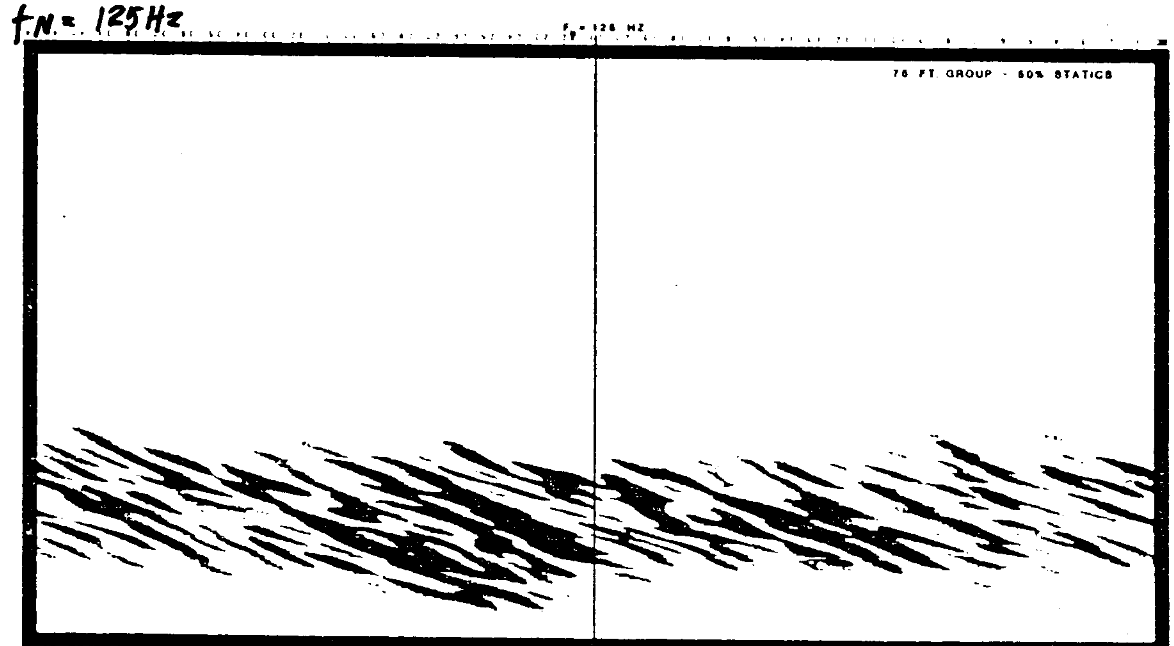

$\Delta x = 75$ Ft

$x = 3525$ Ft

$\bar{V} = 5000$ Ft/sec

Dominant period = 33ms ($f_p \approx 30$Hz)

50% statics $\approx$ 16 ms

Figure 28

1) In the t-x plane various events are separated on the bases of depth, frequency, and apparent velocity. Hence overlapping events often cannot be separated.

   In the f-k plane events are separated based on the apparent velocity. Overlapping events are well separated, therefore, f-k filters may be applied to remove undesirable coherent noise.

2) Linear coherent noise reverberations appear with the primary in the f-k plane, hence are usually well separated from the signal.

f-k displays are a powerful tool in the effective attenuation of the majority of unwanted coherent noise not visible in the t-x domain that often severely reduces the S/N of the final stack.

The major problem with the f-k plots is the difficulty of identifying the various amplitude alignments other than the most obvious, high amplitude linear noise. f-k interpretation requires experience or the result of f-k filtering can be disastrous.

IV. Source and Receiver Arrays

Source and receiver arrays - as discussed in the introduction - are a group of receivers or combination of receivers and/or sources laid out in a pattern.

The objectives of arrays are three-fold:

1) To improve the S/N of data by multiplicity.

2) Provide adequate sampling to avoid spatial aliasing.

3) To attenuate coherent noise waves.

A. Arrays as Temporal and Spatial Frequency Filters

As shown on Figures 10-12, field arrays sample the apparent wavelength of the wavefield as it propagates along the surface. The output of the array is the sum of the amplitudes recorded by the individual receivers. The output for a given array depends on the apparent wavelength of the disturbance: for long wavelengths (Figure 12), all the receivers record ground movement in the same direction, resulting in high amplitude output.

However, if "the apparent wavelength is such, that the receivers experience equally the effect of upward and downward displacement", the net output of such array (Figure 11) is zero. The array has discriminated against a certain apparent wavelength, hence arrays are spatial filters or spatial frequency filters.

When discussing filters in the t-x plane, the term "array" is used. Since arrays are spatial frequency filters in the f-k domain the term "spatial frequency filter" is used when discussing filters in the frequency plane.

The apparent wavelength is a function of the temporal frequency

$$\lambda a = \frac{Va}{f} ,$$

therefore, arrays are also temporal frequency filters.

In summary, arrays have dual effect on the data:

1) Spatial frequency (or wavelength) filtering,

2) Temporal frequency filtering.

B. Types of Arrays

Based on the spacing and weight of the elements, arrays are divided into three classes:

1) Uniform or linear arrays,

2) Linearly tapered arrays,

3) Non-linearly tapered or weighted arrays.

1. Linear Arrays

A linear array consists of a number of equally spaced, uniformly sensitive elements, usually in a straight line with the energy sources (or projected into a straight line for analysis purposes). Linear arrays are the most common type in land acquisition and are used 80 percent of the time.

a. Definitions

Figure 29 summarizes the basic terms used in array design: "n", the number of elements, "s" the element interval, "Δl" the actual array length, and "L", the effective length.

b. The Output of Linear Arrays

Since the recorded seismic wavelet is the sum of its Fourier components (or the sum of sinusoidal waves), the response of an array can sufficiently be described by the summation of sinusoidal waves, properly delayed.

Basic Terms Used in Array Design

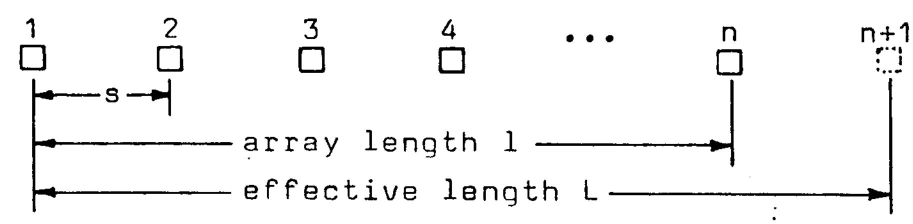

n = number of elements

s = element interval

Δl = actual array length = $(n-1)\,s$

L = effective length = ns

FIG. 1 - THE SUB-ARRAY

Figure 29

According to antenna theory, the "relative amplitude" (normalized) of a uniform array of "n" elements is given by the equation:

$$Ar = \left| \frac{1}{n} \frac{\sin\left(\frac{n}{n-1}\frac{\emptyset}{2}\right)}{\sin\left(\frac{1}{n-1}\frac{\emptyset}{2}\right)} \right| \tag{25}$$

where "Ø" is the phase shift (a static shift or time delay) across the array.

$$\emptyset = 2\pi f \Delta t \tag{26}$$

where f = temporal frequency
Δt = time delay across the array

Equation (25) may also be expressed as the function of "s" and "L" and "λa".

Since $\Delta t = \frac{\Delta l}{Va} = \frac{(n-1)s}{Va}$

Equation 25 becomes

$$Ar = \left| \frac{1}{n} \frac{\sin\left[\frac{n}{n-1}\pi f \frac{(n-1)s}{Va}\right]}{\sin\left[\frac{1}{n-1}\pi f \frac{(n-1)s}{Va}\right]} \right|$$

$$Ar = \left| \frac{1}{n} \frac{\sin\left(\pi ns \frac{f}{Va}\right)}{\sin\left(\pi s \frac{f}{Va}\right)} \right| \quad (27)$$

$$Ar = \left| \frac{1}{n} \frac{\sin\left(\pi \frac{ns}{\lambda a}\right)}{\sin\left(\frac{\pi s}{\lambda a}\right)} \right| \quad (28)$$

$$Ar = \left| \frac{1}{n} \frac{\sin\left(\pi \frac{L}{\lambda a}\right)}{\sin\left(\frac{\pi s}{\lambda a}\right)} \right| \quad (29)$$

Furthermore, since $k = \frac{1}{\lambda a}$

$$Ar = \left| \frac{1}{n} \frac{\sin(\pi\, kns)}{\sin(\pi ks)} \right| \quad (30)$$

or by substituting D = ks into equation (30)

$$Ar = \left| \frac{1}{n} \frac{\sin(n\pi D)}{\sin(\pi D)} \right| \quad (31)$$

Equations 25, 27, 28, 29, 30, and 31 are used interchangeably to suit particular purpose. Only the independent variable displayed on the x-axis varies. The most commonly used equations are 29, 30, and 31.

It is important to note, that the above equations only hold for "mono frequencies". For a band limited seismic wavelet, the spatial filter response given by the above equations is convolved with the frequency response of the seismic wavelet to achieve the filtered response.

For the special case, when $n \to \infty$ (large number of phones), equation 25 becomes a "sync function".

$$Ar = \left| \frac{\sin\left(\frac{\emptyset}{2}\right)}{\frac{\emptyset}{2}} \right| \qquad (32)$$

Similarly, equations 29, 30, and 31:

$$Ar = \left| \frac{\sin\left(\pi \frac{L}{\lambda a}\right)}{\pi \frac{L}{\lambda a}} \right| \qquad (33)$$

$$Ar = \left| \frac{\sin(\pi kL)}{\pi kL} \right| \qquad (34)$$

Note, that for a given group length as $n \to \infty$ $\Delta l \to L$. Furthermore, as $n \to \infty$ for a given group length, $s \to 0$, therefore, the spatial Nyquist $\to \infty$ and the response never repeats.

The output of arrays (Ar) is plotted as the percentage of maximum amplitude (when all receivers record the signal the same instant, hence there is no delay across the array). The percentage may also be expressed in "db", the maximum output being "0" db and smaller outputs in negative "db", hence a certain "db down" from the maximum output.

c. Basic Properties of Linear Arrays

Figures 30 and 31 show the array response for "n" elements. The relative amplitude in db is plotted on the vertical axis. A number of different variables may be plotted on the horizontal axis depending which of the equations are used from equations 27-31.

Figure 30 shows the effective group length (L) or the apparent wavelength (λa) or the temporal frequency (f) on the "x" axis. On Figure 31 the most often used spatial frequency (k) and the dimensionless quantity, "D" are displayed on the "x" axis.

AMPLITUDE RESPONSE FOR "n" ELEMENTS

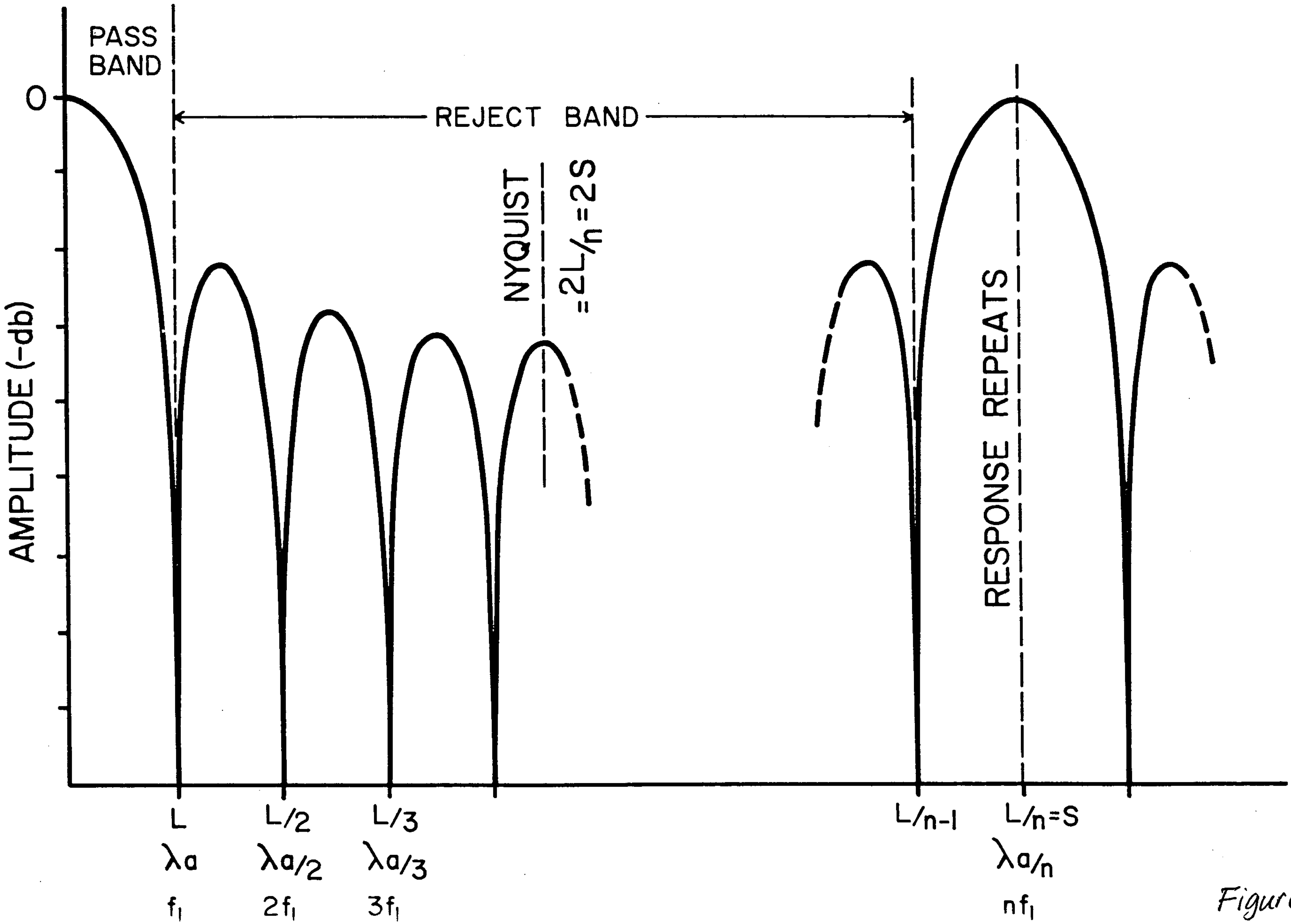

Figure 30

(71)

AMPLITUDE RESPONSE FOR "n" ELEMENTS

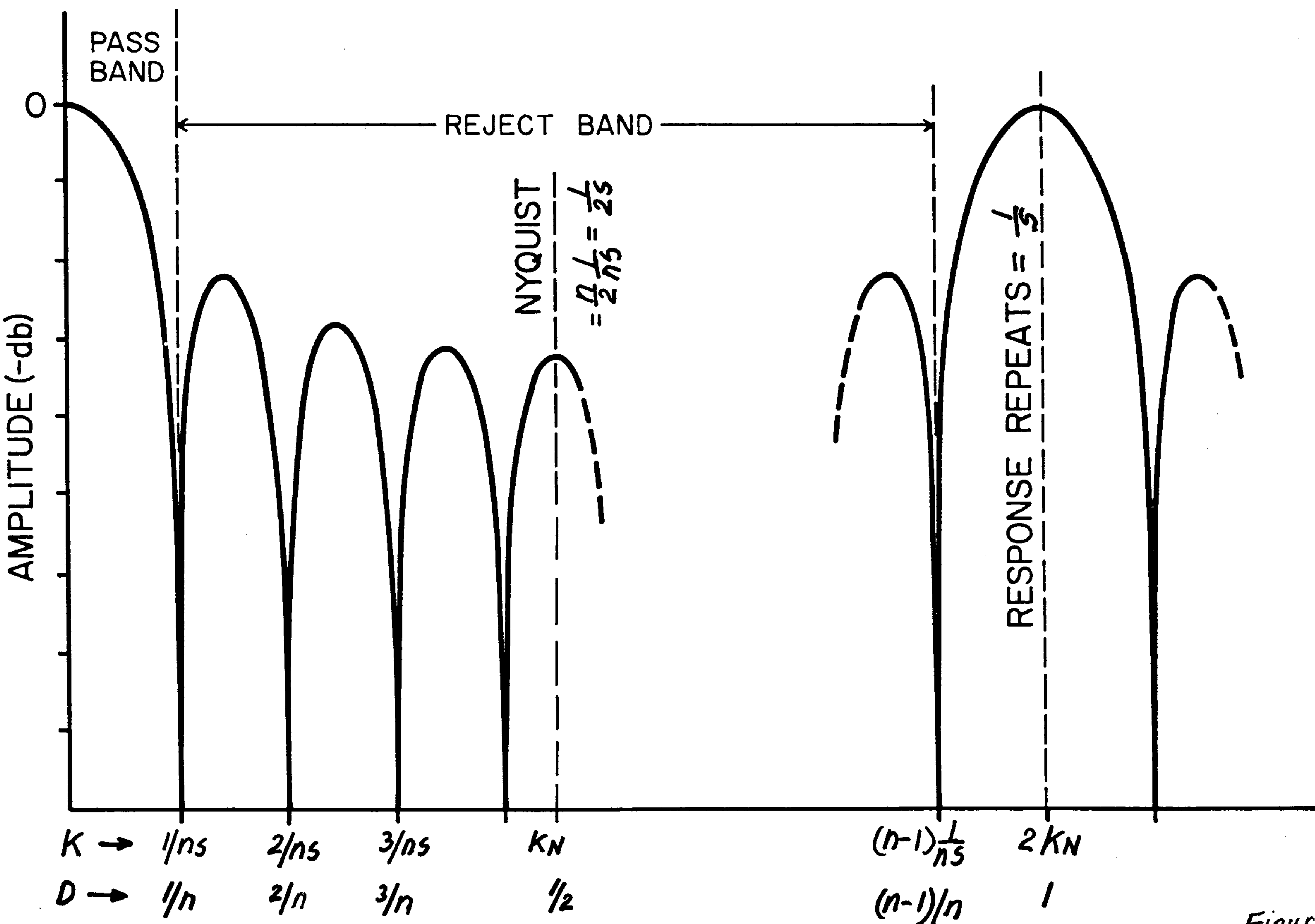

Figure 31

A number of simple properties of linear arrays are shown on Figures 30-31.

1) The first notch occurs at a wavelength equal to the effective group length ($\lambda a=L$) and subsequent notches at L/2, L/3, etc. If the spatial frequency is the independent variable, the first notch occurs at 1/ns and subsequent notches at 2/ns, 3/ns, etc. If "D" is plotted on the "x" axis the first notch is at 1/n and subsequent notches at 2/n, 3/n, etc.

2) The number of notches = n-1.

3) The response is symmetric about the spatial Nyquist. The spatial Nyquist is at 2L/n=2s or k=1/2s or D=0.5. The array will pass spatial frequencies higher than the Nyquist. However, these frequencies will be aliased and masquerade as lower frequencies. The response can be folded back at the Nyquist to determine the aliased spatial frequency.

4) The response repeats at s=L/n or k=1/s or D=1.0. If the response is folded back at the Nyquist, the repeat falls on the main lobe, full wraparound or foldover occurred.

5) The main lobe of the response is the pass band.

6) The region from the first notch to the last notch is called the reject band.

7) The width of the reject band (first notch to last notch):

a) If wavelength (λa) or effective group length is used:

$$\text{Reject bandwidth} = \frac{n(n-2)}{n-1}\, s$$

b) If spatial frequency is plotted:

$$\text{Reject bandwidth} = \frac{n-2}{n}\ \frac{1}{s}$$

c) If "D" is used:

$$\text{Reject bandwidth} = \frac{n-2}{n}$$

It is evident that the width of the reject band may be extended by increasing "n" (for constant "s"). The effective group length will also increase.

8) The width of the pass band is decreasing, by increasing the effective group length.

9) By keeping the effective group length constant and increasing "n", "s" will be smaller. The pass band stays constant, but the reject band is extended.

10) The effective group length, apparent wavelength are decreasing and the temporal frequency, spatial frequency and "D" are increasing in the "x" direction.

11) Physical meaning of notches:

    a) At the notches the output of the array is zero.

b) Equations 27-34 compute the "absolute relative amplitude". In fact, the first lobe has negative amplitudes, the second positive, etc.

c) Therefore, at the notches polarity inversion occurs.

d) The phase shift "flip-flops" at the notches between 0° and 180° as shown on Figure 32.

d. <u>The Performance of Linear Arrays</u>

The purpose of field arrays is to pass the useful signal and reject the coherent noise. The amplitude of coherent noise is often 40-50 db above the signal. Therefore, a minimum of 40 db attenuation is required in the reject band.

The Meaning of Notches on Ampl. Response Plots

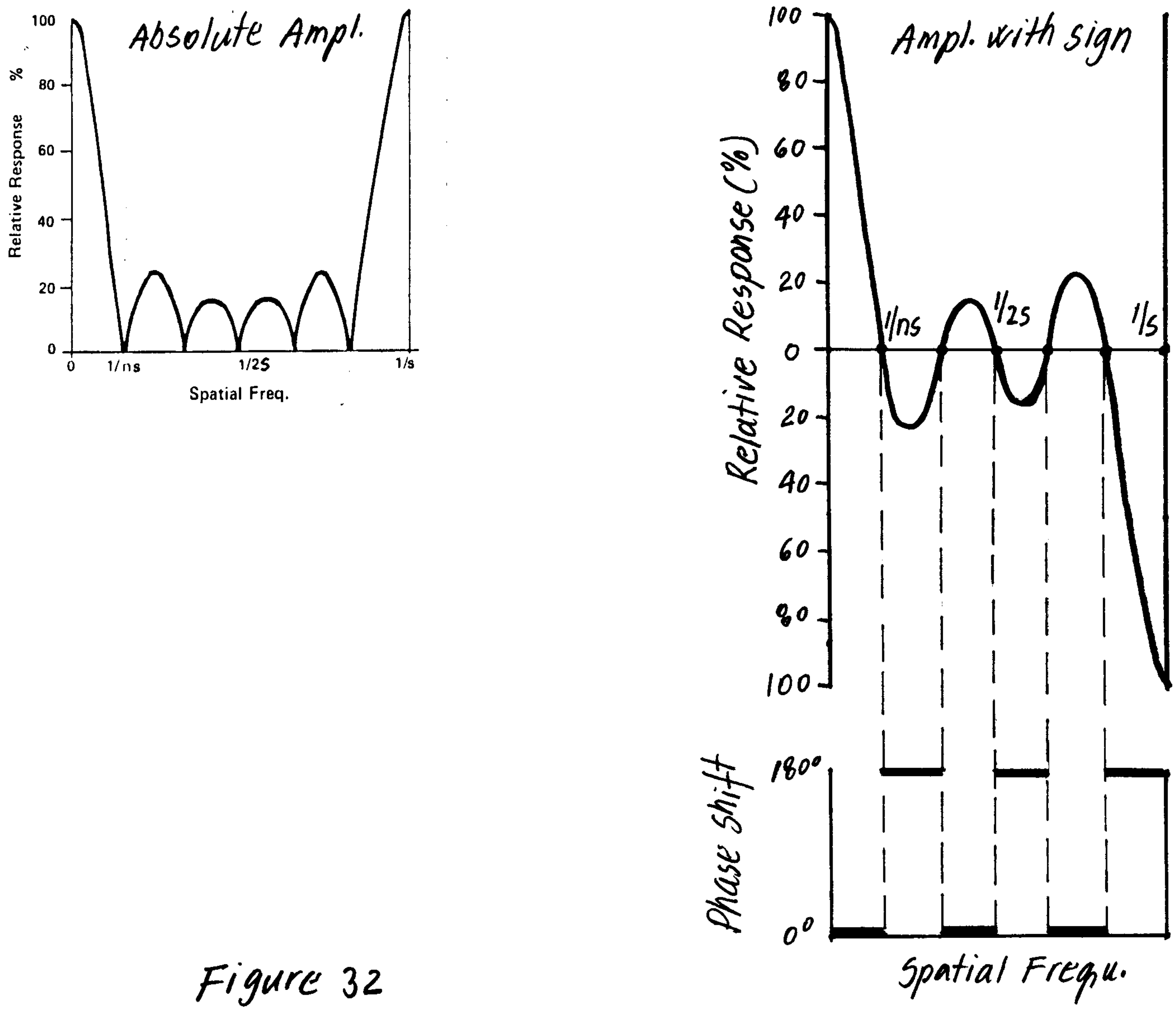

Figure 32

The Effect of Number of Elements on Attenuation and Reject Bandwidth.

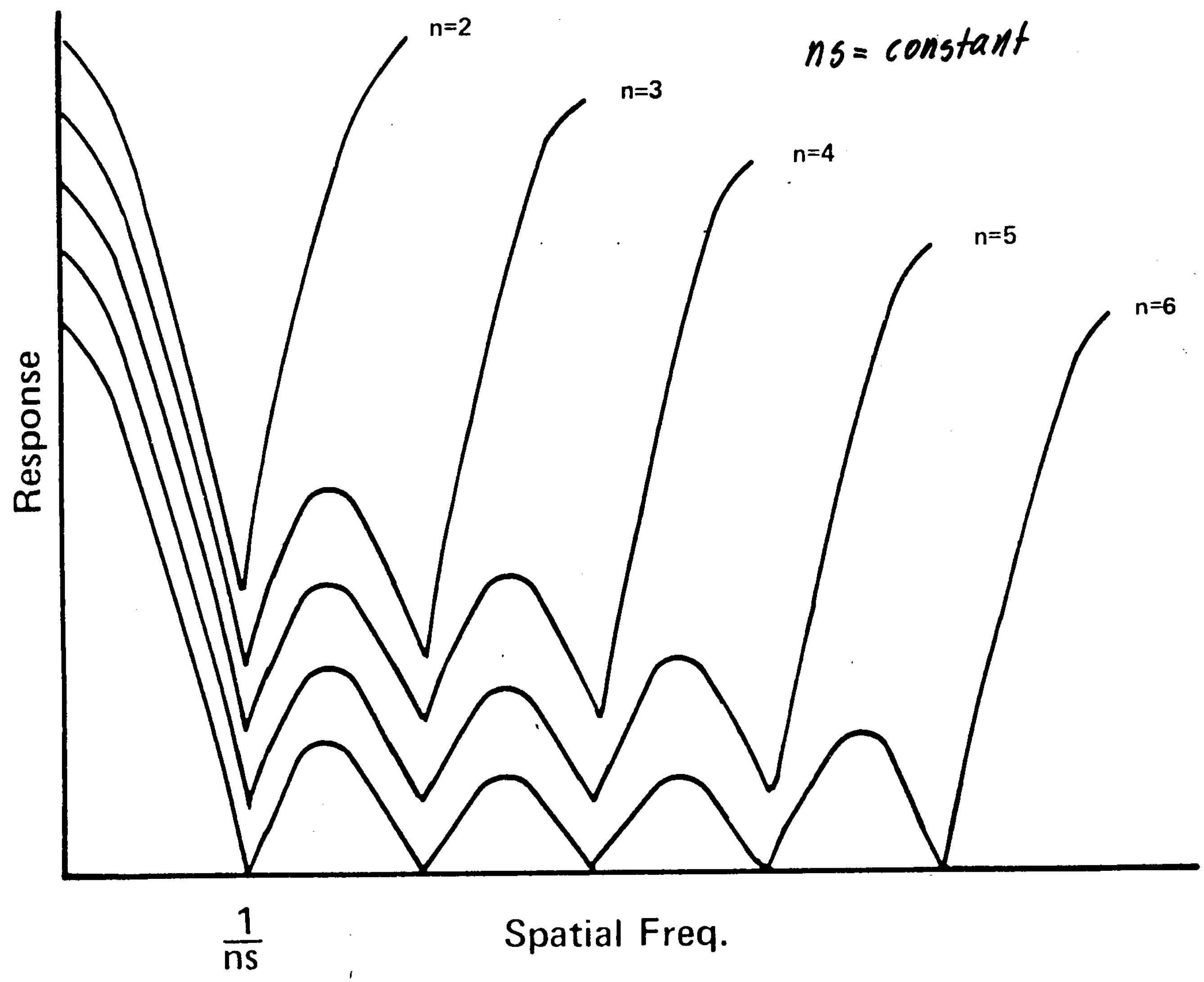

Attenuation:

Same for a particular lobe, regardless of "n"

Reject Bandwidth:

Increasing with "n".

Figure 33

e. The Effect of Number of Elements (n) on Attenuation

Figure 33 displays the superimposed response of arrays from two to six elements at a constant effective group length. The response curves are arbitrarily shifted to show the differences in reject bandwidths. The graph also shows that the attenuation of each successive lobe in the reject band is constant, regardless of the number of receivers. An envelope may be drawn through the peak of lobes (Figure 34) up to the spatial Nyquist.

f. The Fundamental Limitations of Linear Arrays

a) Figure 34 shows: There is no sharp discrimination between pass band and reject band, therefore, linear arrays are best suited to those conditions where signal and noise are well separated in the spatial frequency domain.

b) The average attenuation in the reject band is not more than 25 db for the most commonly occurring number of phones per group.

Example: From Figure 34 at 24 phones per group, the last lobe before Nyquist is the 11th lobe. Attenuation of 11th lobe = 33 db (maximum attenuation). The attenuation of 1st lobe = 13 db. Average = 23 db.

g. Arrays as Antialias Filters

The maximum acceptable group interval to avoid spatial aliasing is given by equation (15). In the selection of group interval the maximum frequency of data (signal and noise) and the minimum apparent velocity must be determined, hence the maximum spatial frequency.

From equation (15), the maximum acceptable group interval.

$$\Delta xmax = \frac{Vapp(min)}{fmax} \qquad (35)$$

Attenuation Envelope of Linear Arrays

The attenuation of the K^{th} lobe in the reject band up to Nyquist : $A = 20 \log \frac{2}{(2K+1)\pi}$

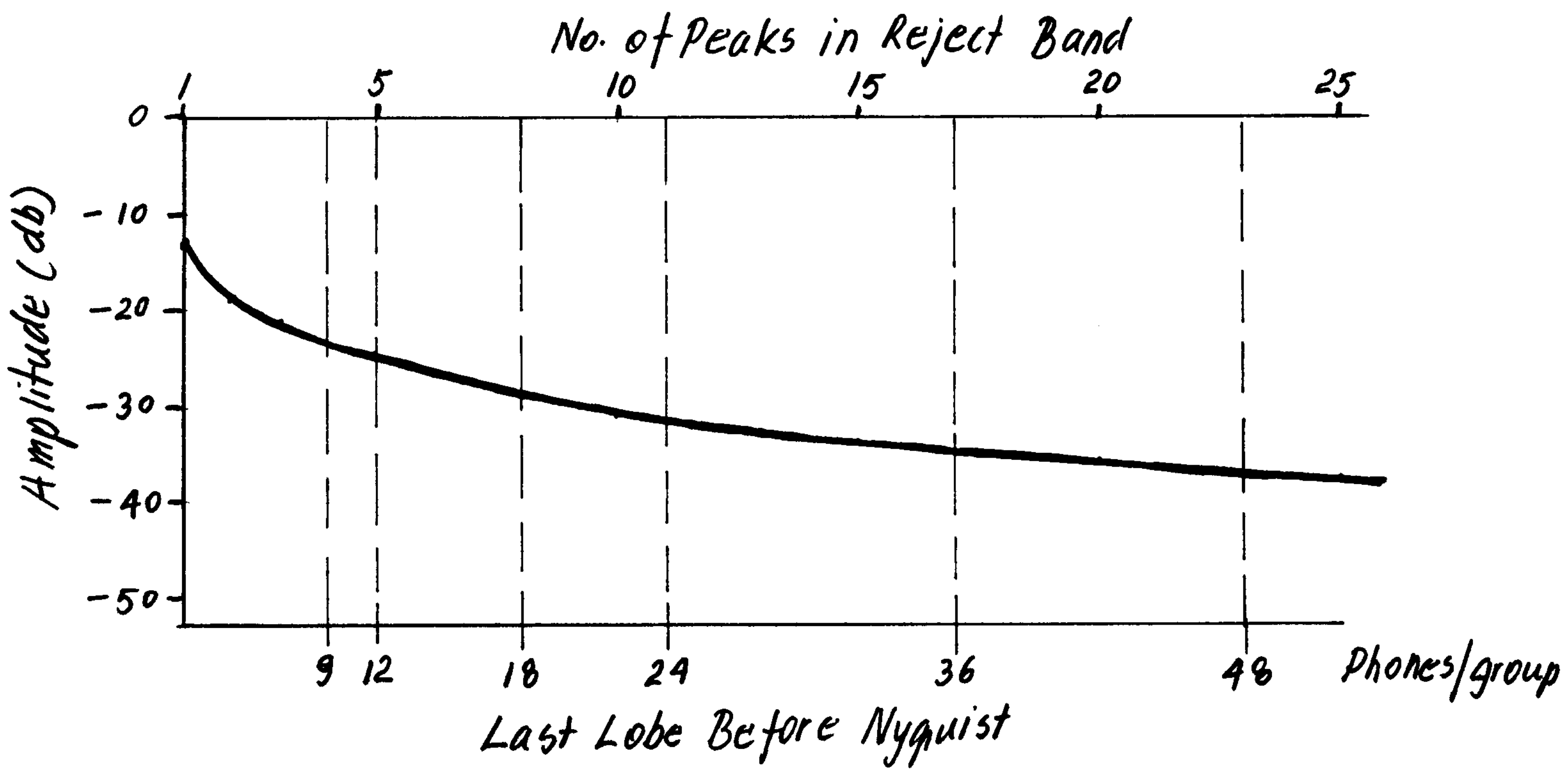

Figure 34

\

If there are no spatial frequencies in the data greater than

$$kmax = \frac{1}{2\Delta xmax}$$

then the seismic data will be properly sampled in space. The function of the subarray (in a group) is to insure that there are negligible contributions in the data for "k"-s higher than kmax. We proceed as follows:

a) The requirement for the subarray is to pass "k"-s lower than kmax and reject "k"-s higher than kmax. Therefore, we place kmax at the first notch of the array response. Assuming above nine phones/group equation (32) may be used to approximate the required subarray length.

At the first notch.

$$Ar = \frac{\sin\left(\frac{\emptyset}{2}\right)}{\frac{\emptyset}{2}} = 0$$

b) since $\frac{\emptyset}{2} = \pi \, \Delta l \, kmax$

$$\frac{\sin(\pi \, \Delta l \, kmax)}{\pi \, \Delta l \, kmax} = 0$$

$$\pi \, \Delta l \, kmax = \pi$$

$$\Delta l = \frac{1}{kmax}$$

Where "Δl" is the minimum group length of the subarray.

c) Since $kmax = \frac{1}{2\Delta xmax}$

$$\Delta lmin = 2\Delta xmax \qquad (36)$$

Therefore, to suppress wave numbers above kmax, the minimum subarray length is twice the group interval.

h. The Effect of Linear Arrays on the Reflected Signal

The upsurge in stratigraphic plays in recent years lead to the development of high resolution techniques requiring higher and higher frequencies. Therefore, the arrays cannot be designed strictly for the purpose of attenuating coherent noise waves, but the degrading effect of arrays on the seismic reflected signal must also be considered.

Geophone arrays are time-distance varying spatial filters and the CDP method is a series of cascaded filters, which may degrade the seismic signal. The magnitude of attenuation depends mainly on six parameters:

a) Reflection time.

b) Distance.

c) Frequency.

d) Velocity.

e) Dip.

f) Group length.

To a lesser extent, attenuation also depends on the number of phones/group and the degree of fold.

When designing arrays for the attenuation of coherent noise, the interpreter must insure that the reflected signal is not attenuated by the array more than 6 db, which is the acceptable limit of attentuation.

The First Notch Frequency

Equations (1) and (5) show, that the apparent spatial wavelength (λa) and the spatial frequency (ka) are the function of apparent velocity (Va) and temporal frequency:

$$\lambda a = \frac{Va}{f} \quad \text{and} \quad ka = \frac{f}{Va}$$

Furthermore, at the first notch of the array response

$$\lambda a = ns$$

Therefore, the first notch temporal frequency:

$$f_1 = \frac{Va}{ns} \tag{37}$$

Subsequent notches are at $2f_1$, $3f_1$, ... nf_1.

The criteria for array design is that the highest desirable reflected signal frequency must be in the pass band.

The apparent velocity (apparent average velocity) of a reflected signal as measured by a "group" of Δl length and offset of "x", assuming straight rays (Figure 35):

$$\bar{V}a = \frac{\Delta l}{\Delta t} = \bar{V}\left[1 + \left(\frac{\cos\alpha}{\frac{x}{\bar{V}To} \pm \sin\alpha}\right)^2\right]^{\frac{1}{2}} \tag{38}$$

Where:

Δt = differential NMO across the group
$\bar{V}$ = average velocity to reflector
α = true dip of reflector
To = two-way normal incidence reflection time.

The plus sign means shooting down dip and the minus updip.

For horizontal reflectors, equation (38) is simplified:

$$\bar{V}a = \bar{V}\left[1 + \left(\frac{\bar{V}To}{x}\right)^2\right]^{\frac{1}{2}} \tag{39}$$

The differential NMO across the group:

$$\Delta t = \frac{\Delta l}{\bar{V}a} \tag{40}$$

$$\Delta t = \frac{1}{\bar{V}} \frac{\Delta l}{\left[1 + \left(\frac{\cos\alpha}{\frac{x}{\bar{V}To} \pm \sin\alpha}\right)^2\right]^{\frac{1}{2}}} \tag{41}$$

Differential NMO (Δt) Across A Group ($\Delta \ell$)

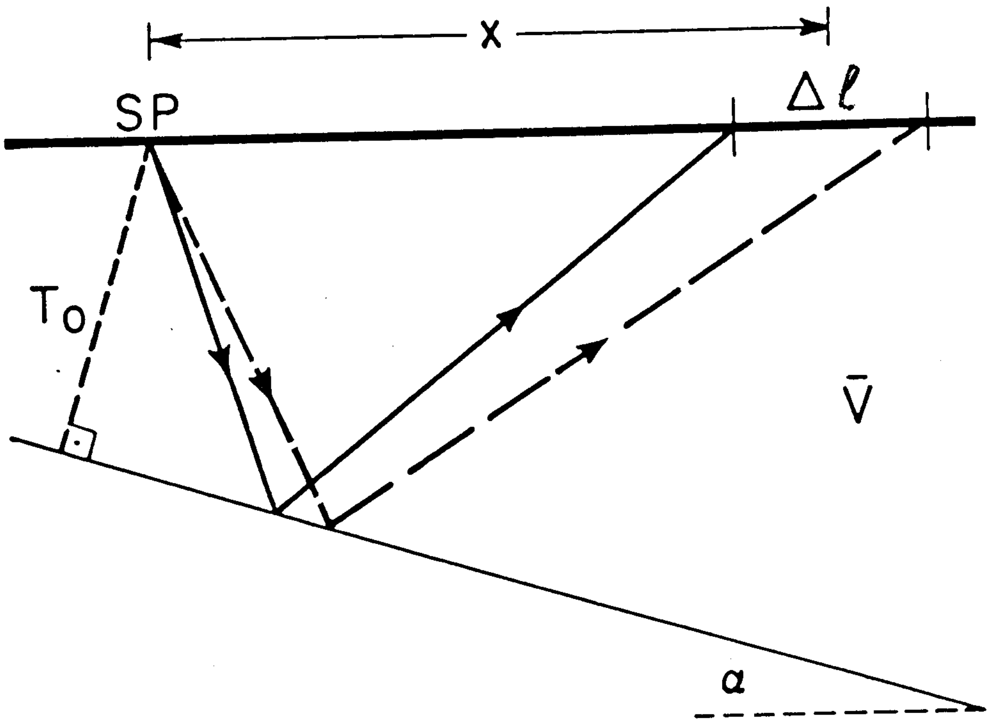

$$\Delta t = \frac{\Delta \ell}{\left[1 + \left(\frac{\cos \alpha}{\frac{X}{\bar{V} T_o} \pm \sin \alpha}\right)^2\right]^{1/2}} \frac{1}{\bar{V}}$$

$$\frac{\Delta \ell}{\Delta t} = \text{Apparent Velocity } (V_a)$$

Figure 35

or for flat layers:

$$\Delta t = \frac{1}{\bar{V}} \frac{\Delta l}{\left[1 + \left(\frac{\bar{V}To}{x}\right)^2\right]^{\frac{1}{2}}} \qquad (42)$$

By using equations (41), (25), and (26) the response of the array to the reflected signal may be computed.

The frequency corresponding to a -6 db attenuation (the acceptable limit) is estimated by:

$$f(-6\ db) = 0.605\ \frac{\bar{V}a}{ns} \qquad (43)$$

The dependence of signal frequency attenuation on the effective array length (ns) and offset is best analyzed by examining the variation of first notch frequency location as the function of these parameters.

<u>The Location of First Notch Frequency as the Function of Effective Group Length</u>

The first notch frequency graph on Figure 36 is normalized to an effective group length of 50 feet. In this manner the first notch frequency values may be expressed as percentages of the first notch frequency at ns = 50 feet (the 50-foot group length is an arbitrary choice).

$$f_1\ (\%) = 100\,\frac{50}{ns} \tag{44}$$

The graph shows, that the largest decrease in the first notch frequency occurs when the effective group length is increased from 50 feet to 300 feet. For longer array lengths the relative decrease is minimal.

The Location of First Notch Frequency as the Function of Offset

The graphs on Figure 37 are normalized to an offset of 1000 feet. Therefore, the first notch frequencies are expressed on the vertical axis as percentages of the first notch frequency at x = 1000 feet. For flat reflections:

$$\Delta f_1\ (\%) = 100 \left[\frac{1 + \left(\frac{2z}{xn}\right)^2}{1 + \left(\frac{2z}{1000}\right)^2}\right]^{\frac{1}{2}} \tag{45}$$

where z = depth to reflector.

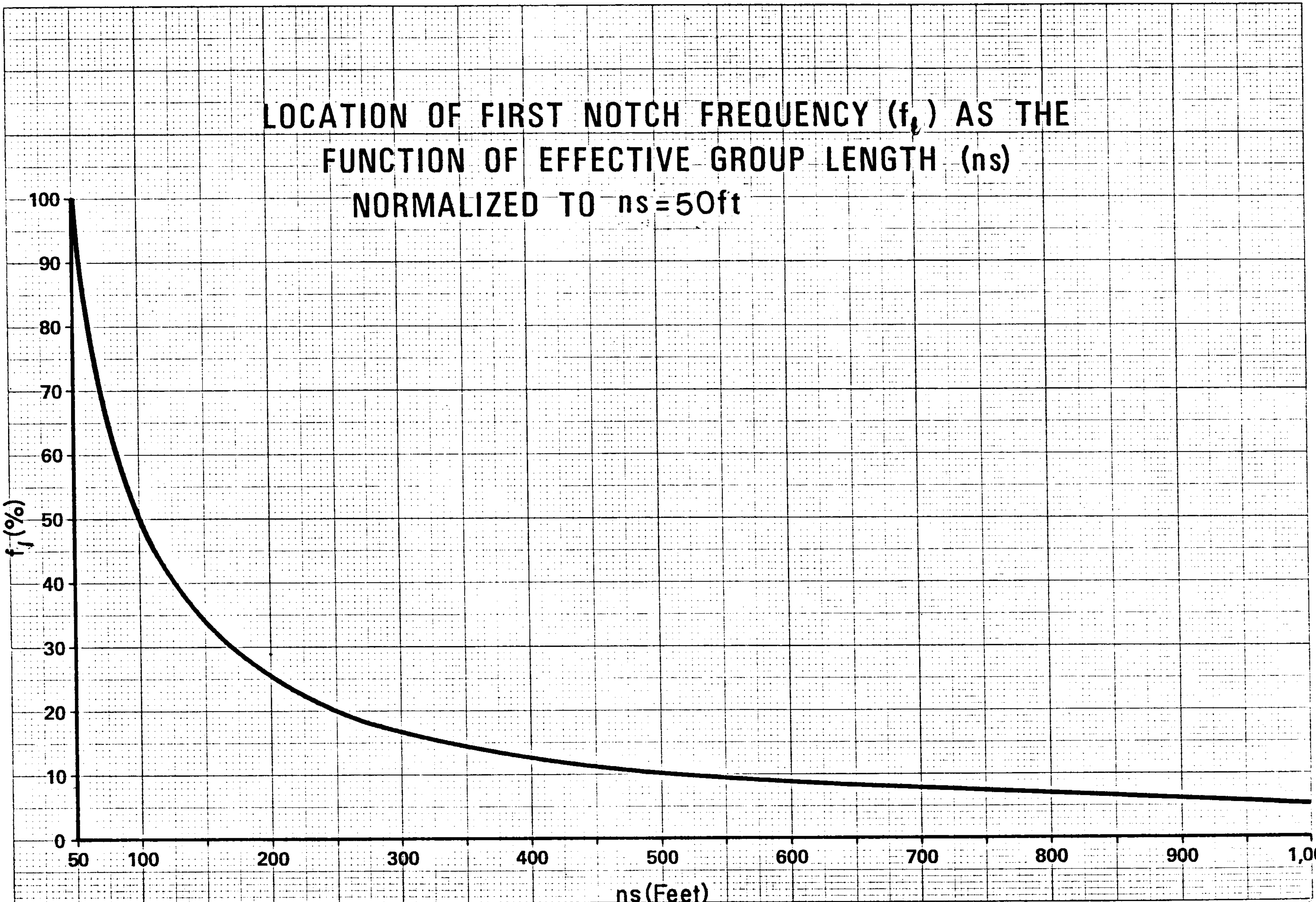
LOCATION OF FIRST NOTCH FREQUENCY (f_1) AS THE
FUNCTION OF EFFECTIVE GROUP LENGTH (ns)
NORMALIZED TO ns=50ft
f_1(%)
100
90
80
70
60
50
40
30
20
10
0
50
100
200
300
400
500
600
700
800
900
1,000
ns (Feet)

Figure 36

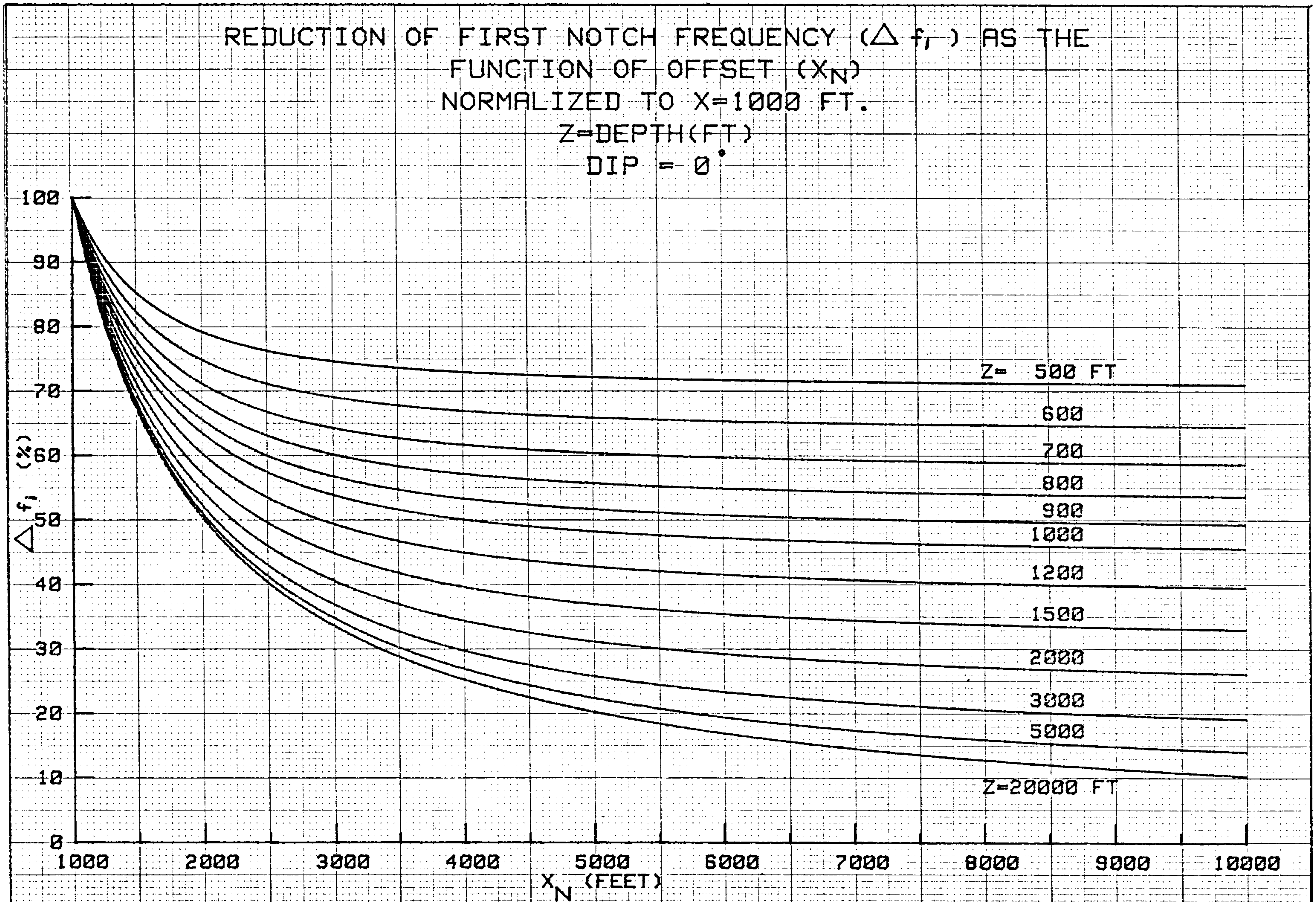

REDUCTION OF FIRST NOTCH FREQUENCY (△ f1) AS THE FUNCTION OF OFFSET (XN) NORMALIZED TO X=1000 FT.
Z=DEPTH(FT)
DIP = 0°
100
90
80
70
60
50
40
30
20
10
0
△ f1 (%)
Z= 500 FT
600
700
800
900
1000
1200
1500
2000
3000
5000
Z=20000 FT
1000
2000
3000
4000
5000
6000
7000
8000
9000
10000
XN (FEET)

Figure 37

Two important conclusions are evident from the graphs:

a) The greatest reduction in first notch frequency occurs when the offset is increased from 1000 feet to 4000 feet. For longer offsets the additional reduction is minimal.

b) The reduction in first notch frequency depends on the depth: the greater the depth, the larger the reduction. Furthermore, as the depth is decreased, the curves flatten out. Therefore, at shallow depths the first notch frequency is very sensitive to depth changes, but insensitive to offset variations. At depths greater than 5000 feet, the depth change is not a significant factor, but the offset is critical.

The combined effect of array length, offset and depth is computed by multiplying the percentages on Figures 36 and 37.

The Effect of Dip on First Notch Frequency

1) The relative first notch frequency reduction due to effective group length is independent of dip, as shown by equation (44).

2) The first notch frequency--according to equations (37) and (38)--is always less for shooting downdip. Therefore, only the downdip first notch frequency variations with dip are displayed on Figures 38-40. The following conclusions are evident from the graphs:

   a) At long offsets (over 6000 feet) the first notch frequency is not sensitive to dip.

   b) For shorter ranges, the reduction dramatically increases with dip. The curves flatten out at steep dips, indicating the insensitivity of first notch frequency variations with offset.

The Maximum Acceptable Group Length

The maximum acceptable attenuation of the reflected signal due to the frequency filtering effect of an array is usually set at 6 db. If "Ar" is set at

6 db in equation (25), Ø/2 may be computed and with the help of equations (26) and (41) the maximum acceptable group length (Δlmax) can be computed for any combinations of "$\bar{V}$", "To", "x", "α, and "n". Seven nomographs are enclosed (Figures 41-47) to estimate "Δlmax" (from 0°-40° dip). The graphs were computed for n=2 phones/group and frequency f=1 Hz. The "Δlmax" for any frequency is computed by dividing the "Δlmax" for 1 Hz by the desired frequency "Δl"max from n=2 may be converted to any "n" by multiplying the value of "Δlmax" for n=2 by the "C" value (on Figure 48) correspond to the desired "n".

Example:

To = 1.000 sec
xmax (longest offset) = 10 000 ft
$\bar{V}$ = 24 000 ft/sec
α = 0°
n = 6
f = 60 Hz

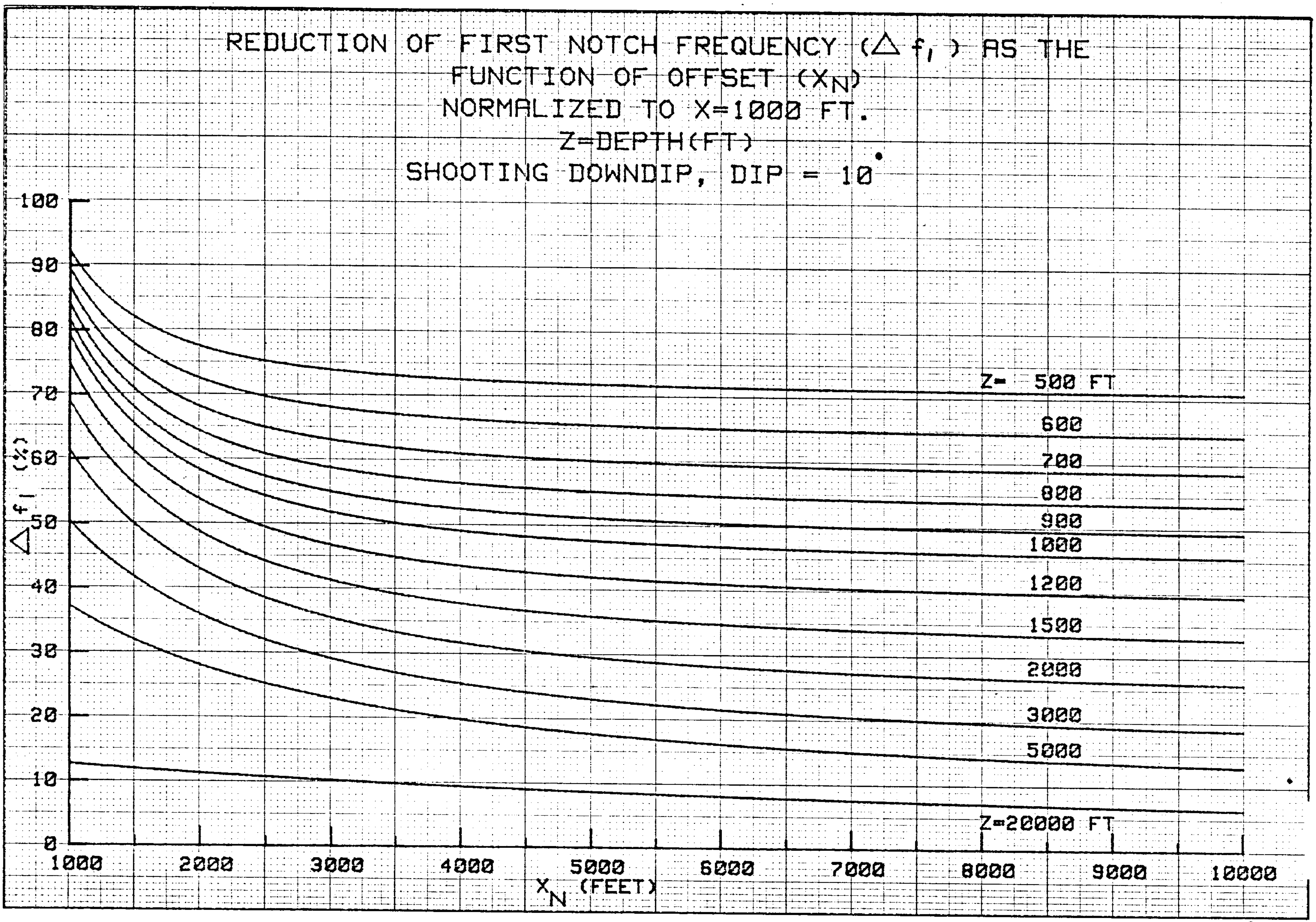
REDUCTION OF FIRST NOTCH FREQUENCY (Δf_1) AS THE
FUNCTION OF OFFSET (X_N)
NORMALIZED TO X=1000 FT.
Z=DEPTH(FT)
SHOOTING DOWNDIP, DIP = 10°
Z= 500 FT
600
700
800
900
1000
1200
1500
2000
3000
5000
Z=20000 FT
Δf_1 (%)
0
10
20
30
40
50
60
70
80
90
100
1000
2000
3000
4000
5000
6000
7000
8000
9000
10000
X_N (FEET)

(95)

Figure 38

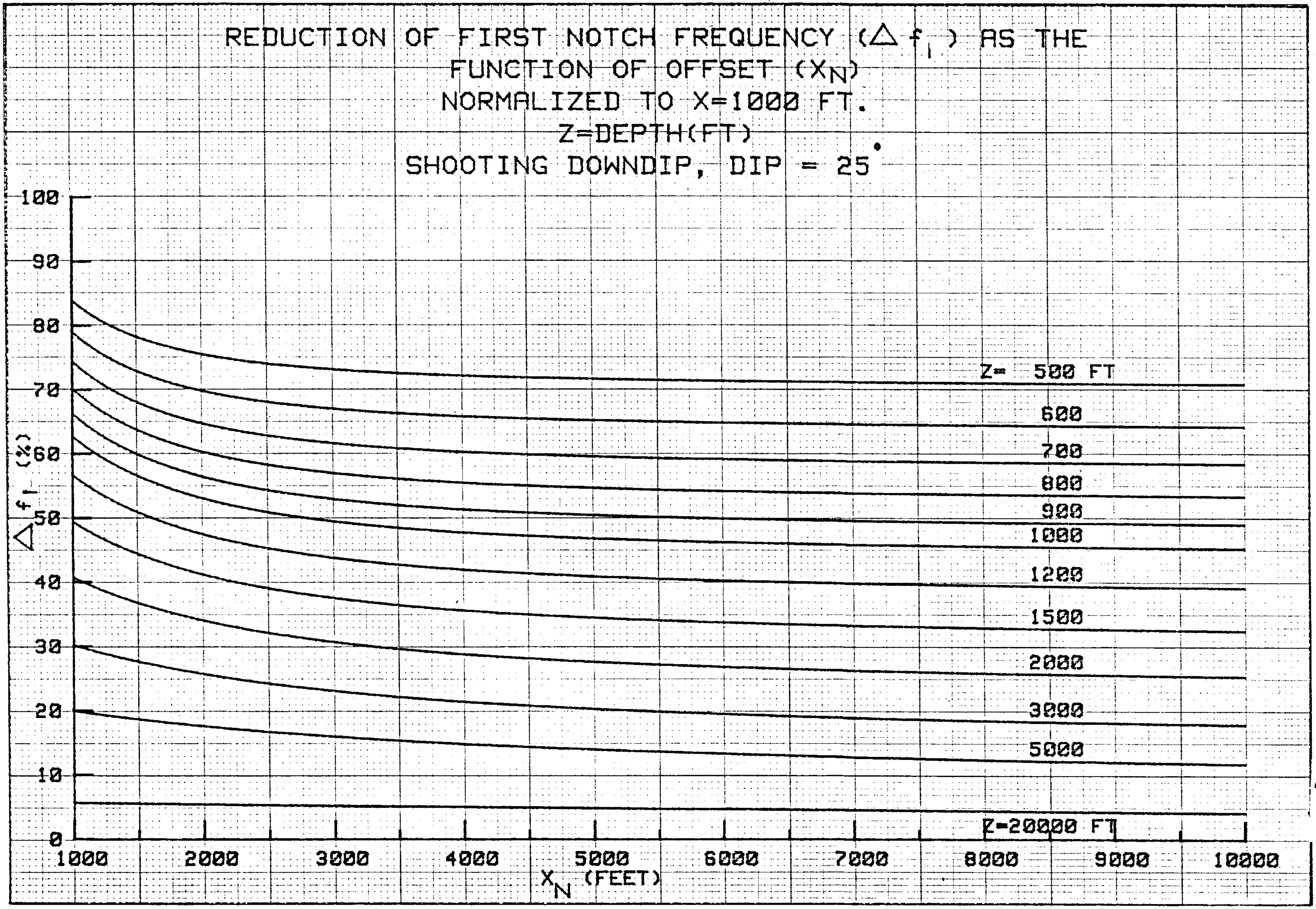
REDUCTION OF FIRST NOTCH FREQUENCY (Δ f1) AS THE
FUNCTION OF OFFSET (XN)
NORMALIZED TO X=1000 FT.
Z=DEPTH(FT)
SHOOTING DOWNDIP, DIP = 25°
Δf1 (%)
0
10
20
30
40
50
60
70
80
90
100
Z= 500 FT
600
700
800
900
1000
1200
1500
2000
3000
5000
Z=20000 FT
1000
2000
3000
4000
5000
6000
7000
8000
9000
10000
XN (FEET)

Figure 39

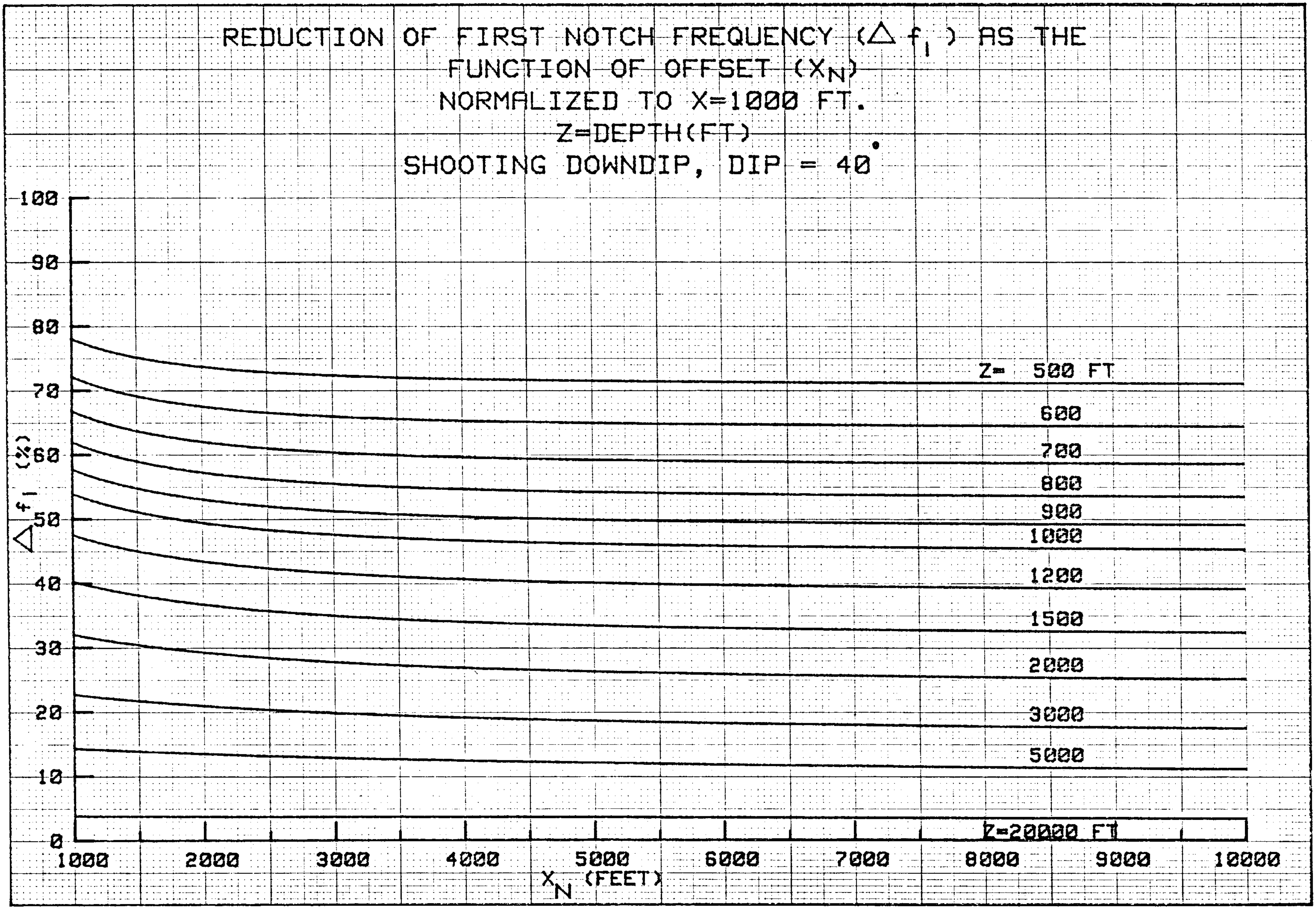
REDUCTION OF FIRST NOTCH FREQUENCY (Δ f1) AS THE FUNCTION OF OFFSET (XN)
NORMALIZED TO X=1000 FT.
Z=DEPTH(FT)
SHOOTING DOWNDIP, DIP = 40°
Δ f1 (%)
100
90
80
70
60
50
40
30
20
10
0
1000
2000
3000
4000
5000
6000
7000
8000
9000
10000
XN (FEET)
Z= 500 FT
600
700
800
900
1000
1200
1500
2000
3000
5000
Z=20000 FT

(91)

Figure 40

Starting on the lower graph of Figure 41, the intersection of the horizontal line through To = 1.0 sec and the slant line x = 10 000 ft defines a point. The intersection of the vertical line through this point and the $\bar{V}$ = 24 000 ft/sec curve on the upper graph projected horizontally to the maximum acceptable group length axis determines the value of "Δlmax" for n = 2 and f = 1 hz:
Δlmax = 2.1 x 10^4ft. For f = 60 Hz, Δlmax = 2.1 x 10^4/60 = 350 ft. For n = 6, from Figure 48 C = 1.52. Hence the final Δlmax = 532 ft.

The graphs may also be used in a reverse sense. Example: to attenuate some coherent noise wave a graph length of 532 feet is required. Determine the maximum offset xmax by starting with Δl = 532 ft, the xmax = 10 000 ft.

A number of conclusions may be drawn from Figures 41-48.

a) The "C" curve on Figure 48 shows that the improvement in "Δlmax" (hence the output of array) is very small above ten phones/group.

MAXIMUM ACCEPTABLE GROUP LENGTH

FOR TWO PHONES/GROUP AND f = 1hz SIGNAL

DIP = 0°

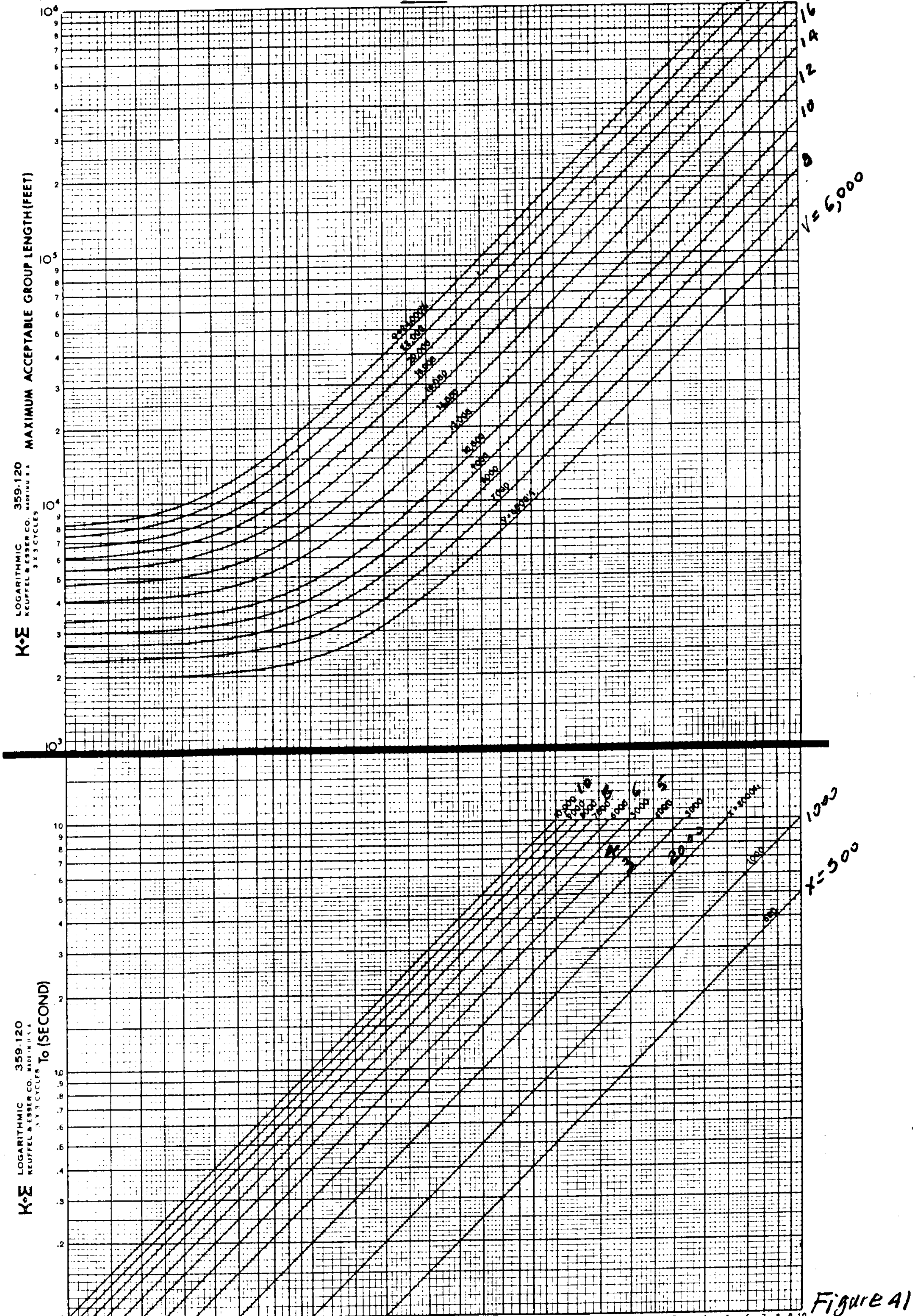

Figure 41

MAXIMUM ACCEPTABLE GROUP LENGTH

SHOOTING DOWN DIP

FOR TWO PHONES/GROUP AND f = 1hz SIGNAL

DIP = 5°

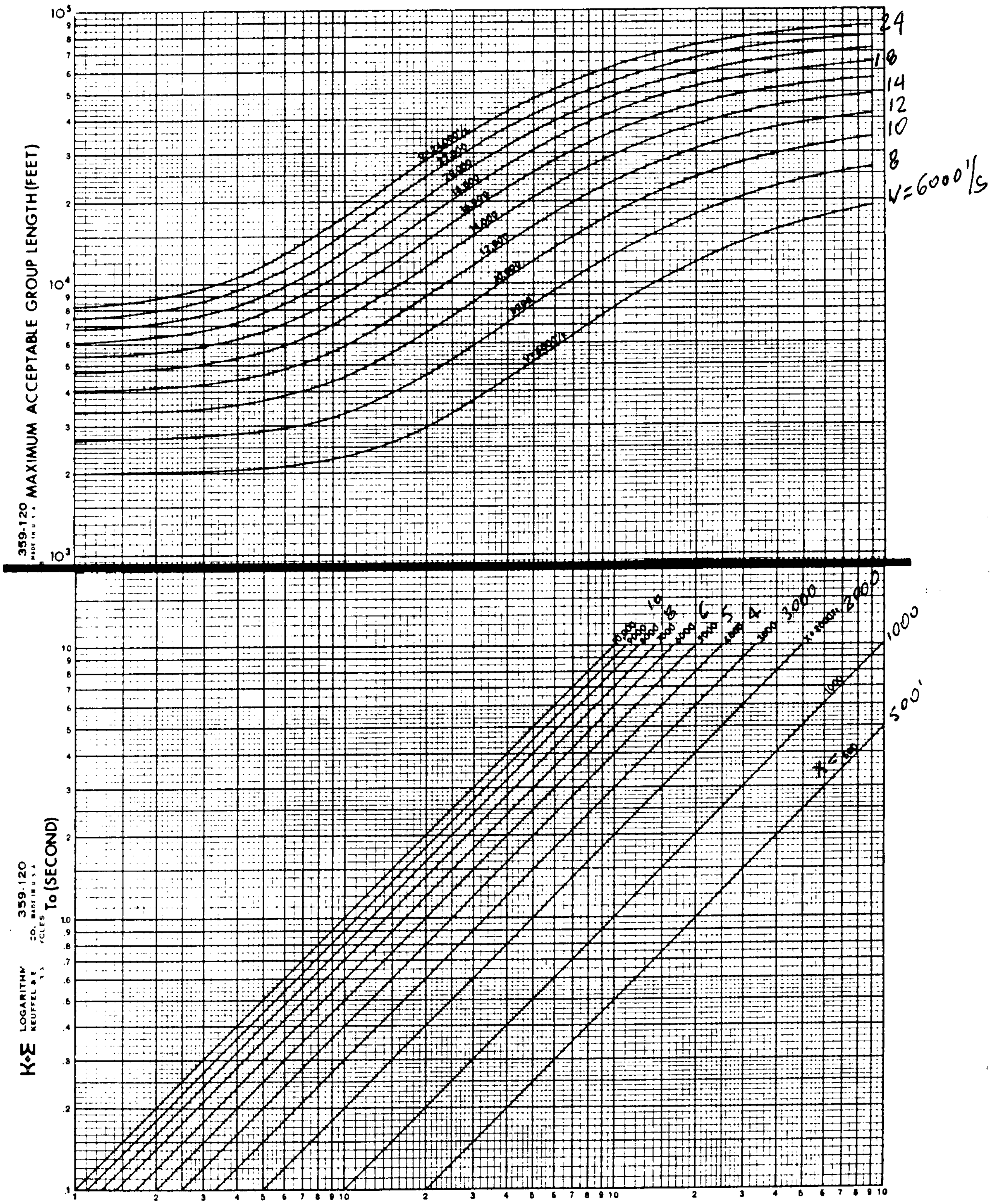

Figure 42

MAXIMUM ACCEPTABLE GROUP LENGTH

SHOOTING DOWN DIP

FOR TWO PHONES/GROUP AND f=1hz SIGNAL

DIP=10°

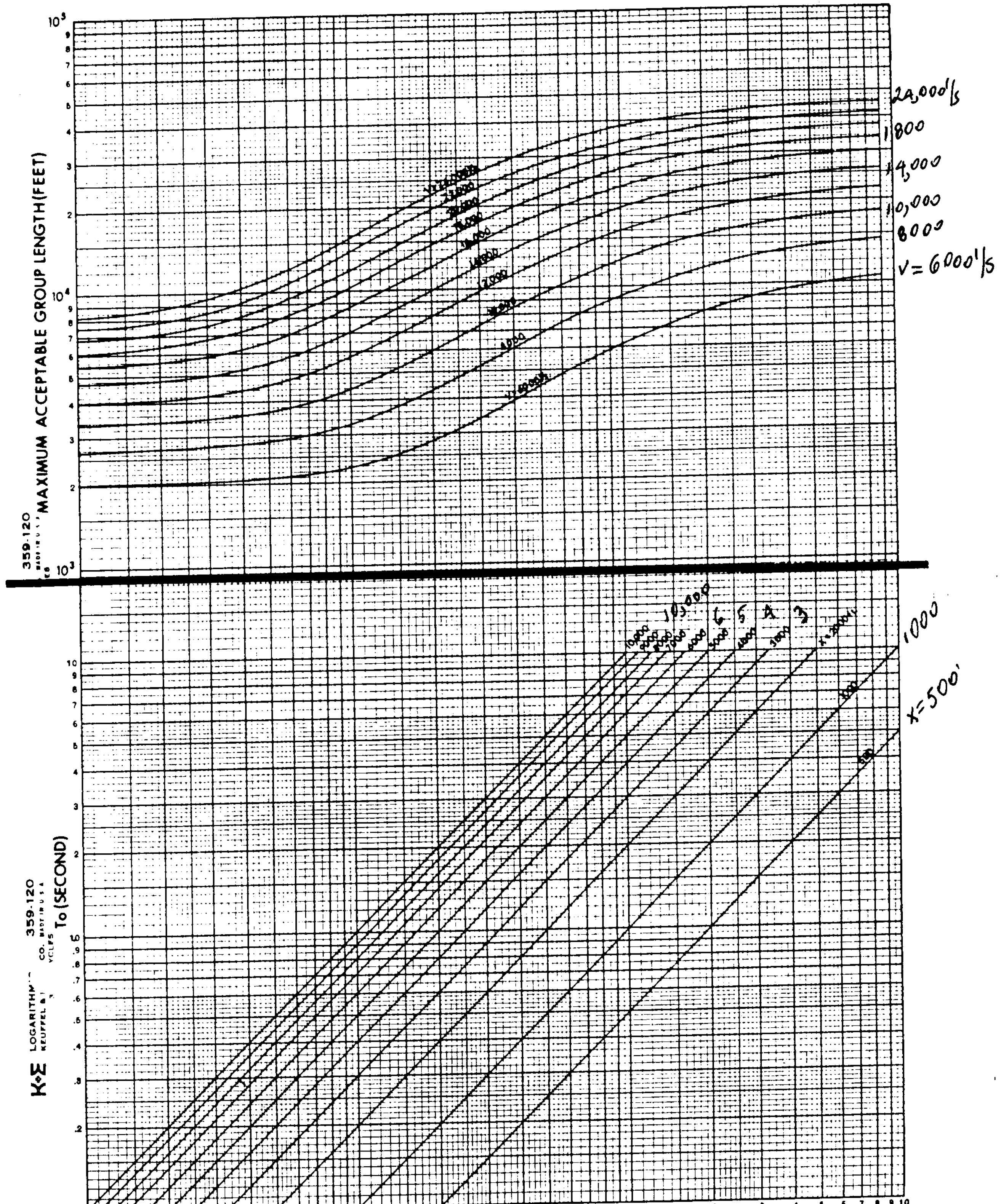

Figure 43

MAXIMUM ACCEPTABLE GROUP LENGTH
SHOOTING DOWN DIP
FOR TWO PHONES/GROUP AND f=1hz SIGNAL
DIP=15°

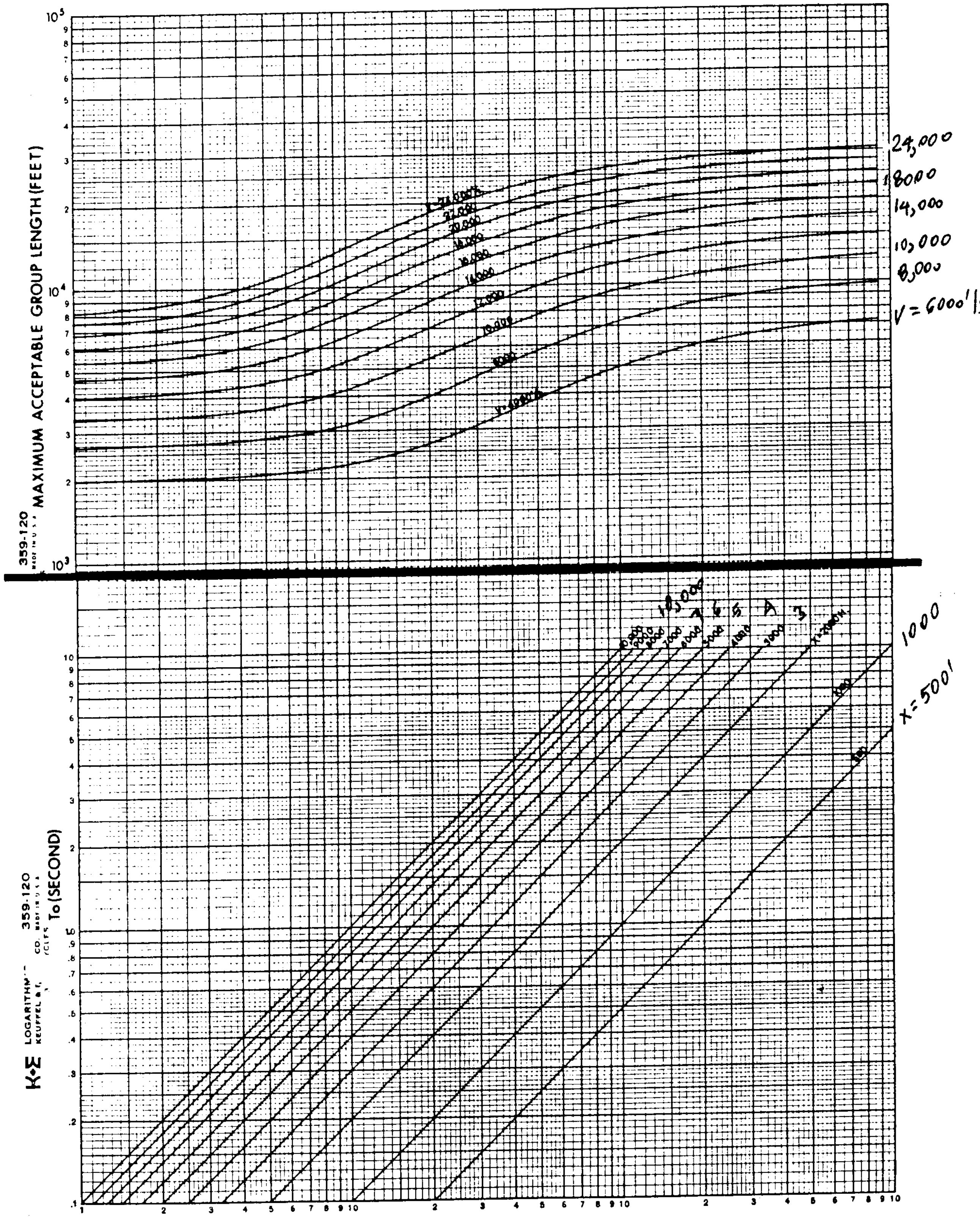

Figure 44

MAXIMUM ACCEPTABLE GROUP LENGTH

SHOOTING DOWN DIP

FOR TWO PHONES/GROUP AND f=1hz SIGNAL

DIP = 20°

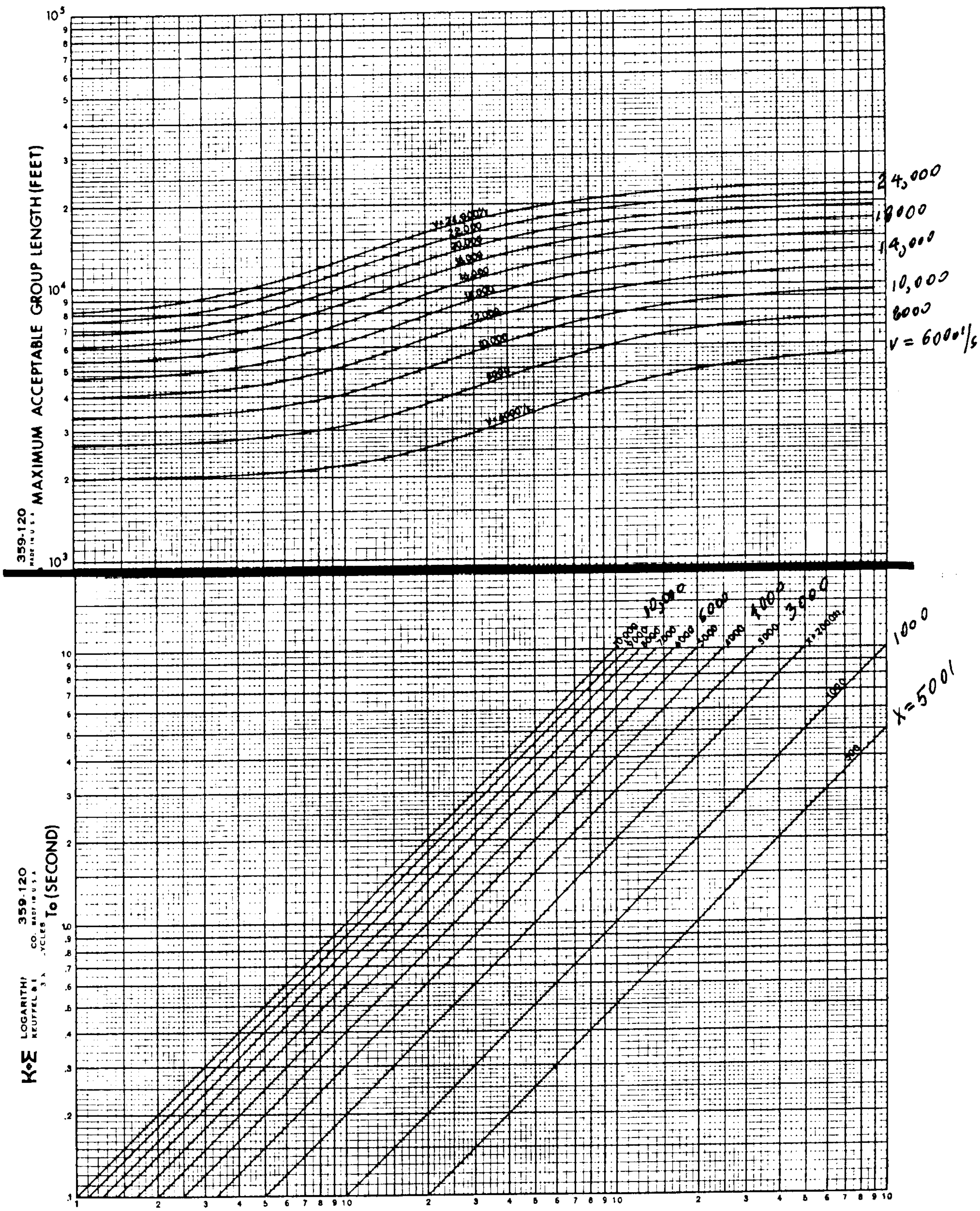

Figure 45

MAXIMUM ACCEPTABLE GROUP LENGTH

SHOOTING DOWN DIP

FOR TWO PHONES/GROUP AND f=1hz SIGNAL

DIP=30°

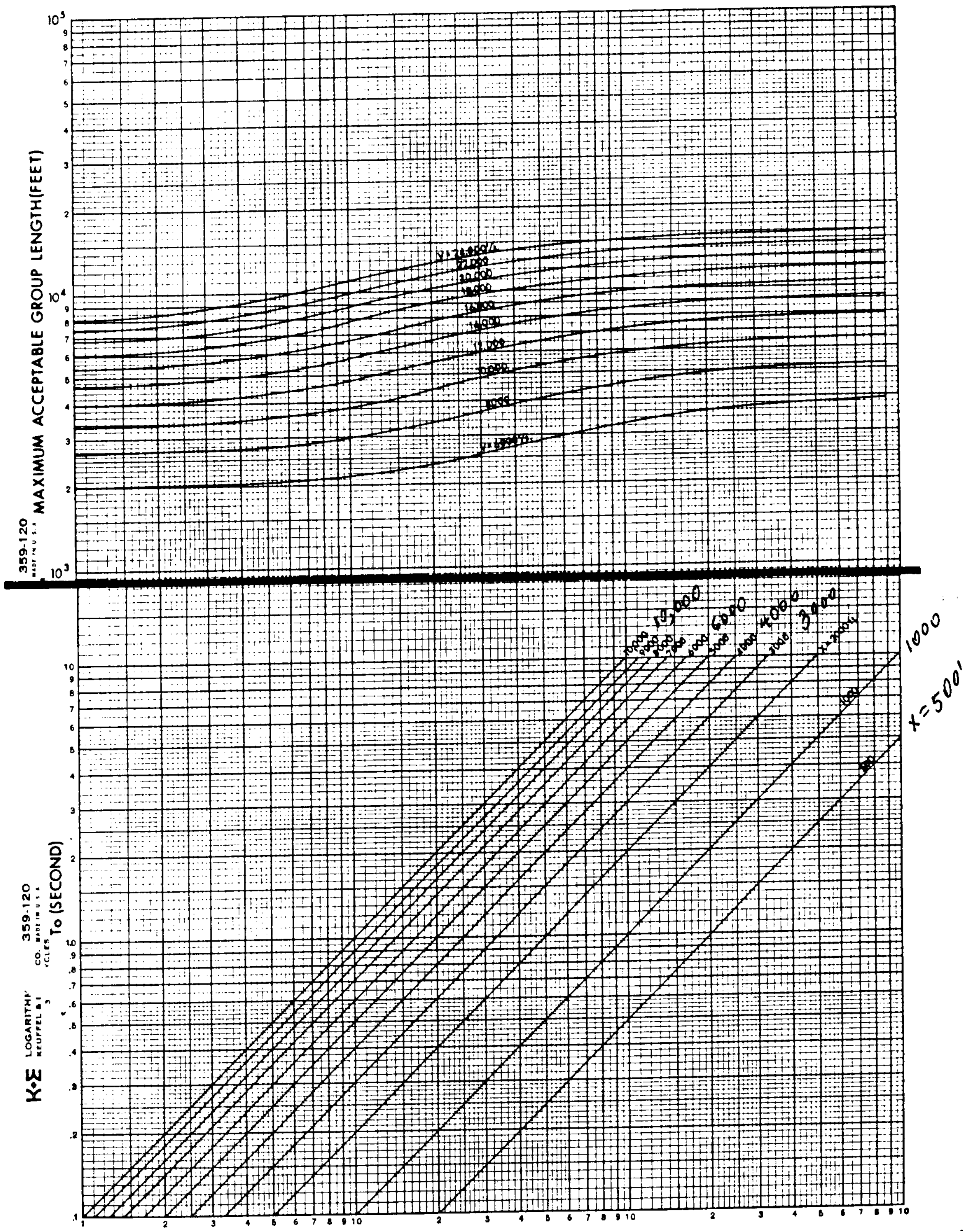

Figure 46

MAXIMUM ACCEPTABLE GROUP LENGTH
SHOOTING DOWN DIP
FOR TWO PHONES/GROUP AND f=1hz SIGNAL

DIP = 40°

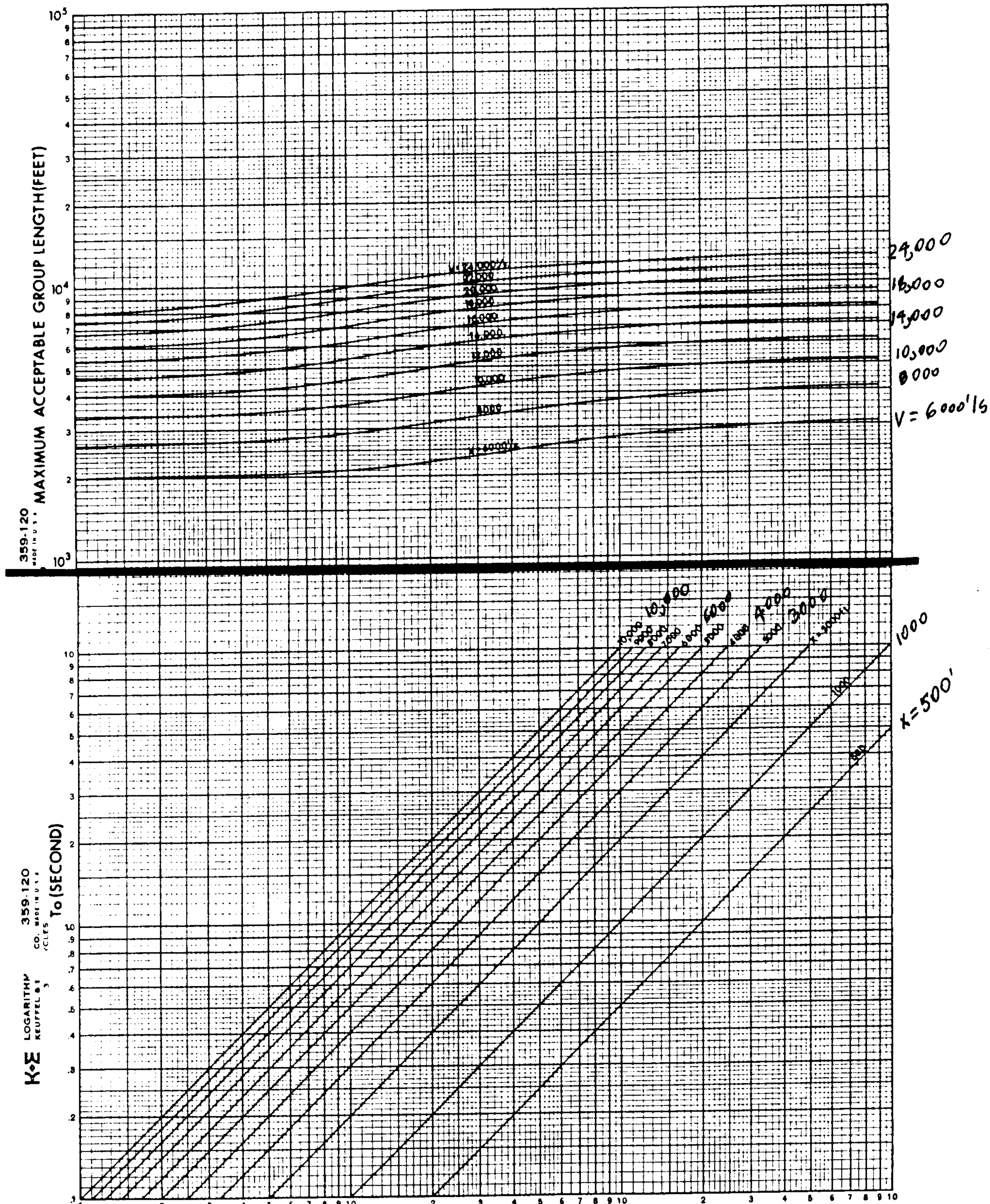

Figure 47

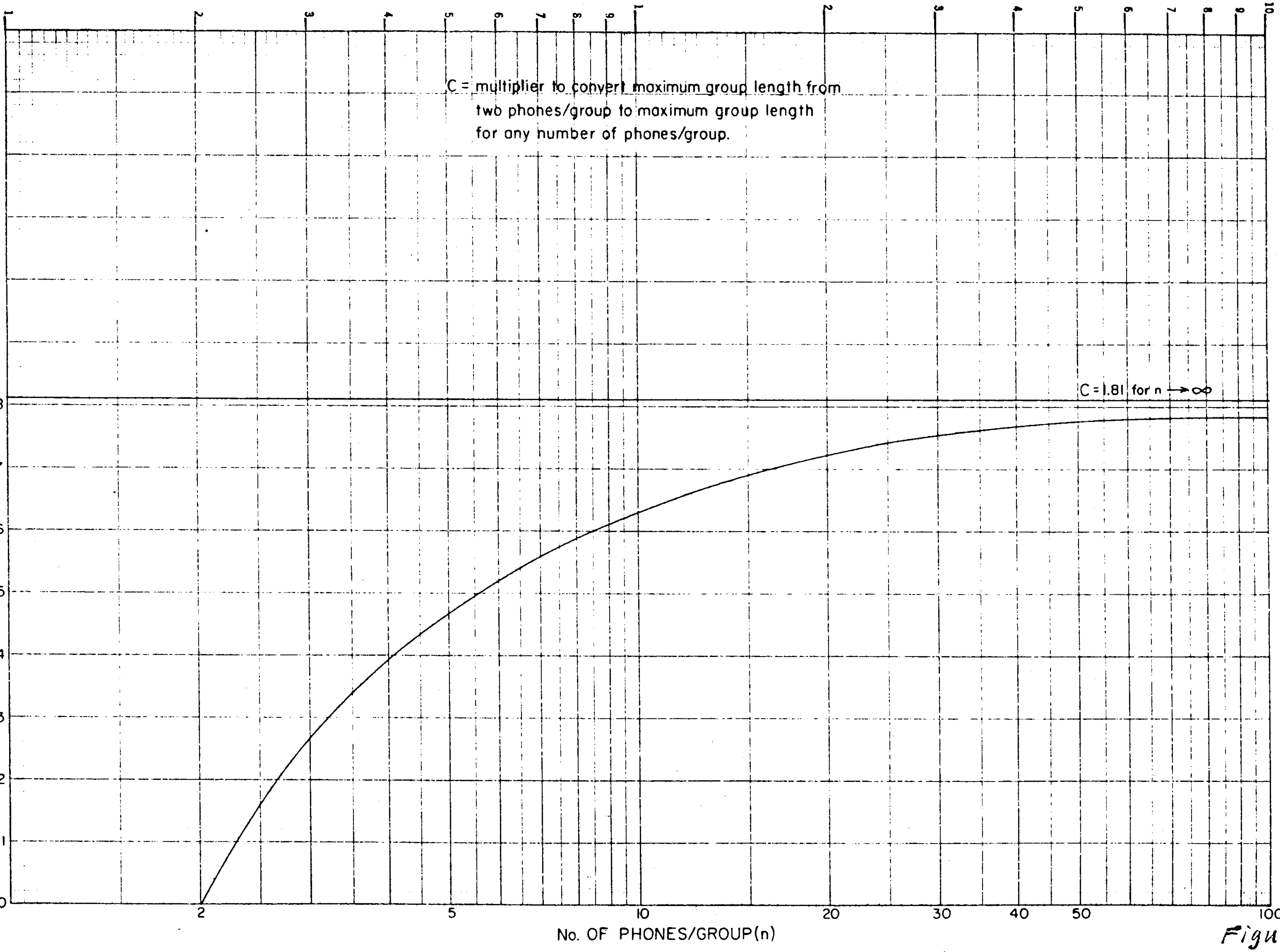
C = multiplier to convert maximum group length from two phones/group to maximum group length for any number of phones/group.
C = 1.81 for n → ∞
No. OF PHONES/GROUP(n)
2
5
10
20
30
40
50
100

Figure 48

b) For a constant velocity, at shallow depths and large offsets "Δmax" is independent of dip.

c) "Δlmax" is inversely proportional to the frequency, therefore, arrays are very strong high frequency filters.

d) For steep dips, "Δmax" is not sensitive to variations in depth and offset.

e) The steepest part of the curves is the mid range of depths and distances, indicating that "Δlmax" is most sensitive to changes in depth and offset in that range.

Attenuation of the CDP Trace

The maximum acceptable group length is usually computed for the longest offset trace in the CDP. However, each trace in the CDP is attenuated by a different amount. The longest offset attenuation is the worst and it is usually smaller for a CDP trace. Therefore, in array design the attenuation of the CDP trace should also be examined.

The 600% Symmetric CDP Trace

Spread: 48 trace split

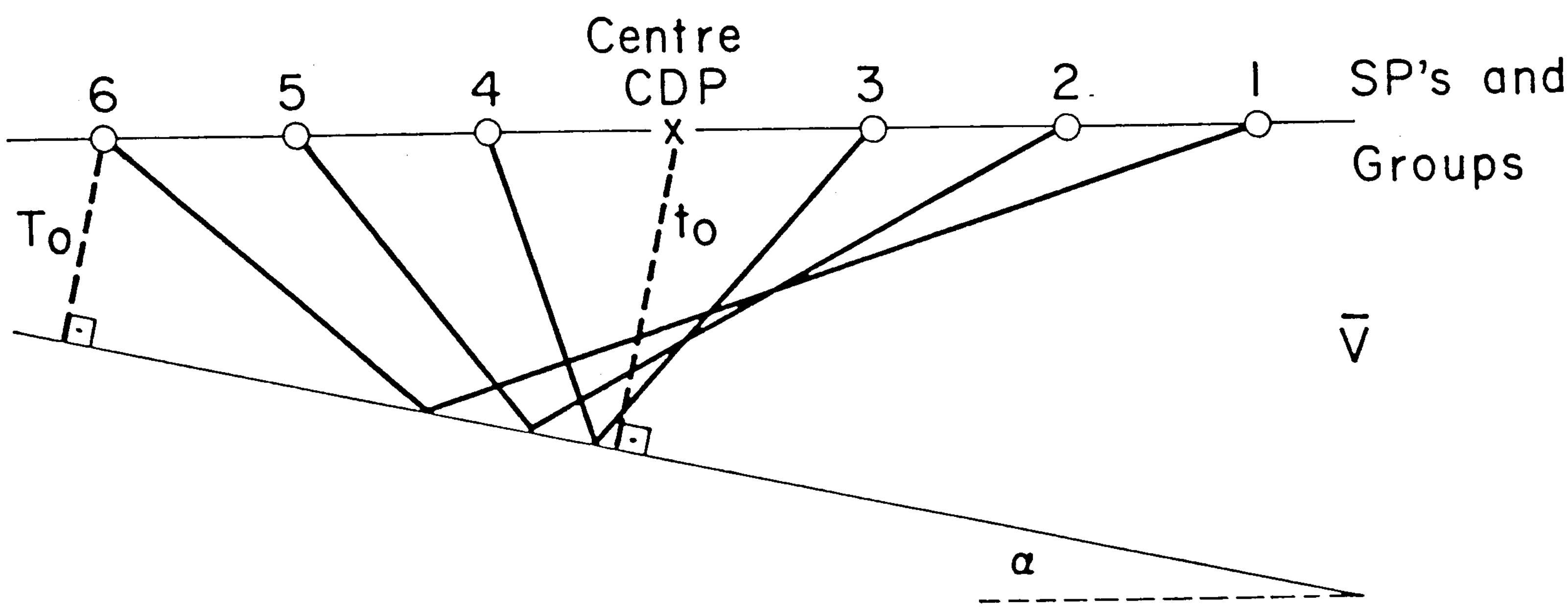

T_o = Normal Incidence Reflection Time At SP's.

t_o = Normal Incidence Reflection Time At Centre Of CDP.

Ranges: 110 Ft. Group Interval: 880 Ft., 1760 Ft., 2640 Ft.

220 Ft. " " : 1760 Ft., 3520 Ft., 5280 Ft.

440 Ft. " " : 3360 Ft., 6720 Ft., 10,080 Ft.

Figure 49

Figure 49 shows a 600 percent CDP configuration. For ease of computation the symmetric configuration is used.

In the CDP trace, "N" sinusoidal signals are summed with various amplitudes and phase shifts.

The relative amplitude of "N" traces in a symmetric CDP configuration is determined from the equation:

$$Ar = \frac{1}{n}\left[\left(\sum_{k=1}^{N} \left|Ak\right| \cos \frac{\emptyset k}{2}\right)^2 + \left(\sum_{k=1}^{N} \left|Ak\right| \sin \frac{\emptyset k}{2}\right)^2\right]^{\frac{1}{2}} \quad (46)$$

where "Øk/2" and "Ak" are the phase shift and relative amplitude of the individual traces as defined by equations (25) and (26).

Figures 50-52 are summary graphs to help observe conclusions.

<u>Conclusions</u>

a) The attenuation of the CDP trace is considerably less than that of the longest offset downdip trace. Therefore, if the maximum acceptable group length is computed only for the longest offset downdip case, the array will be shorter than required by the CDP stack. Shorter arrays mean more shots/mile, higher expense and less attenuation of coherent noise waves.

b) The top left plot on Figure 50 shows strong attenuation at low velocities, hence long arrays are strong low velocity filters.

c) For higher frequencies the attenuation is more severe.

d) If dip is introduced, the curves flatten out, hence the attenuation is not sensitive to changes in depth (To).

e) At steep dips and high frequencies the attenuation is extremely severe even at high velocities. Therefore, dip is a very strong high frequency filter. The graphs on Figure 51 confirm this observation even at short arrays.

ATTENUATION OF A 600% CDP TRACE

$\Delta X = 420$ Ft. $X_{max.} = 10080$ Ft. $n = 6$

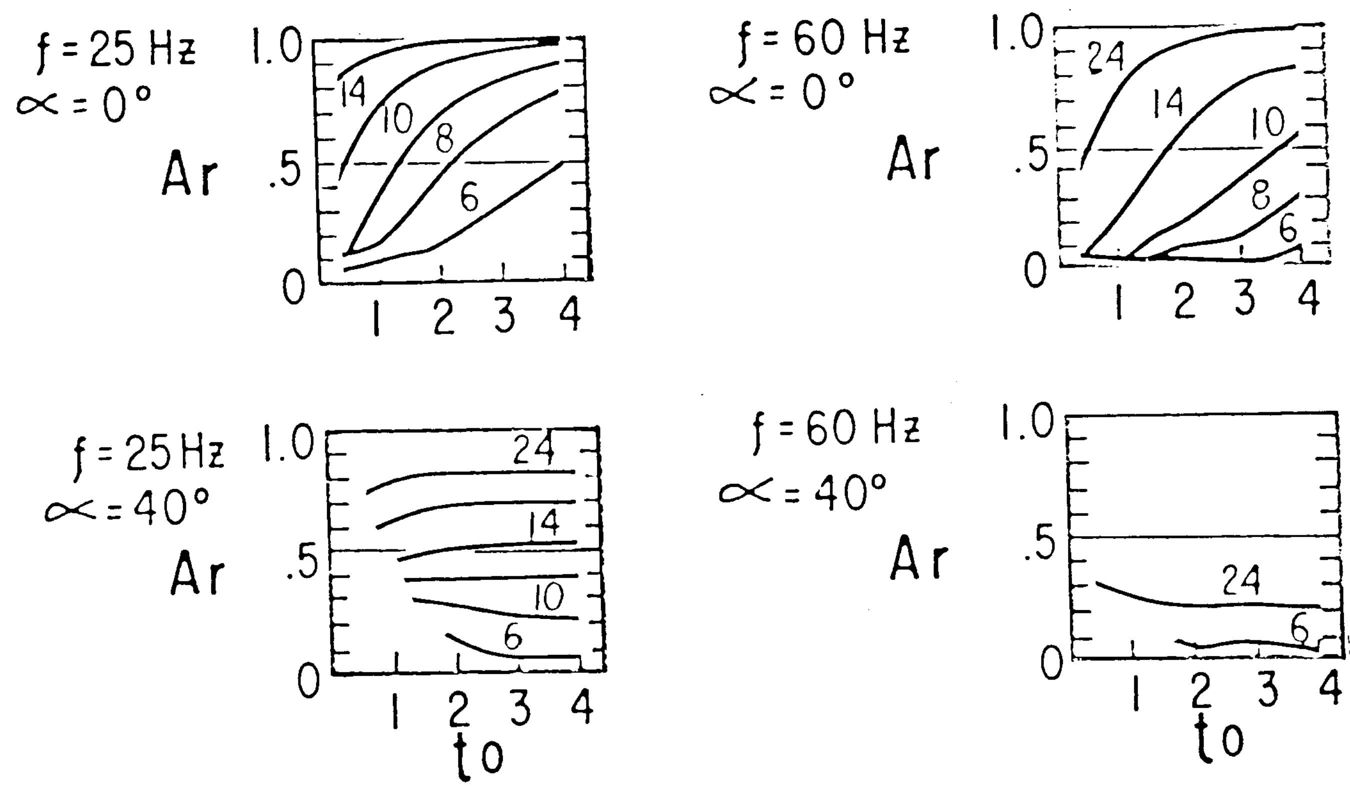

Figure 50

ATTENUATION OF A 600% CDP TRACE

$\Delta X = 110$ Ft. $X_{max.} = 2640$ Ft. $n = 6$

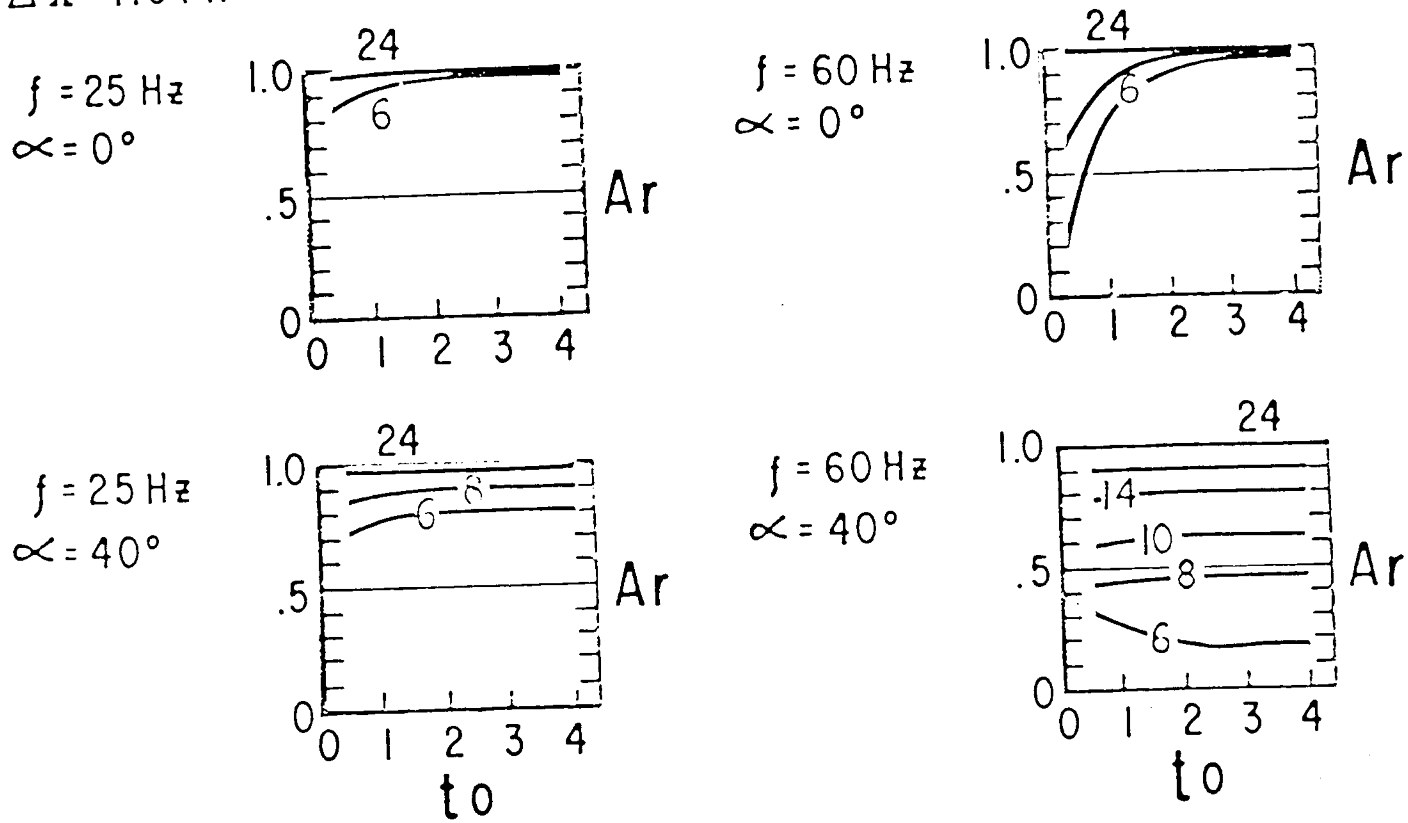

Figure 51

ATTENUATION OF A CDP TRACE

600% & 2400%; n=6 & 24

ΔX = 420 Ft. X_{max} = 10,080 Ft. f = 60 Hz α = 0°

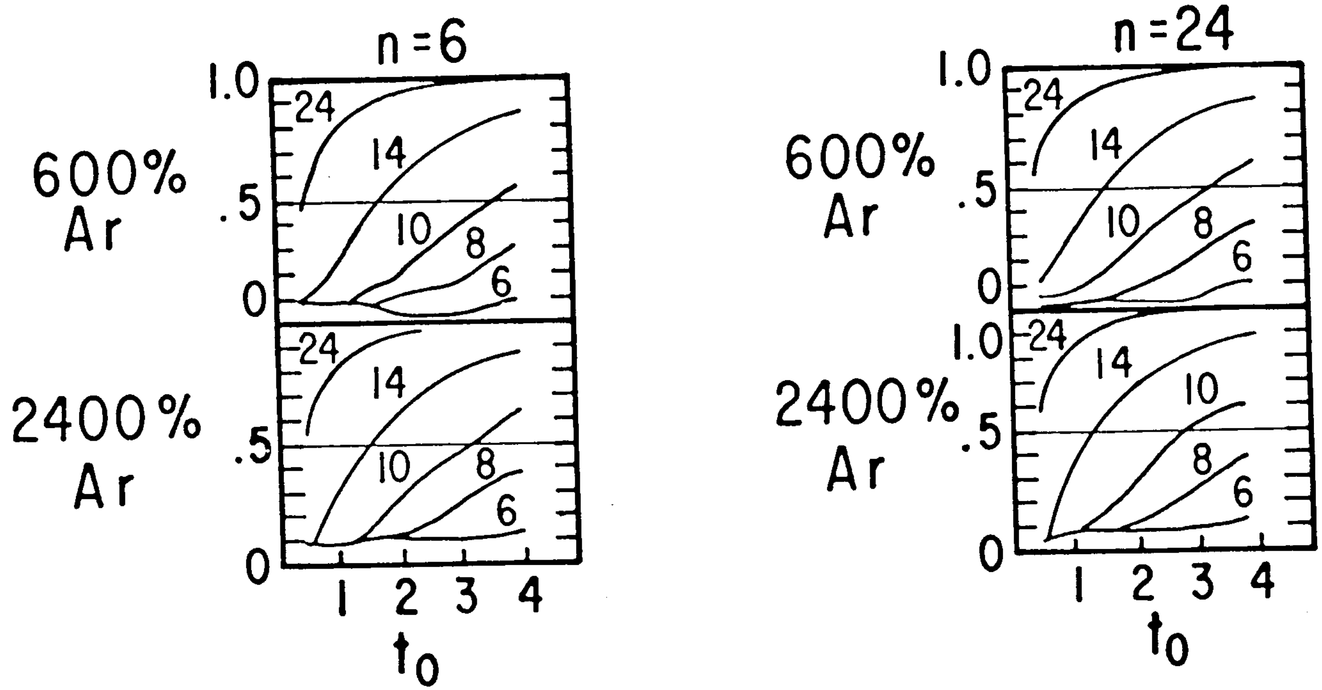

Figure 52

f) It is evident from Figure 52, that neither the increase in the number of phones per group nor the increase in CDP coverage changes the attenuation significantly.

i. Maximum Acceptable Elevation Change Across a Group

Attenuation across a group occurs not only due to NMO cancellation in a group, but also because of the static shift caused by elevation changes across a group. An acceptable array may be designed to pass the required frequencies, but large elevation changes across the group may place the output signal in the reject band, especially at low near surface velocities.

Figure 53 summarizes the equations used in the computation of maximum acceptable elevation change ($\Delta Emax$). "Δt" in this case is the static time shift across the group.

Maximum Acceptable Elevation Change Across A Group ($\Delta E max$)

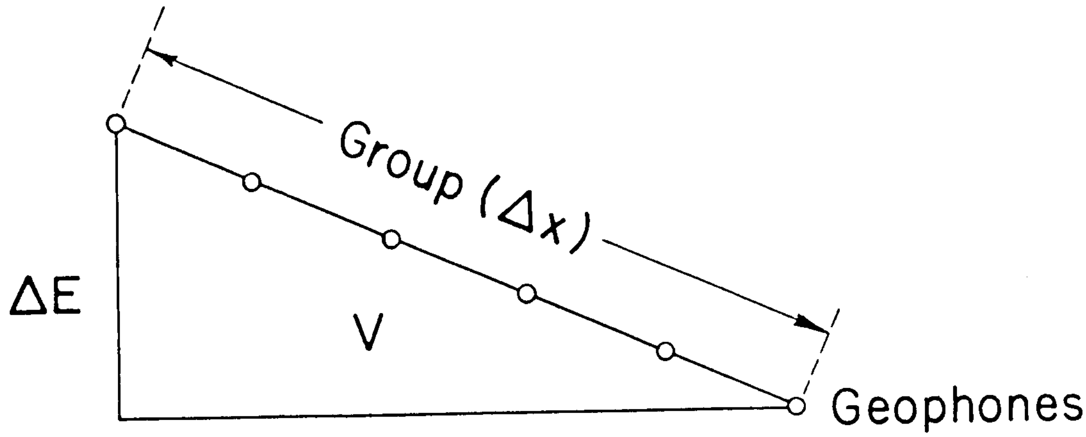

ΔE = El. Change Across Group

V = Near Surface Velocity

Δt = Vertical Time Difference Across Group

$$\Delta t = \frac{\Delta E}{V}$$

$$\emptyset/2 = 180 f \Delta t = 180 f \frac{\Delta E}{V}$$

$$Ar = \frac{1}{n} \Bigg/ \frac{\sin\left(\frac{n}{n-1}\frac{\emptyset}{2}\right)}{\sin\left(\frac{1}{n-1}\frac{\emptyset}{2}\right)} \Bigg/$$

For $Ar = .5 \quad \Delta E = \Delta E max$

$$\Delta E max = \frac{\emptyset/2}{180}\ \frac{V}{f}$$

$$\Delta E max = B \frac{V}{f} = B \lambda a$$

Figure 53

MAXIMUM ACCEPTABLE ELEVATION CHANGE ACROSS A GROUP (△Emax)
FOR n = 2 PHONES/GROUP)

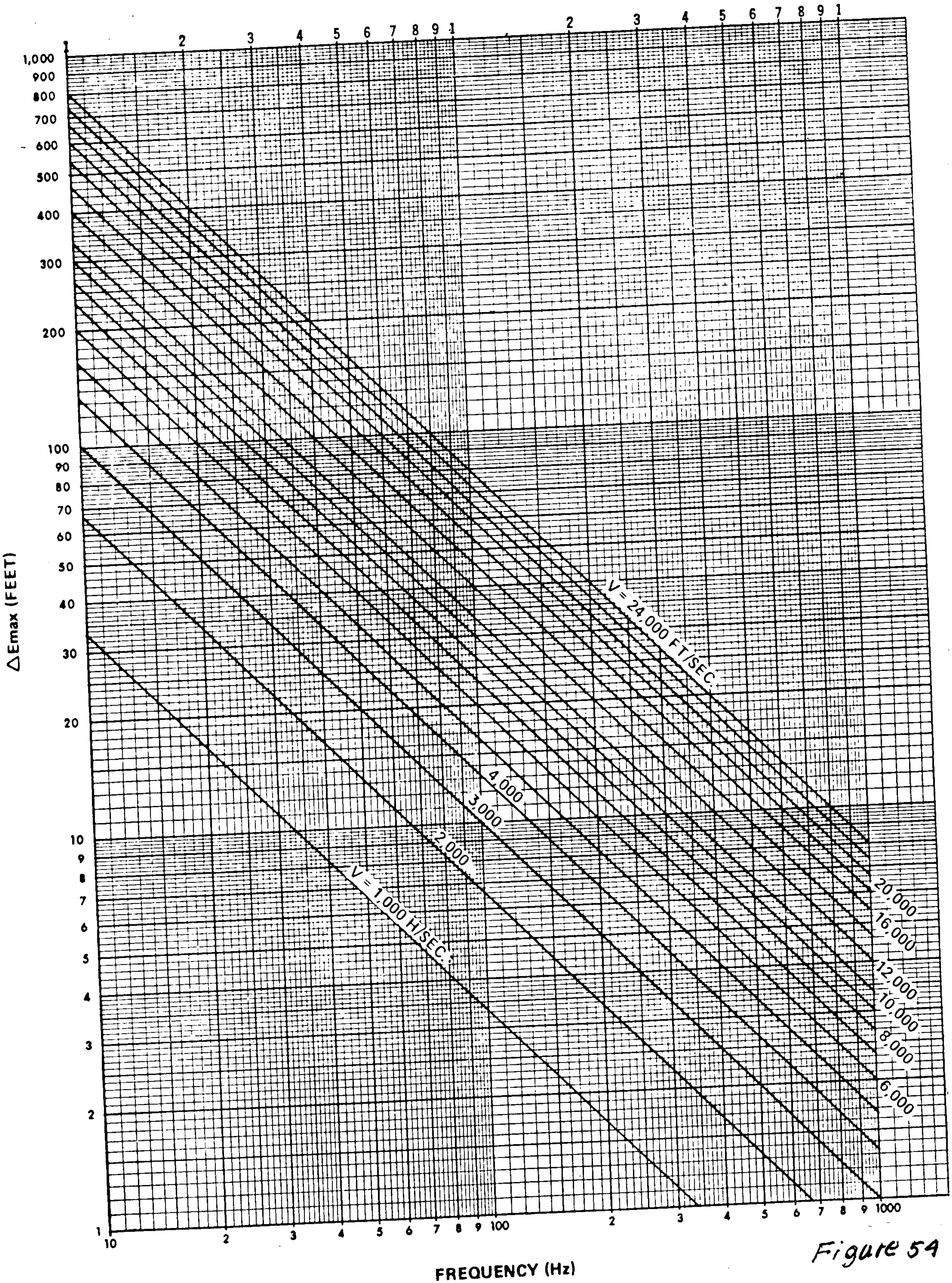

Figure 54

From Figure 54 "ΔEmax" may be determined for any combination of frequency and near surface velocity pairs. The graph is computed for n=2 phones per group. The answer is converted to any number of phones per group by multiplying the results with the appropriate "C" factor from Figure 48.

The following conclusions are evident from Figure 54:

1) "ΔEmax" is inversely proportional to the frequency and, therefore, very sensitive to frequency change in the 5-25 Hz range.

2) "ΔEmax" is directly proportional to the near surface velocity. Therefore, the higher the near surface velocity, the more elevation change is allowed across the group.

3) If the elevation change across the group is more than ΔEmax, the phones should be bunched.

4) ΔEmax is independent of the actual or effective group length and the depth of target.

5) Note, that by allowing 6 db attenuation for NMO cancellation in a group and an additional 6 db for the elevation across the array, the cascaded attenuation is 12 db, which in fact may be excessive in certain cases.

2. Linearly Tapered Arrays

The fundamental limitation of linear arrays is the lack of sharp discrimination between pass band and reject band. Therefore, linear arrays are not efficient spatial filters.

a. Methods to Increase Reject Band Attenuation

The most common approach is to define an ideal response in the wave number domain and then determine what type of spatial function (array) is required to achieve such a response.

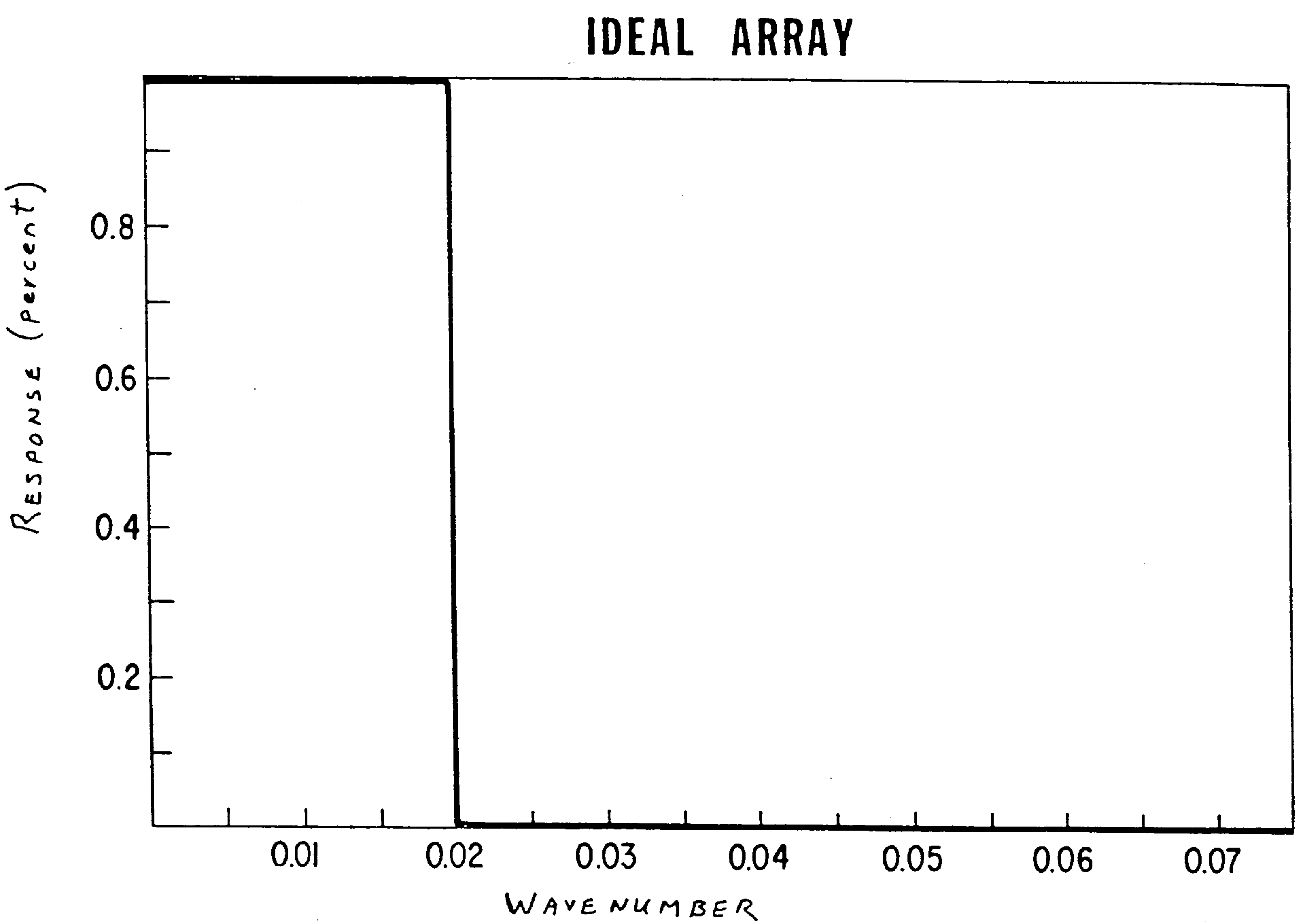

FIGURE 55 Typical desired response of an ideal array in the wavenumber domain.

SPATIAL WEIGHTS FOR IDEAL ARRAY

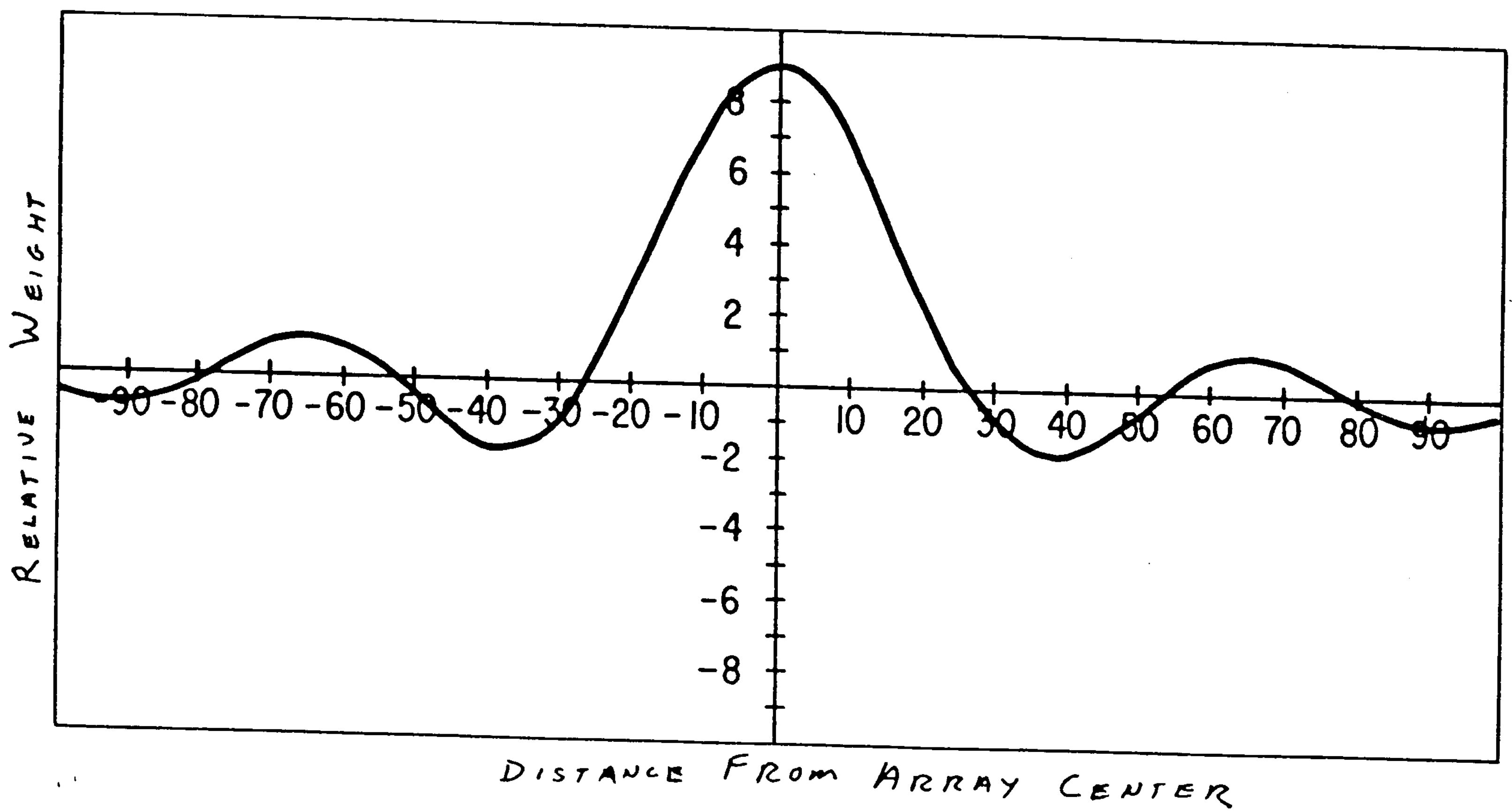

FIGURE 56 Spatial weighting function required for the ideal array of figure 55

Figure 55 shows an ideal response, which will completely pass wave numbers from 0-0.02 and completely rejects any higher wave numbers. Note, that this is a "box car" function in the "k" domain and its spatial equivalent is a "sync" function and its response is shown on Figure 56. In order to achieve the ideal response an infinitely long array is required with strong weighting of the center elements and alternating negative and positive weighting of the elements away from the center.

Since such arrays are impractical to implement in the field approximations must be made to the sync function. However, any approximations will distort the ideal response.

All weighted arrays are designed in such a manner, that the weighting function approximates the main lobe of the sync function shown on Figure 56. In other words, the weighting function is truncated at the first zero crossing.

<u>The first approximation</u> to the main lobe is a triangle as shown on Figure 57. The weights in this array are linearly tapered, hence the array is a <u>linearly tapered array</u>, where the weights are

tapered in integral steps away from the array center. The response is shown on Figure 58. The difference in attenuation between a linear and linearly tapered array of same dimensions is only 10 db as may be deducted from the comparison of Figures 58 and 60. A better approximation of the main lobe is by a "flat top" design shown on Figures 61 and 62. The cutoff of the "flat top" array is sharp, the reject band is flat with an average attenuation of 30 db as compared with 25 db on the triangular array and 15 db with the linear array. In fact, the closer the weighting function is to the main lobe of the sync function, the more rejection is obtained and the flatter the response will be in the reject band.

b. The Implementation of Linearly Tapered Arrays in the Field

Linearly tapered arrays are achieved in the field by:

1) The combinations of receiver subarrays.

2) The combinations of source and receiver arrays.

In other words, the desired tapered response is achieved by multi-staged filtering.

For example, the "flat top" ten-element weighting function on Figures 61 and 62 can be laid out in the field as three equivalent spatial receiver arrays shown on Figure 63.

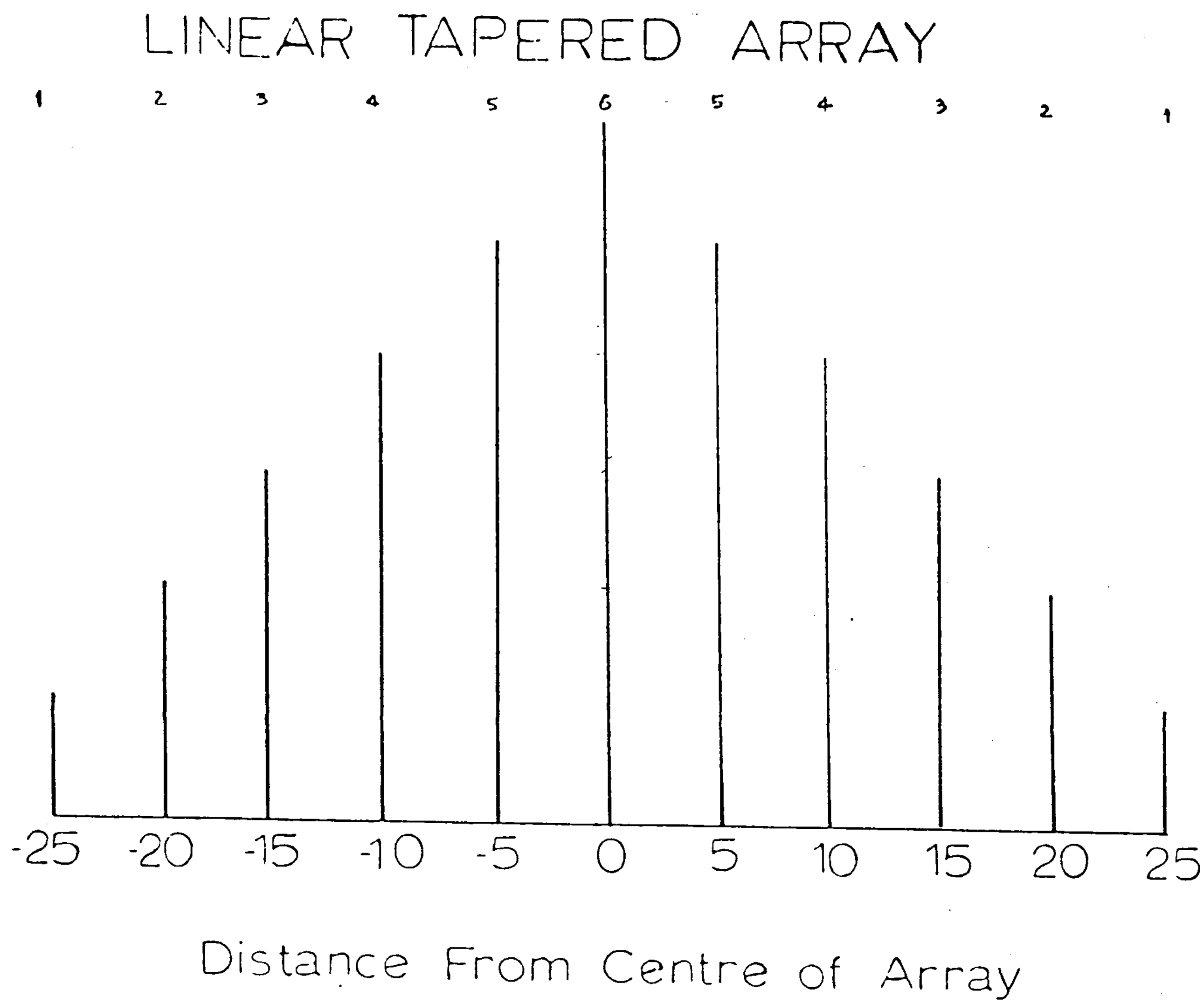

FIGURE 57 Spatial domain representation of a linearly tapered array. The amplitude of the spikes represents the relative weight of each element.

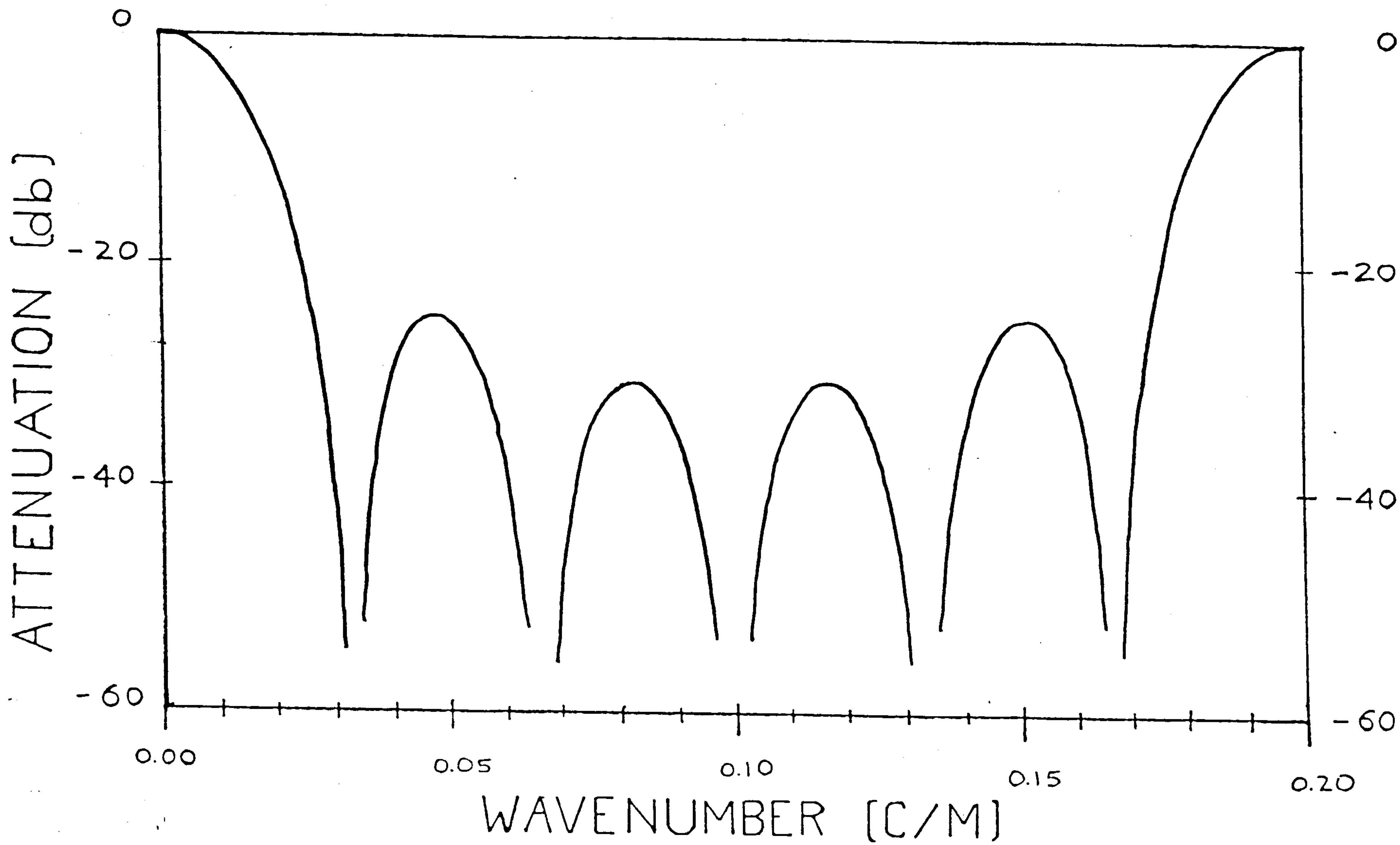

FIGURE 58 Wavenumber domain response of linearly tapered array depicted in figure 57

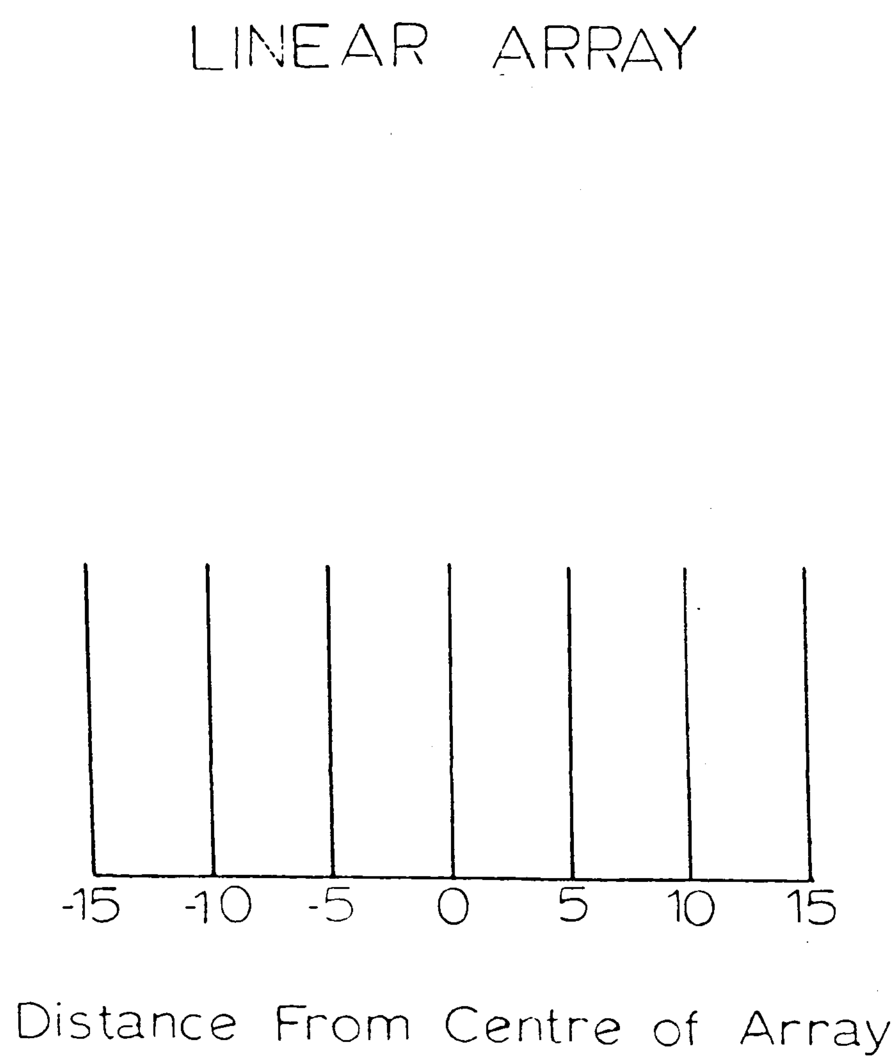

FIGURE 59 Spatial domain representation of a simple linear array. The amplitude of the spikes represents the relative weight of each element.

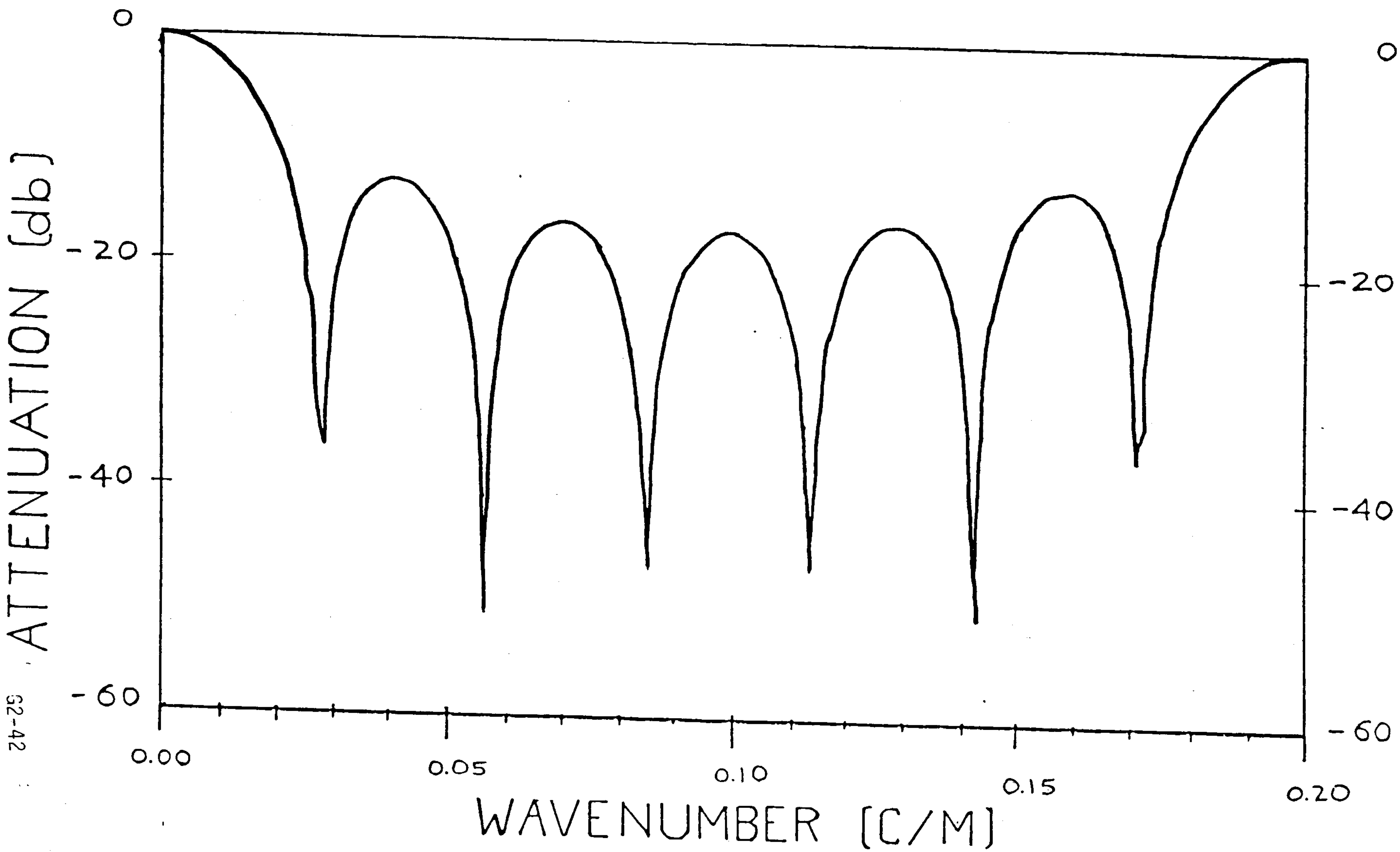

FIGURE 60 Wavenumber domain response of the simple linear array depicted in figure 59

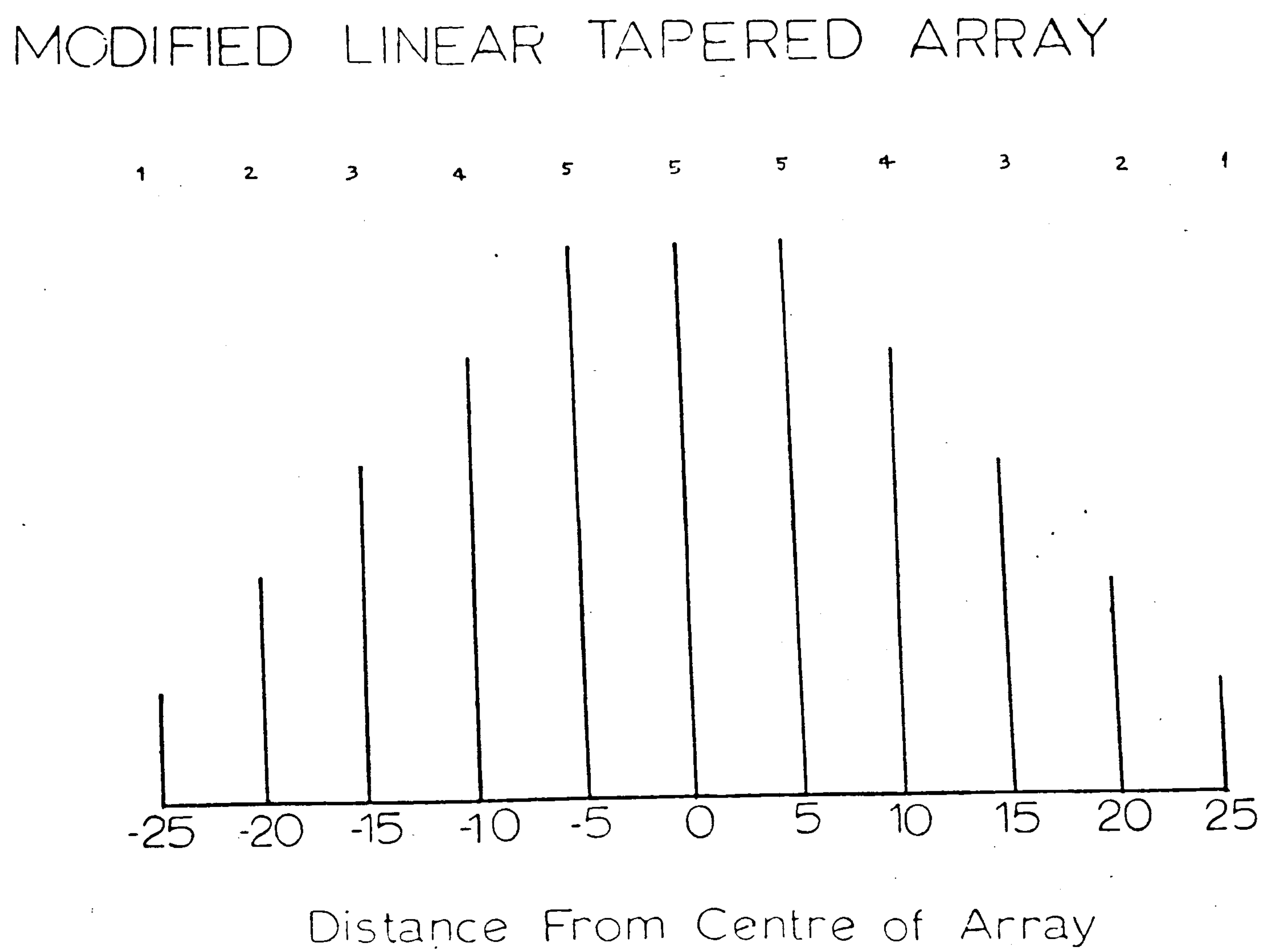

FIGURE 61 Spatial domain representation of a modified linearly tapered array. The amplitude of the spikes represents the relative weight of each element.

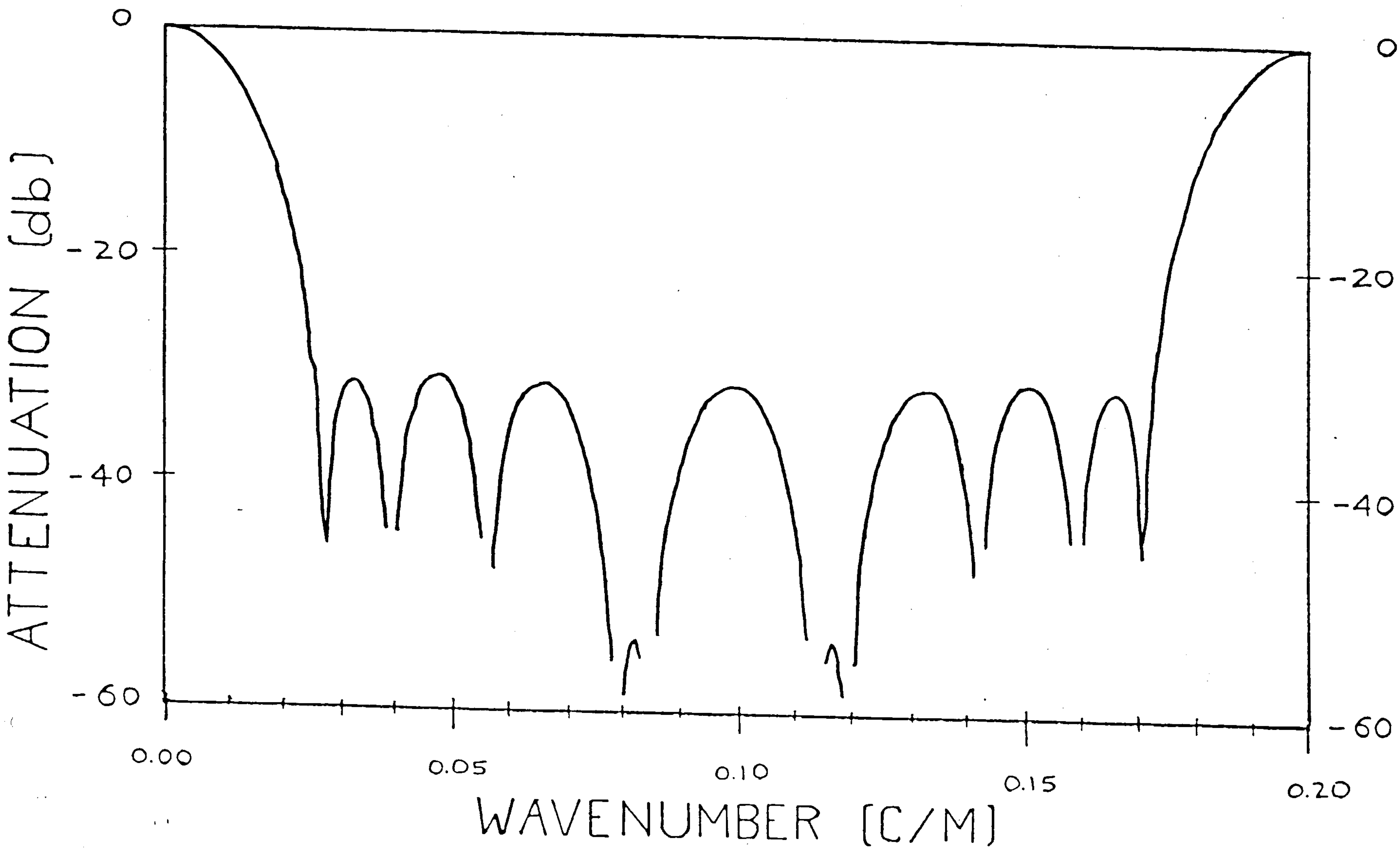

FIGURE 62 Wavenumber domain response of the modified linearly tapered array. Note the improvement from figure 61

Layout "A" consists of five strings of 2-10 phones per string in a house top arrangement. This is not a very field efficient layout, since it requires strings of variable number of phones. A better layout is indicated by "B": five strings of six phones each. Layout "C" is also possible: six strings of five phones each. The most practical layout is "B" since is requires only five strings. The element spacing is constant in all the layouts. The subarrays (five in layout "A", five in layout "B", and six in layout "C") are linear arrays.

Linearly Tapered Arrays as the Combination of Linear Subarrays

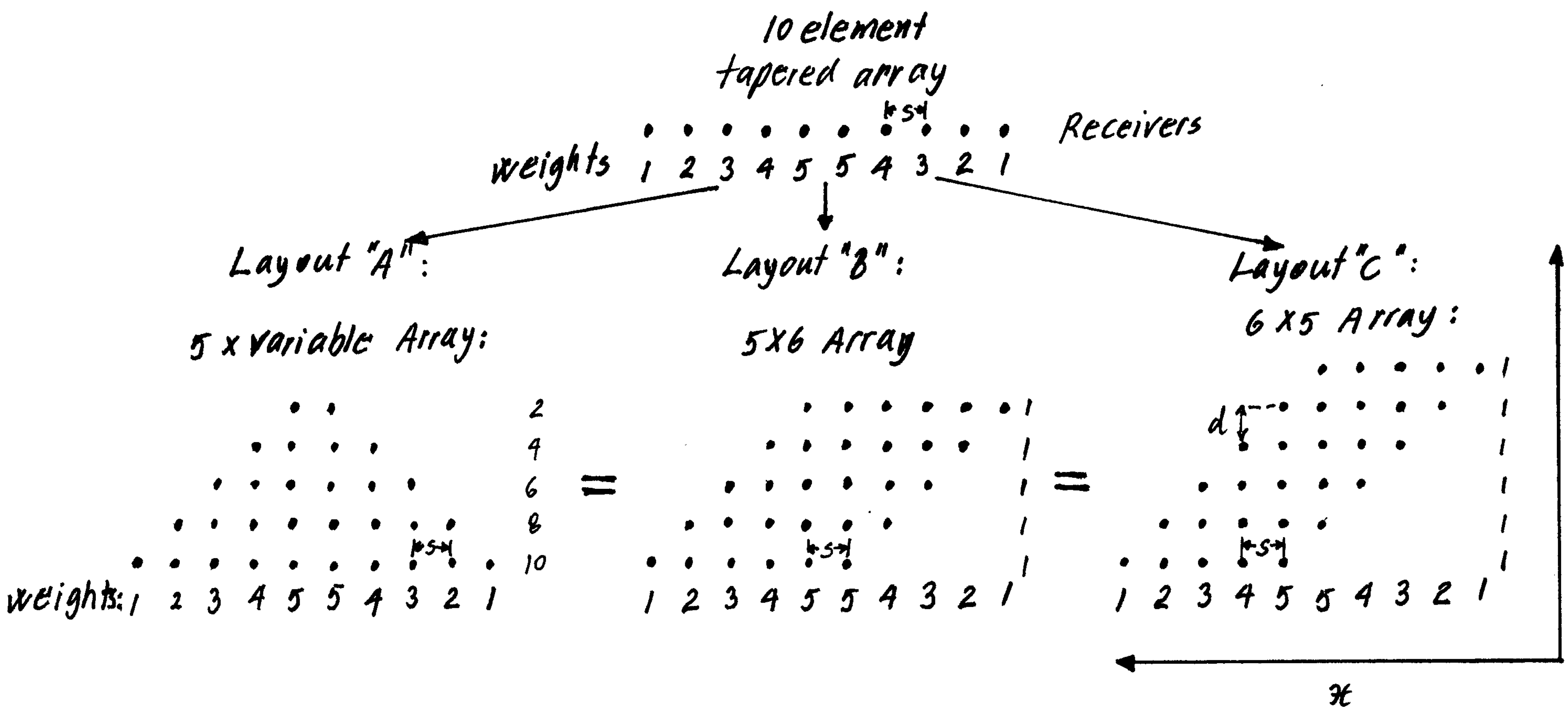

Figure 63

c. <u>The Response of Two or More Subarrays</u>

Applying two or more linear (or other) subarrays simultaneously is equivalent to:

1) Spatial convolution of the individual patterns on the ground.

2) This is equivalent to the multiplication of their amplitude responses in the spatial frequency domain, if the amplitudes are expressed in percentages.

3) If the amplitudes are plotted in db, the spatial convolution of the subarrays is simply the sum of their respective amplitude values at each "k" (or λ or D).

For example: The amplitude response of the ten-element tapered array on Figure 63 in the "x" direction is equivalent to the sum (in db) of:

a) Layout "A": 2, 4, 6, 8, and 10-element linear arrays.

b) Layout "B" and "C": a six-element and a five-element linear array.

Note: The arrays are only equivalent in the "x" direction. In the "y" direction: layout "A" is equal to an asymmetric five-element tapered array, layout "B" is a five-element linear array, and layout "C" is a six-element linear array.

Combined subarrays are most often used with surface sources (vibroseis) where both the receiver and source arrays are linear arrays. In some areas (Middle East) large, two dimensional source and receiver arrays are used to attenuate strong coherent noise waves and to achieve substantial S/N improvement through redundancy.

d. <u>The Properties of Combined Subarray Responses</u>

1) Linearly tapered array (such as shown on Figure 63) can always be laid out as the combination of linear subarrays.

2) The notches of the combined response will be located and only located at the notches of the individual responses.

Figures 64, 65, and 66 illustrates the position of notches when a four-element source and a six-element receiver arrays are convolved.

3) The first notch occurs at the first notch of the subarray with the longest effective group length.

4) The combined array response repeats at the first repeat wavelength (or k) common to all the subarrays. For example, on Figures 64-66, the element spacing for the four-element array is S = 150 ft, hence the four-element array repeats at λ = 150, 75, 37.5, etc. The element spacing for the six-element array is 75 ft, hence the response repeats at λ = 75, 37.5, etc. The first common repeat wavelength for the combined array is 75 ft, hence the combined response repeats at 75 ft as shown on Figure 66.

(135)

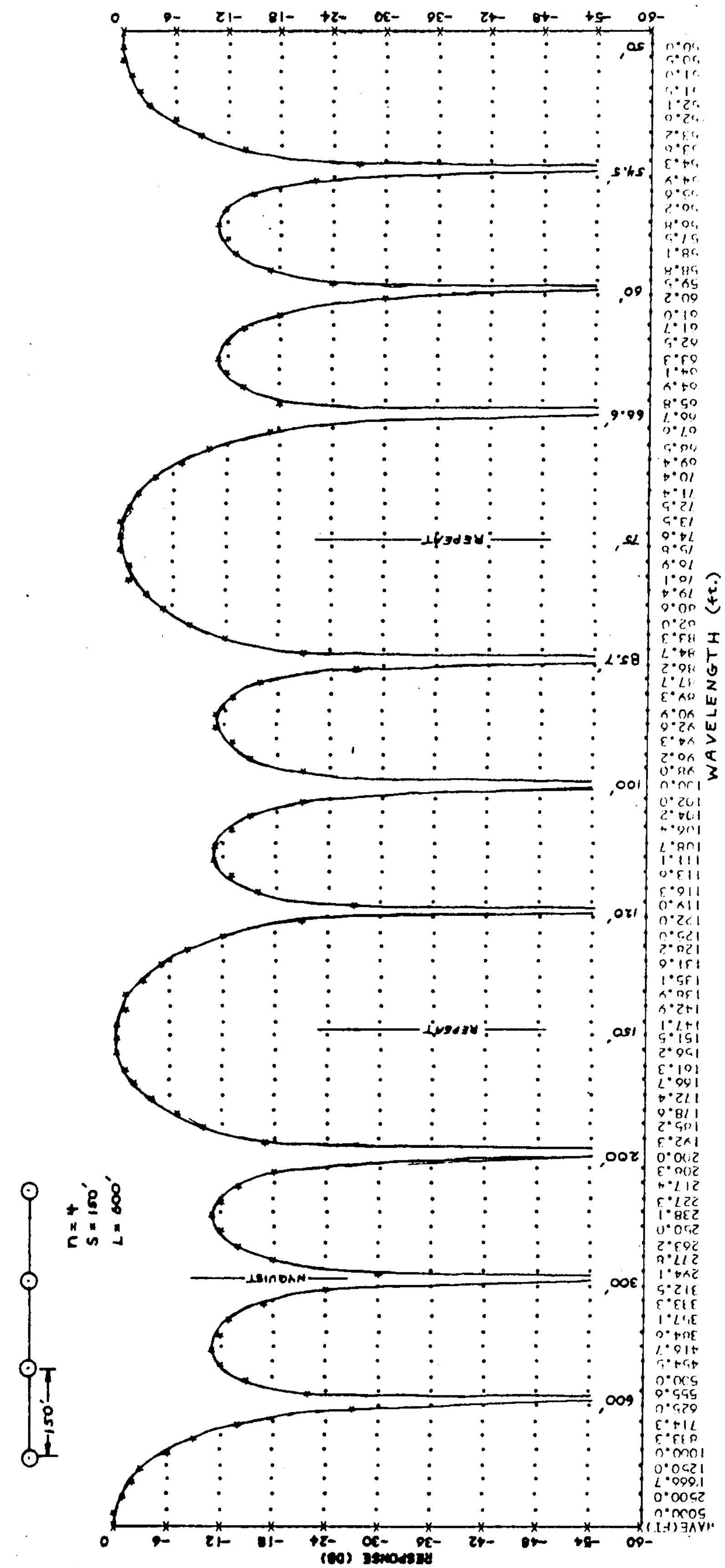

SOURCE RESPONSE

FIG. 64

(136)

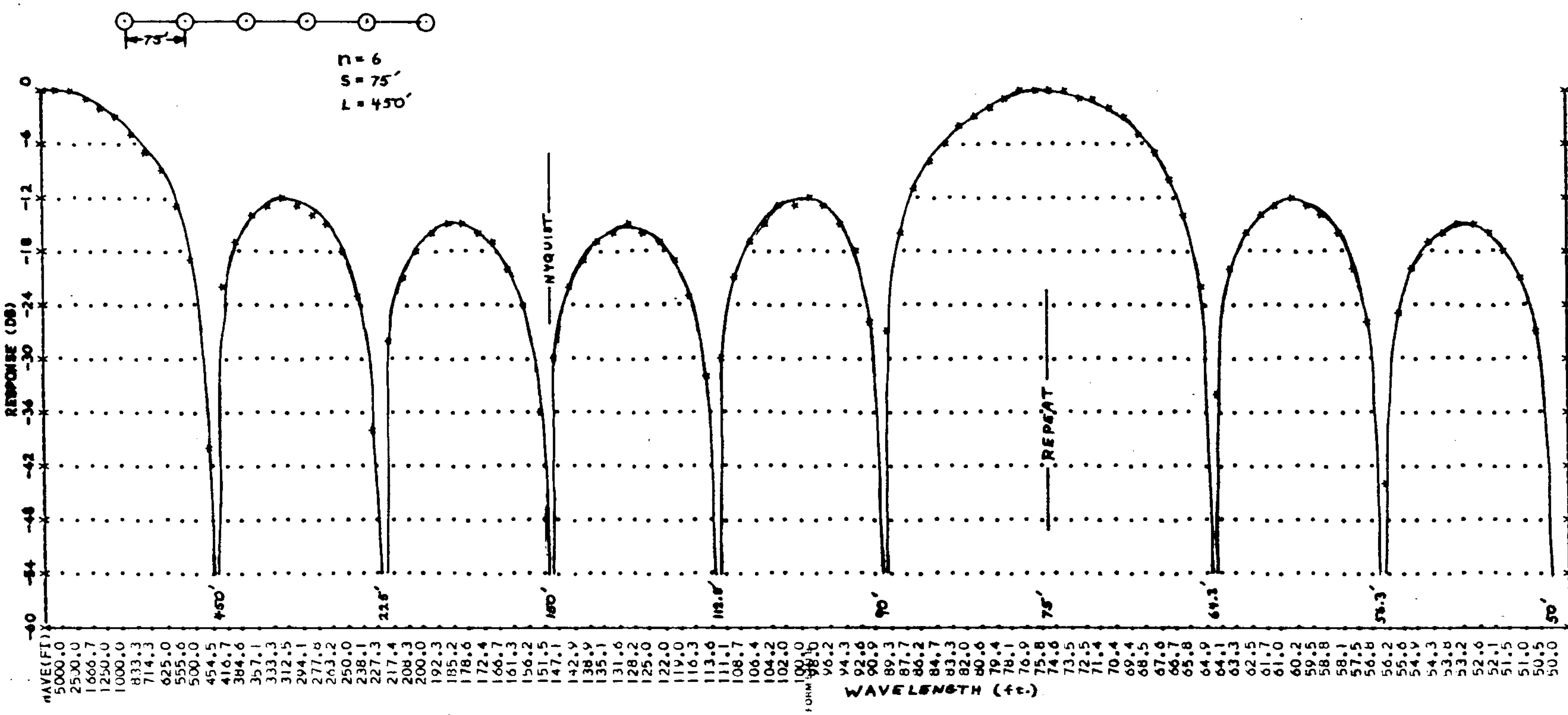

RECEIVER RESPONSE

FIG. 65

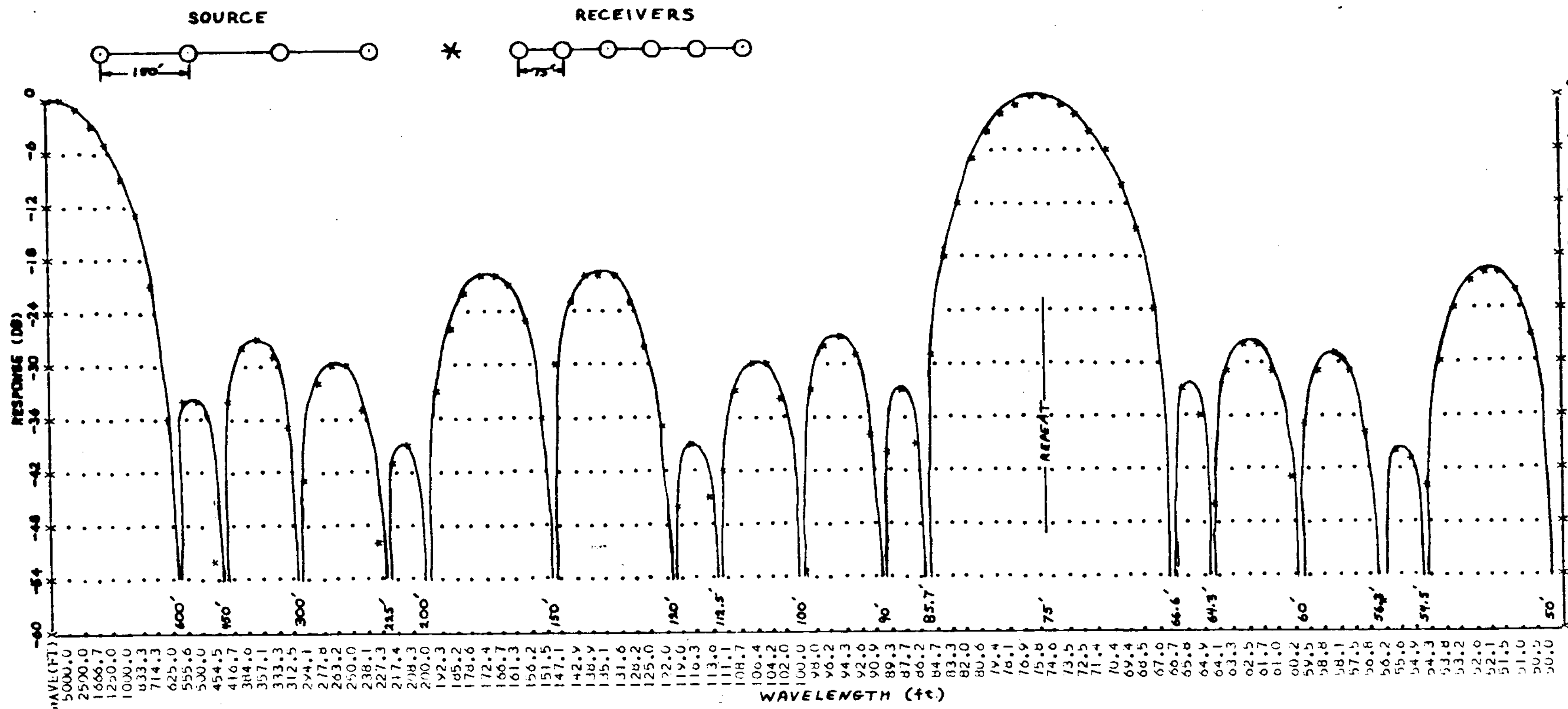

COMBINED RESPONSE

FIG. 66

5) The spatial Nyquist is twice the wavelength (or half the "k") of the first repeat of the combined response.

6) The width of the reject band, hence the last notch before repeat depends on the position of the first repeat common to all subarrays, but never before the repeat of the subarray with the shortest element spacing.

e. Practical Considerations in Tapered Array Design

Lavender (1973) and Kallweit (1976) have designed "rules of thumb" to arrive at "optimum" arrays when using the combination of two or three linear arrays. Figure 67 summarizes the rules for both.

3. Non-Linearly Tapered Arrays (Weighted Arrays)

The maximum achievable attenuation in the reject band by linearly tapered arrays is 30 db. However, the coherent noise is often 40 db above the signal, therefore, the theoretical requirement for any spatial array is 40 db.

THE "OPTIMUM" ARRAY

Modified from Lavender (1973)*

1. Two Subarrays Convolved:

   A. Make the effective length of the longer subarray equal to, or greater than, the longest wavelength one wishes to attenuate.

   B. Make the effective length of the shorter subarray approximately 70 percent of the effective length of the longer subarray. This will result in about 30 db attenuation across the reject-band.

   C. Make the subarray with a fewer elements the shorter one. This tends to broaden the reject-band by pushing the first repeat wavelength (zero attenuation) towards the shorter wavelengths.

---

* Lavender, L. L., 1973, Rule of Thumb Array Design, New Orleans Division, Amoco Production Company.

Figure 67

2. Three Subarrays Convolved:

A. Make the effective length of the longer subarray equal to, or greater than, the longest wavelength one wishes to attenuate.

B. Make the effective length of each remaining subarray 80 percent of the effective length of the next longer sub-array. This will result in about 45 db attenuation across the reject-band.

C. Make the subarray with a fewer elements the shortest array. This tends to broaden the reject-band by pushing the first repeat wavelength (zero attenuation) towards the shorter wavelengths.

A better approximation to the required theoretical response shown on Figure 55 may be achieved by a closer fit to the main lobe of the sync function on Figure 56.

This can only be achieved by non-linear taper of the weights. Savit and Holzman solved the weighting coefficient functions for elements of an equispaced array constrained to be of finite length with only positive weights.

In Savit's solution the RMS errors between the ideal and computed array responses are minimized.

In Holzman's solution the Chebyshev optimization criterion is applied, which confines the maximum allowable error in the solution to a specified amount.

a. <u>Savit Array</u>

An array designed by Savit's criterion is called a "Savit Array".

b. <u>Chebyshev Array</u>

An array designed by Holzman's criterion is called a "Chebyshev Array".

Figures 68-71 show the weighting functions and amplitude responses of the Savit and Chebyshev arrays. The Chebyshev array has better response and a flat reject band. The level of attenuation may be arbitrarily great depending on the design parameters. In most cases 40 db is specified.

Since the Chebyshev and Savit arrays require complex weighting functions, such arrays are difficult and in most cases impractical to implement in the field. The Chebyshev array is used to marine streamers. However, on land only the electronically weighted geophones are a practical method of implementing such arrays. The "Mini Max" system by Geosource uses electronic weighting to implement Chebyshev arrays in an easy to use practical manner.

<u>Determination of Initial Chebyshev Array Parameters</u>

Given: λ_L = longest wavelength in reject band

λs = shortest wavelength in reject band
Ro = rejection ratio (usually 100 = 40 db)

Calculate:

$$Do = \frac{\lambda_L + \lambda s}{\lambda_L + \lambda s} = \text{spacing of array elements}$$

$$\sigma o = \frac{1}{\cos\left[\pi Do/\lambda_L\right]} = \text{transformation constant}$$

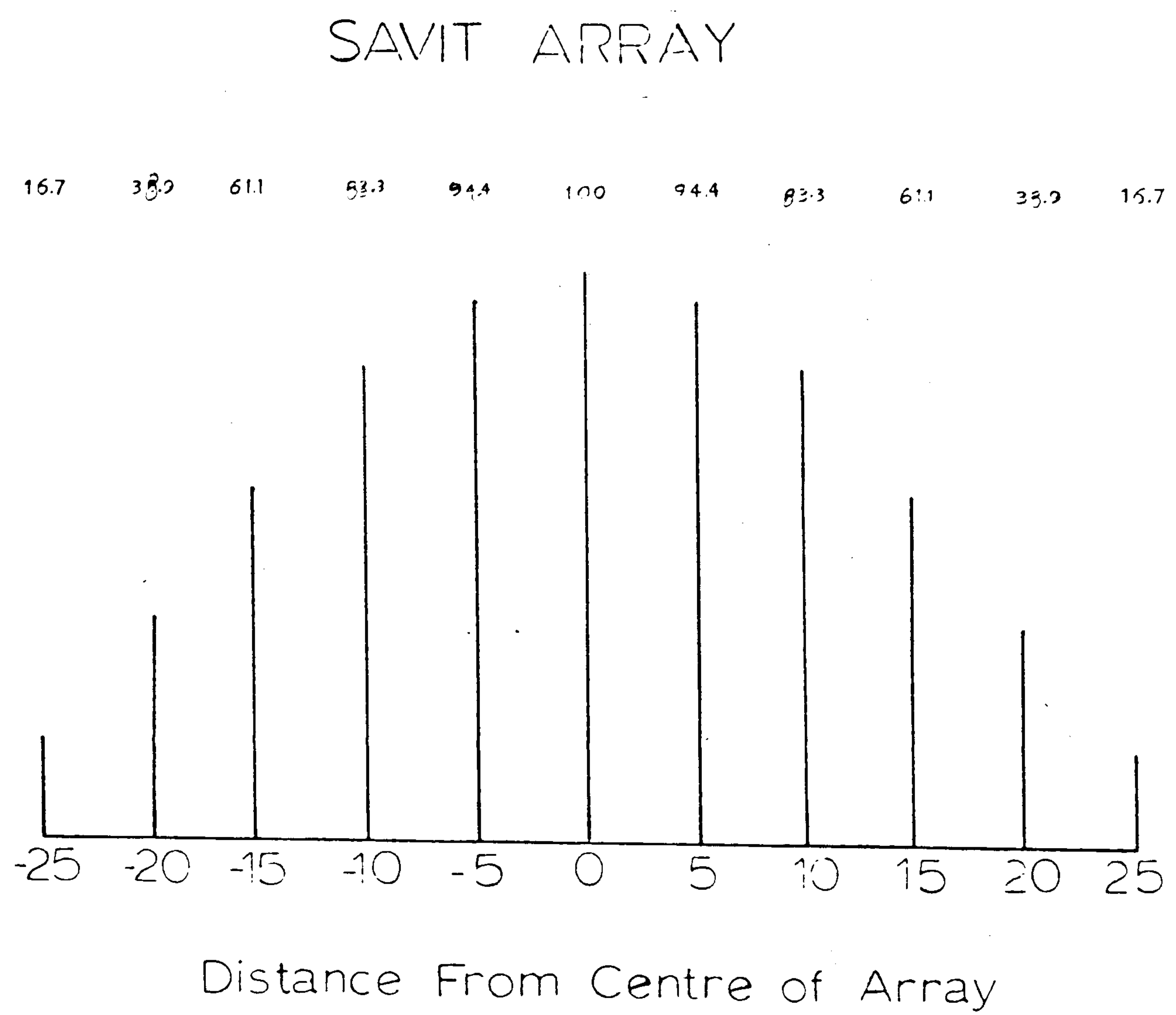

FIGURE 6.8 Spatial domain representation of a Savit array. The amplitude of the spikes represents the relative weight of each element.

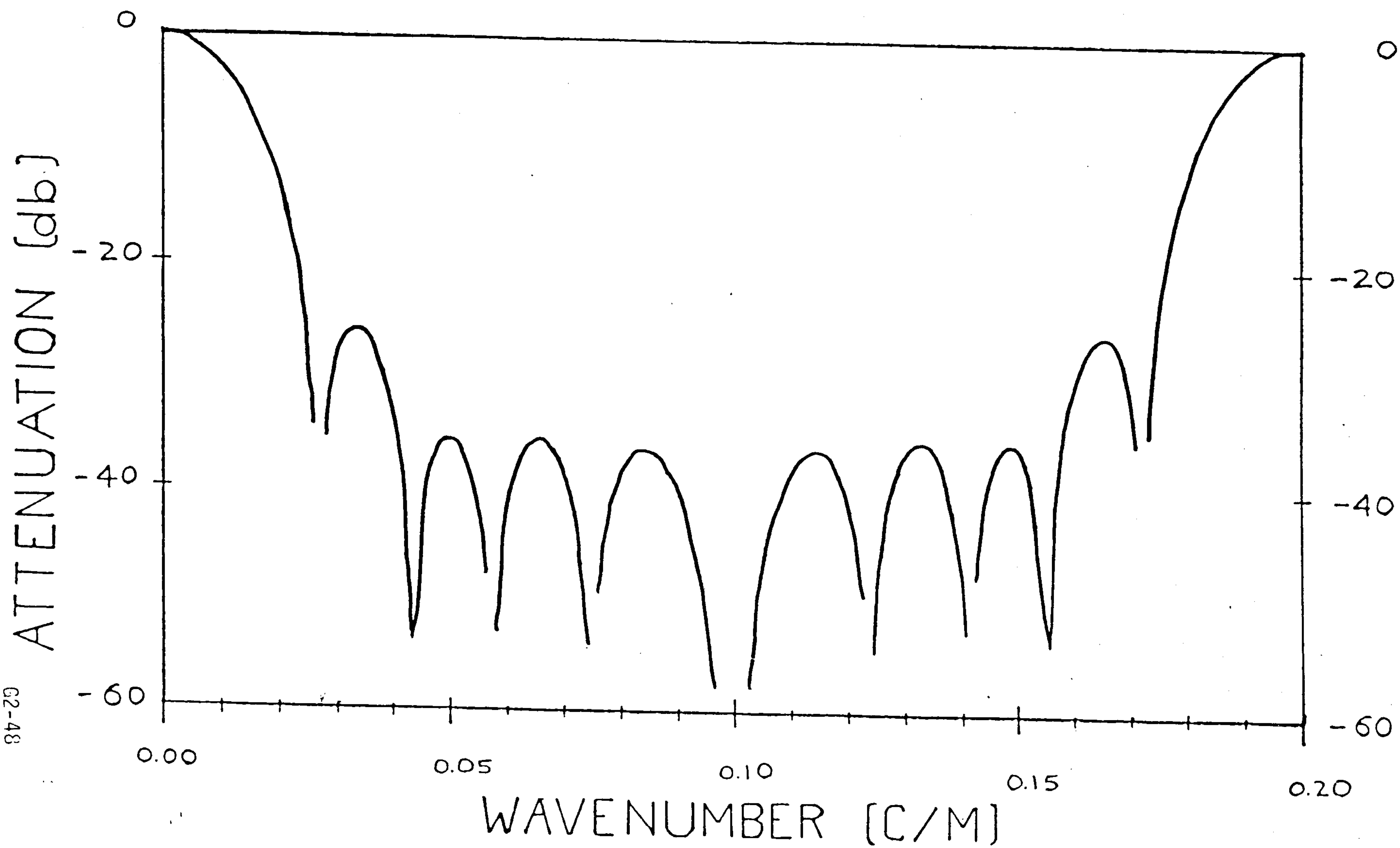

FIGURE 69 Wavenumber domain response of the Savit array depicted in figure 68

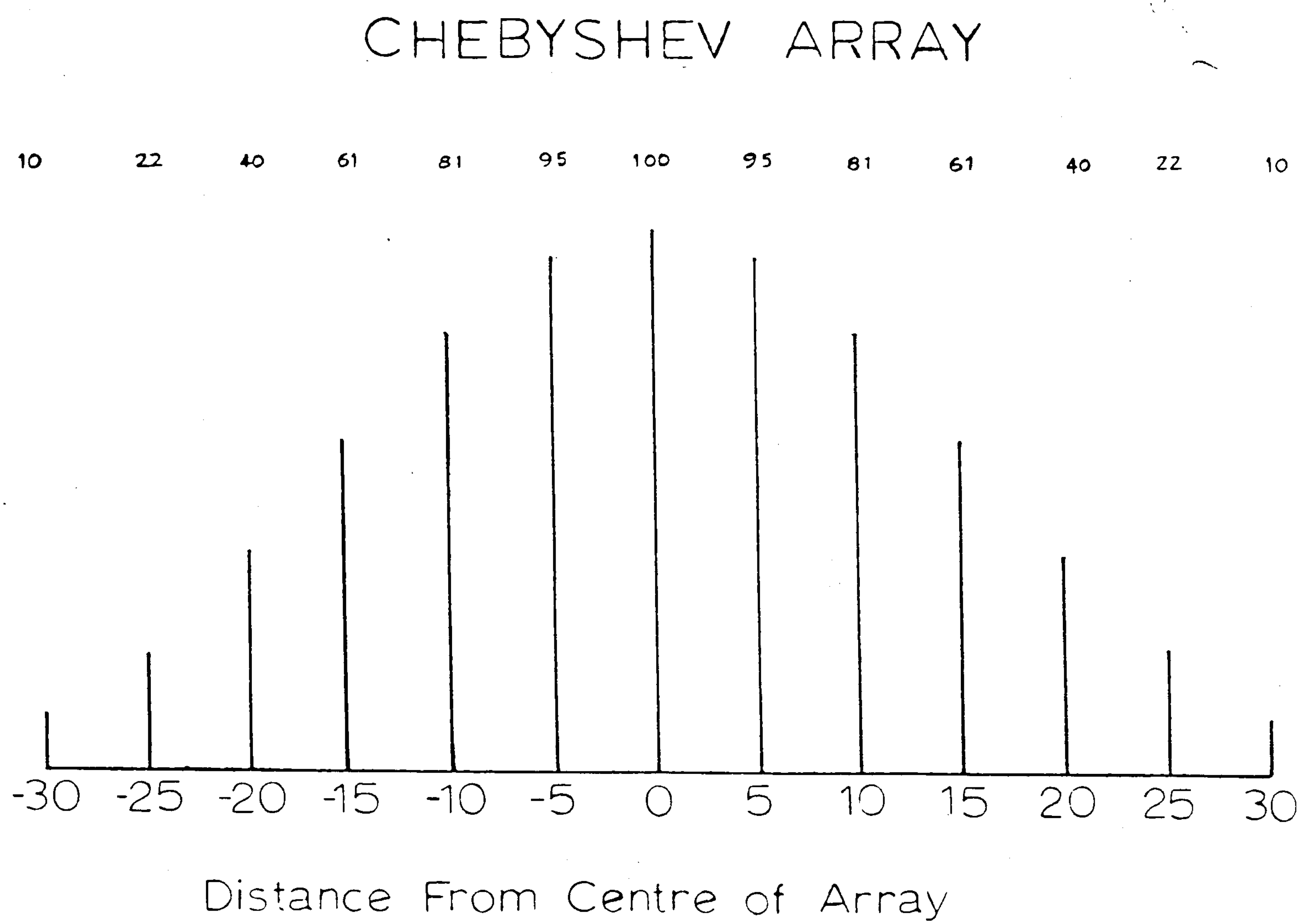

FIGURE 70 Spatial domain representation of a Chebyshev array. The amplitude of the spikes represents the relative weight of each element.

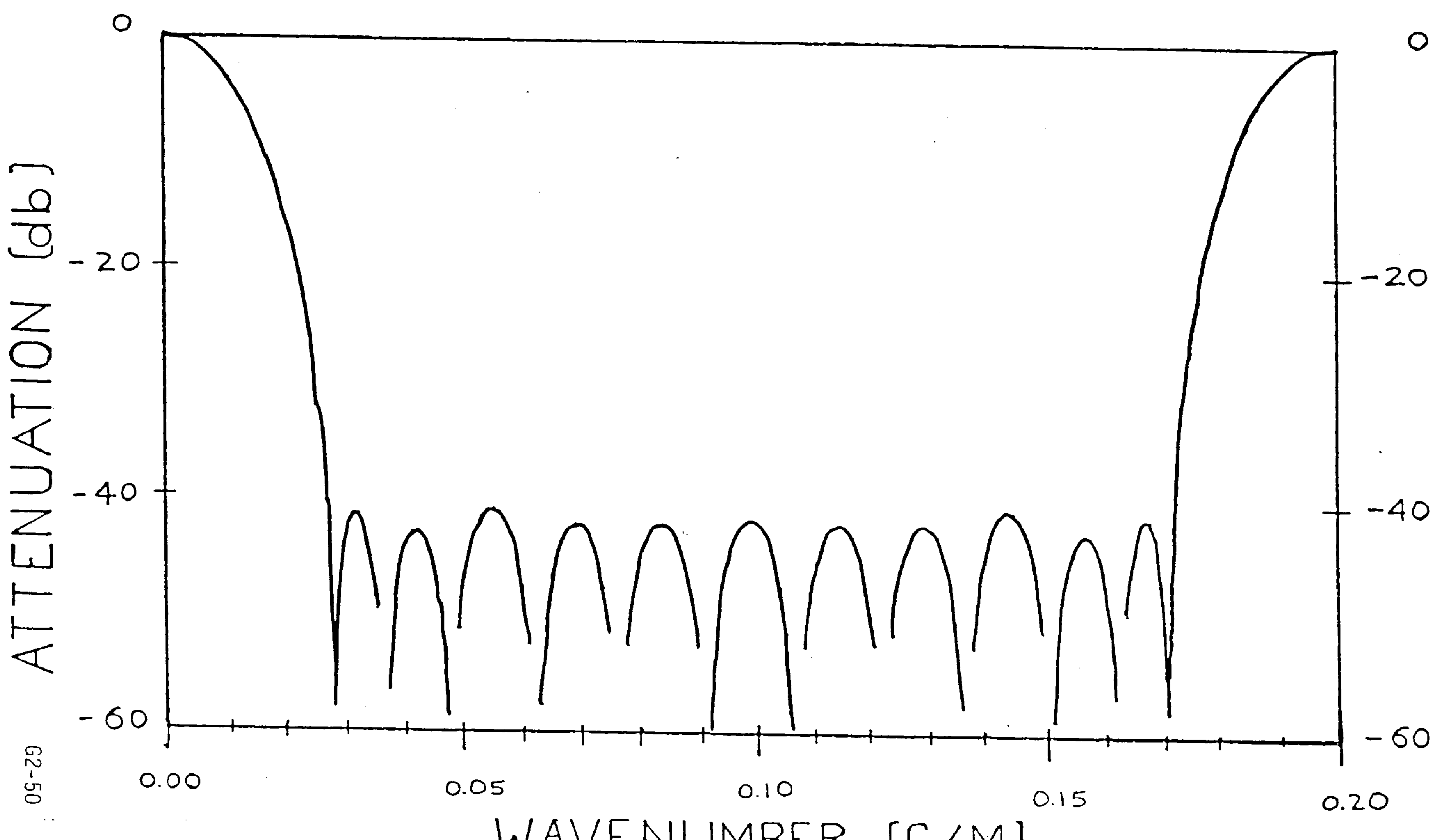

FIGURE 71 Wavenumber domain response of the Chebyshev array depicted in figure 70

$$m = \frac{\cosh^{-1}(Ro)}{\cosh{-1}(\sigma o)} = \text{order of solution}$$

$$n = m + 1 = \text{number of array elements}$$

The weights are given by the equation:

$$Wi = \frac{2}{N} \sum_{s=0}^{[m/2]} Es\ Tm\left[\sigma o \cos\left(\frac{s\pi}{N}\right)\right] Tm-2i \left[\cos\left(\frac{s\pi}{N}\right)\right] \quad (46)$$

Where: Wi = the ith weight with increasing from "0" at the array centre

$\left[\frac{m}{2}\right]$ = largest integer

Es = 1 if s = 0; Es = 2 if s ≠ 0

$$Tm = \sum_{R=0}^{[m/2]} (-1)^R \binom{m}{2R} X^{m-2R} (1-X^2)^R$$

The Chebyshev Polynominal

Example:

λ_L = 62.5 m

λs = 6.00 m

Ro = 100 (40 db)

Then,

Do = 5.4 m

σo = 1.0391

m = 19

N = 20

The weights are: 207, 291, 463, 668, 897, 1131, 1352, 1541, 1678, 1750. The output of the array is calculated from the general equation:

$$Ar = \frac{\sum_{i=1}^{M} Wi \cos\left[2\pi k\,(di-dc)\right]}{\sum_{i=1}^{M} Wi} \text{ (in \%)} \qquad (47)$$

Where:

- k = wave number
- Wi = the relative weight of the ith element
- di = distance of the ith element from an arbitrary reference point
- dc = distance of array centre from reference point
- M = total number of weights (elements) in array

The amplitude response of the example is shown on Figure 72.

C. Practical Limitations of Arrays

A prominent geophysicist stated: "It is easy to sit in an office, with a computer, and design exotic arrays which give fantastic attenuation. For any particular survey, however, there are limitations in the field as to what can be accomplished".

Newman and Mahoney have investigated the effect of errors in weights and element spacing (positioning) on the performance of uniform, linearly tapered, Savit and Chebyshev arrays.

Figures 73-75 summarize the results for errors of 2 percent, 5 percent, 10 percent, and 20 percent. A 10 percent error is common in field work.

The following conclusions may be drawn from the study:

1) Highly tuned arrays with sharp distinction between reject and pass bands are very sensitive to errors in weight and element positioning. As shown on Figure 75, a 10 percent error in positioning and weights limits a 60 db attenuation Chebyshev array to 30 db.

TOTAL OPTIMUM CHEBYSHEV RESPONSE

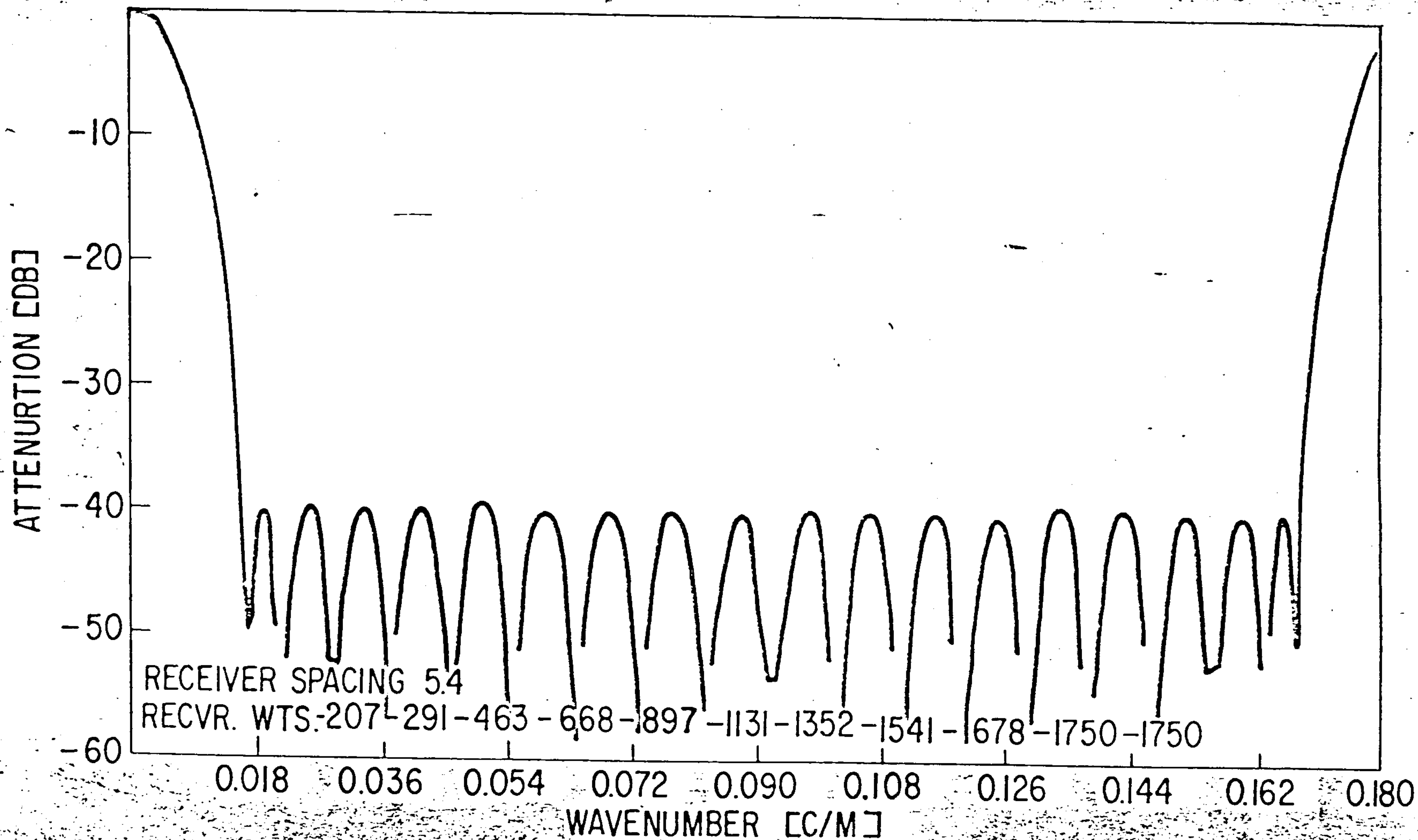

ARRAY RESPONSE

FIGURE No. 72

2) Linear arrays are not sensitive to errors. As shown on Figures 73 and 74 a 30 db attenuation can be reached by a simple linear array.

3) The practical limit of any array is 30 db. This is the reason why highly tuned, complex arrays are seldom used. They are difficult to implement in the field and the errors inherent in layout destroy the advantage of the array.

4) In spite of the limitations of non-linearly tapered arrays, the distinction between pass and reject bands is sharper with the Chebyshev than linear arrays.

5) Other disadvantages of highly tuned arrays is that coherent noise modes and their bandwidth in the spatial domain may vary rapidly, especially if near surface conditions change, hence a sophisticated array highly tuned to a certain bandwidth is not going to be very effective a "few miles down the road", where the noise bandwidth is different.

6) Because of the above reasons, the most commonly used arrays are simple linear arrays or linearly tapered arrays.

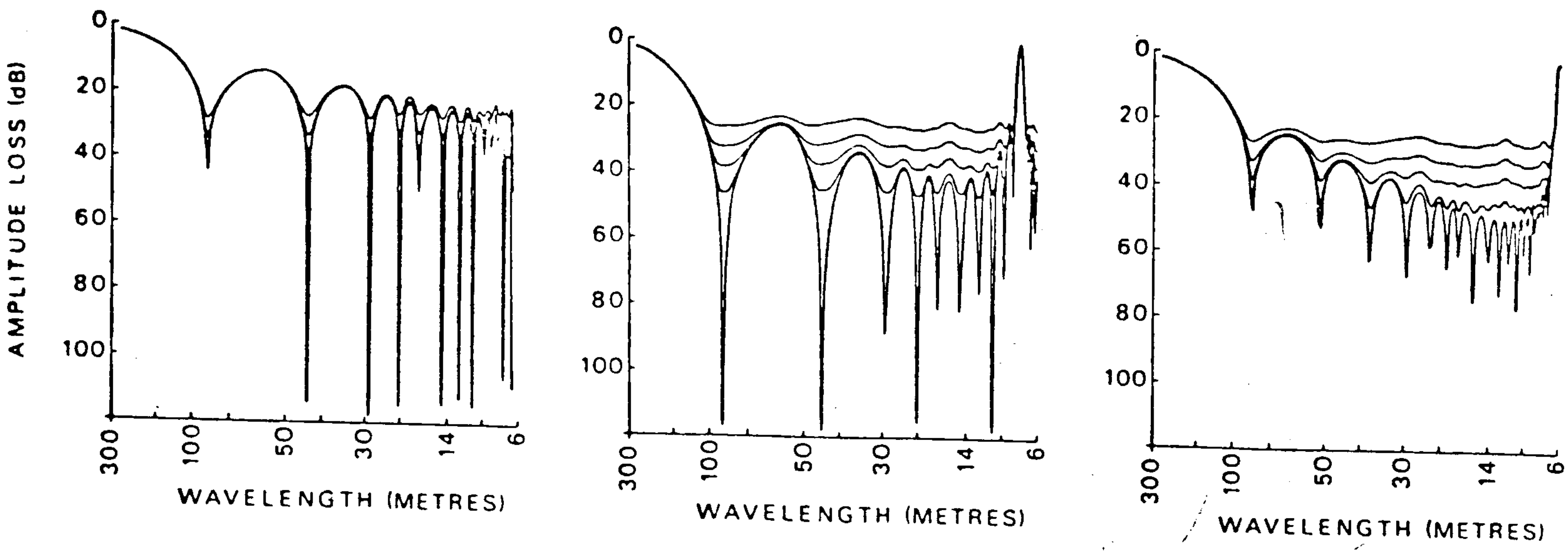

FIGURE 73 Ensemble mean responses for different 21 element arrays with applied errors in weights of zero, 2, 5, 10, and 20 percent standard deviation. (Left) Uniform array. (Center) Linearly tapered array. (Right) Savit array. (Newman and Mahoney, 1973, figure 11)

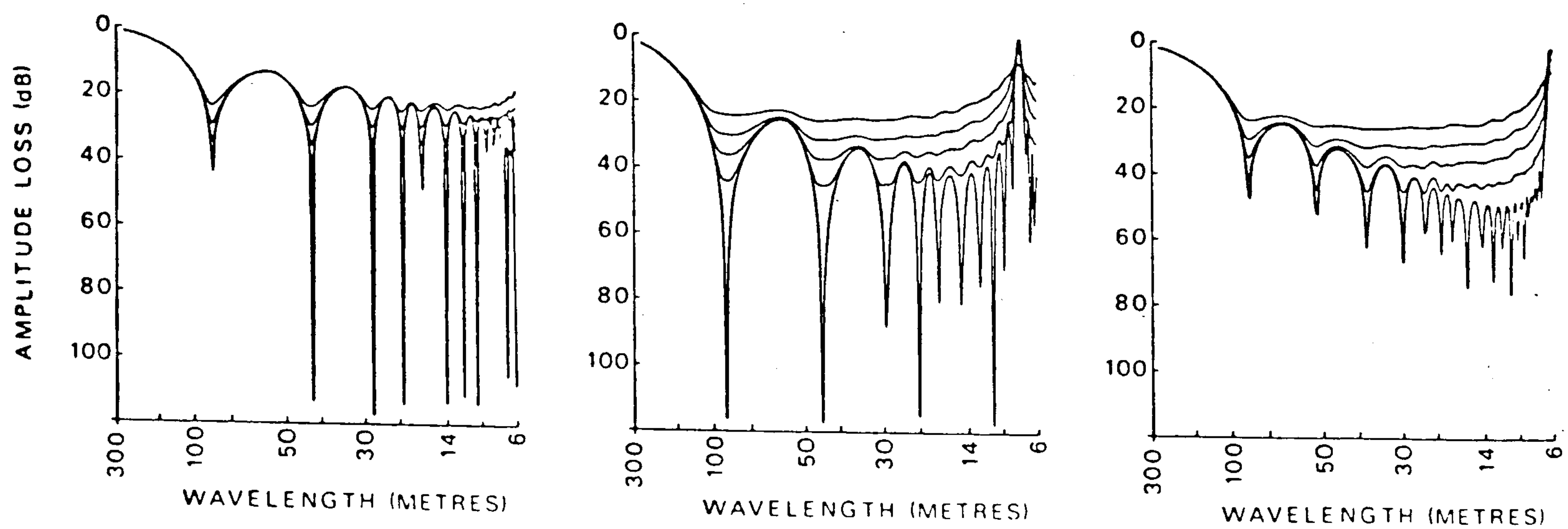

FIGURE 74 Ensemble mean responses for different 21 element arrays with applied errors in element spacing of zero, 2, 5, 10, and 20 percent standard deviation. (Left) Uniform array. (Center) Linearly tapered array. (Right) Savit array. (Newman and Mahoney, 1973, figure 14)

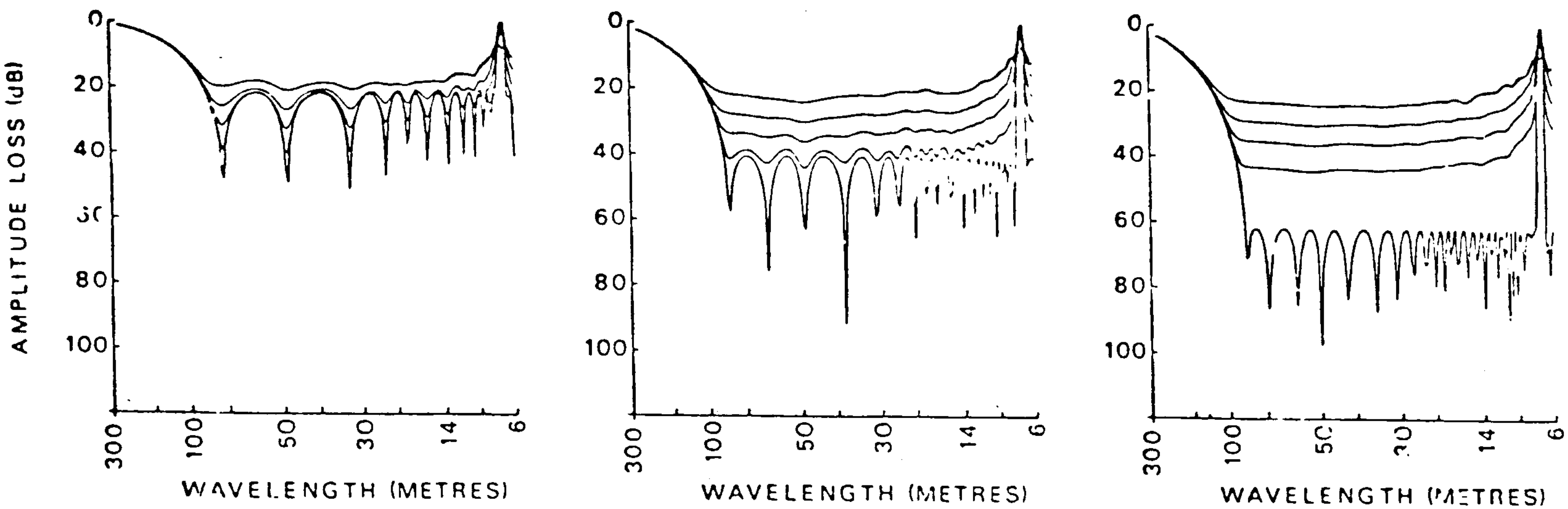

FIGURE 75 Ensemble mean responses for Chebyshev arrays of differing nominal performance and for joint errors in element weights and spacing of zero, 2, 5, 10 and 20 percent standard deviation. (Left) Nominal 20 db array (13 elements). (Center) Nominal 40 db array (21 elements). (Right) Nominal 60 db array (30 elements). (Newman and Mahoney, 1973, figure 15)

V. The Design of Source and Receiver Arrays

The main purpose of field arrays is two-fold:

1) To improve the S/N through multiplicity.

2) To attenuate coherent, mostly linear noise.

Field arrays are high cut spatial frequency filters. However, the spatial frequency is directly proportional to the temporal frequency. Therefore, field arrays are also high cut temporal frequency filters. The basic requirements for the design of spatial filters are:

1) To pass the useful signal--usually the maximum required signal frequency--with a minimum of attenuation.

2) To reject the coherent noise events.

Coherent noise trains are often high amplitude (30-40 db above signal level), but in the majority of cases restricted to lower temporal frequencies (below 20 Hz). Therefore, the first step in array design is to determine whether the coherent noise can be attenuated by simple low cut temporal filters without degrading the lower frequencies of the signal. Over 60 percent of the cases this may be achieved and array design becomes academic.

If, it has been determined that spatial filters are necessary, one may proceed with the array design.

Arrays are designed to attenuate coherent noise, but at the same time, it is necessary to check the reflected signal attenuation by the array. Usually a compromise must be reached between effective noise attenuation and signal passing. It is usually better to pass some noise rather than to attenuate signal.

A. Field Tests Necessary for Array Design

The only field test necessary for array design is a "simple wave test". A simple wave test consists of recording a single ender spread of closely spaced single receivers. If back scattered noise is suspected, a 3D wave test must be designed.

The length of spread should always be as long as the production spread.

The spacing of receivers in a wave spread: the shortest wavelength noise and/or signal should not be aliased. From equation (13) the max group interval:

$$\Delta xmax = \frac{Vamin}{2fmax}$$

Where Vamin = the minimum expected apparent velocity
fmax = the maximum expected frequency

The minimum velocity is usually the airwave (Vamin = 1100 ft/sec) with a max. frequency of 100 Hz. Therefore, the spacing of phones should not be more than 6 feet. However, it is very difficult to avoid spatial aliasing of the higher frequencies of airwaves. Noise frequencies are below 50 Hz, hence a maximum phone spacing of 20 feet is usually adequate.

Using a simple wave test, arrays can be designed in the time-distance or f-k domain.

B. Array Design in the Time-Distance Domain

As a first approximation, design a simple linear receiver array.

1. Coherent Noise Attenuation

a) Steps in Linear Array Design

The following steps are recommended:

1) Identify all coherent noise events on the wave test and measure their phase velocity, predominant frequency and relative amplitude to the weakest signal. The measurements can be made by a simple "db" scale or by program "DLLI".

   Figure 76 shows a wave test and Figure 77 the identified events. Two sections should be made. One in true amplitude to measure amplitudes and one with DAVC to identify events.

2) Compute the wavelengths (or spatial frequency) of each of the events. Since noise trains have a range of phase velocities and predominant frequencies, a range of wavelengths are computed using the simple formulae:

$$\lambda a = \frac{Va}{fp}; \qquad Va = \frac{\Delta x}{\Delta t}$$

The data is listed in a table on Figure 78.

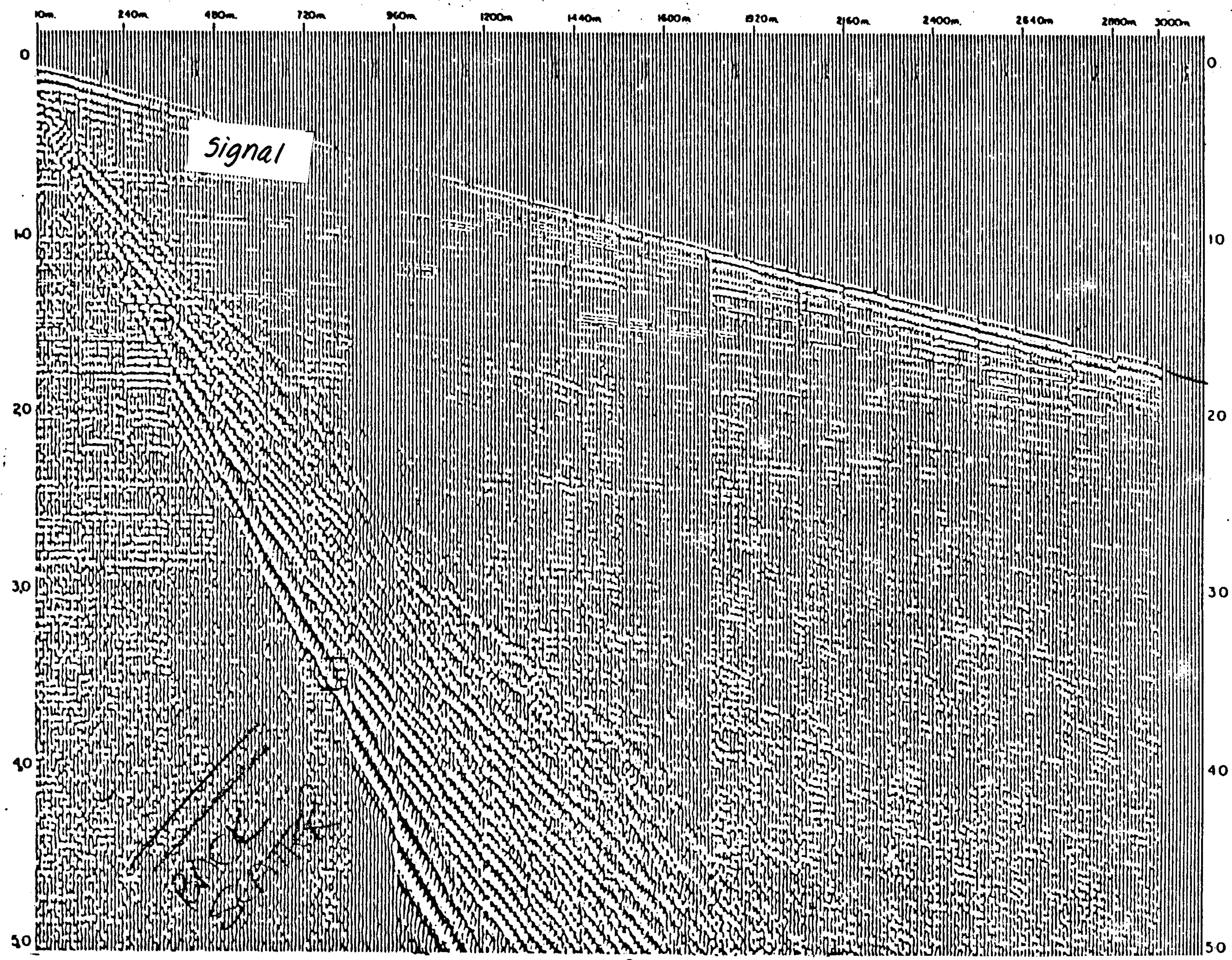

Dispersive Rayleigh Waves

Figure 76 - Processed Noise Analysis Data

Transposed Wave Test

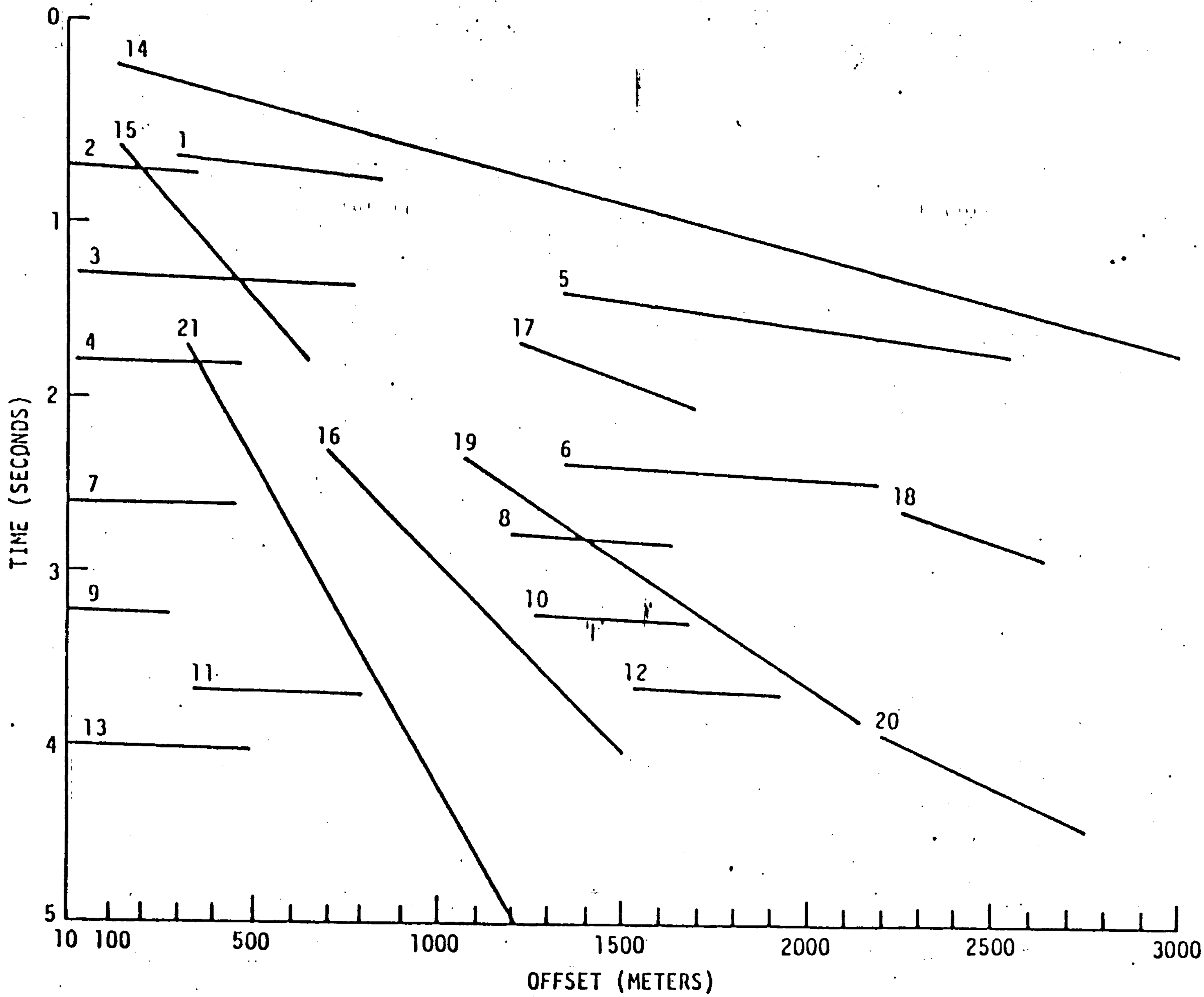

Figure 77 - Interpretation of Noise Analysis Section on Figure 76

3) Plot the data in a histogram form as shown on Figure 79. The amplitude histogram is plotted as the function of range of apparent wavelengths. This presentation has the merits of not only identifying--in visual form--the wavelengths needed to be attenuated but also by how many db's relative to the weakest signal.

4) Compute (or read off the histogram) the longest wavelength noise (λmax) and place it at the first notch of a simple linear receiver array. At the first notch:

$\lambda max = ns$ (the effective array length)

$\lambda max = 70$ m in the example shown on Figure 79.

5) Compute (or determine from histogram) the shortest wavelength noise (λmin). Place λmin at the last notch before repeat. At the last notch (from Figure 30):

$$\lambda min = \frac{ns}{n-1}$$

$\lambda min = 20$ m for the example

Characteristics of Signal and Noise

Event No.	Mode	V	f	λ	K	A	db
1	S(0-2)	5 600	40	140.0	0.00714	1.3	2.2
2	S(0-2)	17 000	25	680.0	0.00147	1.7	4.6
3	S(0-2)	9 480	20	474.0	0.00211	2.0	6.0
4	S(0-2)	21 000	20	1050.0	0.00095	2.0	6.0
5	S(0-2)	2 960	17	170.6	0.00586	1.3	2.2
6	S(2-3)	6 520	20	326.0	0.00307	1.7	4.6
7	S(2-3)	17 000	20	850.0	0.00116	1.7	4.6
8	S(2-3)	6 520	25	260.8	0.00383	1.0	0.0
9	S(3-5)	21 000	25	840.0	0.00119	1.3	2.2
10	S(3-5)	11 000	20	550.0	0.00182	1.0	0.0
11	S(3-5)	17 000	18	914.4	0.00106	1.0	0.0
12	S(3-5)	11 000	20	550.0	0.00182	1.0	0.0
13	S)3-5)	21 000	25	840.0	0.00119	1.3	2.2
14	N1	1 720	50	34.4	0.02910	1.3	2.2
			40	43.0	0.02300		
15	N2	420	20	21.0	0.02760	1.7	4.6
16	N2	430	13	33.1	0.03000	1.7	4.6
17	N3	1 280	20	64.0	0.01563	2.0	6.0
18	N3	1 280	25	51.2	0.01953	1.7	6.0
19	N3	830	33	25.15	0.03980	1.3	2.2
20	N3	1 130	25	45.2	0.02210	1.0	0.0
21	N4	270	13	20.77	0.04800	3.0	9.5
			10	27.00	0.03700		

Event No.	As shown on Figure 4.2.4B
Mode	S(0-2) signal between 0 and 2 seconds
V	Apparent velocity in meter/sec
f	Frequency in Hz (cycle/sec) computed from period
λ	Apparent wavelength - V/f in meter/cycle
K	Apparent wavenumber - 1/g in cycle/meter
A	Amplitude in mm
db	Relative amplitude (relative to event no. 10) in db

Figure 78

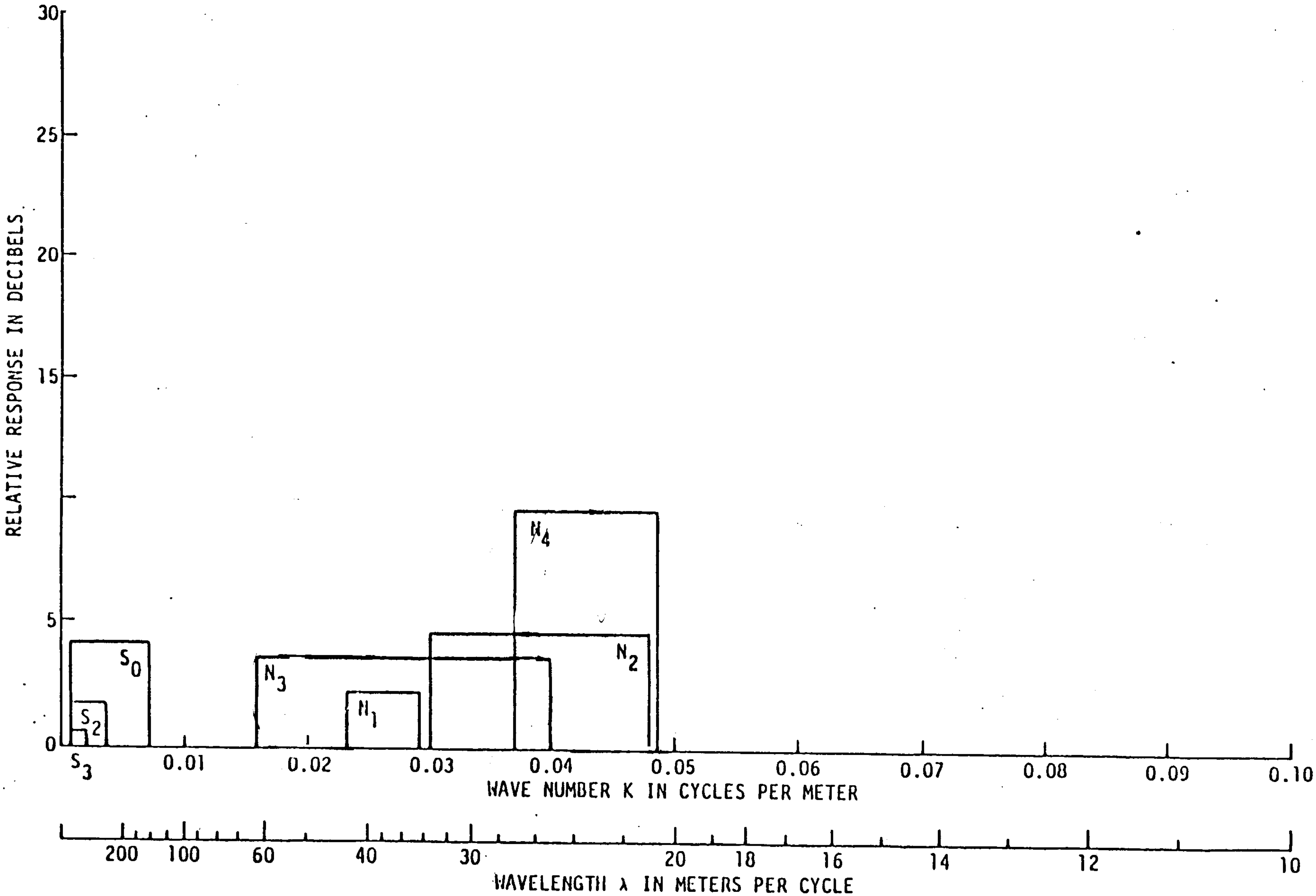

Figure 79 - Signal and Noise Characteristics (See Table on Figure 78)

6) Determine the number of elements in the linear array:

$$n = \frac{\lambda max + \lambda min}{\lambda min}$$

$$n = \frac{70 + 20}{20} = 5 \text{ in the example}$$

7) Determine the spacing of elements:

$$s = \frac{\lambda max}{n}$$

$$s = \frac{70}{5} = 14 \text{ m in the example}$$

Therefore, the parameters for the simple linear receiver array are:

effective group length (ns) = 70 m
number of phones/group = 5
phone spacing = 14 m
actual group length = 56 m

8) Determine the degree of noise attenuation needed from the histogram. The noise amplitude should be at least 12 db below signal. The strongest noise (NA) is 10 db above the signal, hence a 22 db attenuation in the reject band is required in our example.

9) Compute the array response with the parameters determined in steps 5-7. The crew in the example is equipped with strings of six phones (the minimum number of phones per group). Therefore, the revised parameters are:

effective group length	= 72 m	= ns
number of phones/group	= 6	= n
phone spacing	= 12 m	= s
actual group length	= 60 m	= 41

The array response for a six-element linear array is shown on Figure 80. The response is computed using equations (29) or (30).

$$Ar = \left| \frac{1}{n} \frac{\sin\left(\pi \frac{ns}{\lambda a}\right)}{\sin\left(\frac{\pi s}{\lambda a}\right)} \right|$$

or

$$Ar = \left| \frac{1}{n} \frac{\sin(\pi k\ ns)}{\sin(\pi ks)} \right|$$

Amplitude Response— 6 element Linear Array

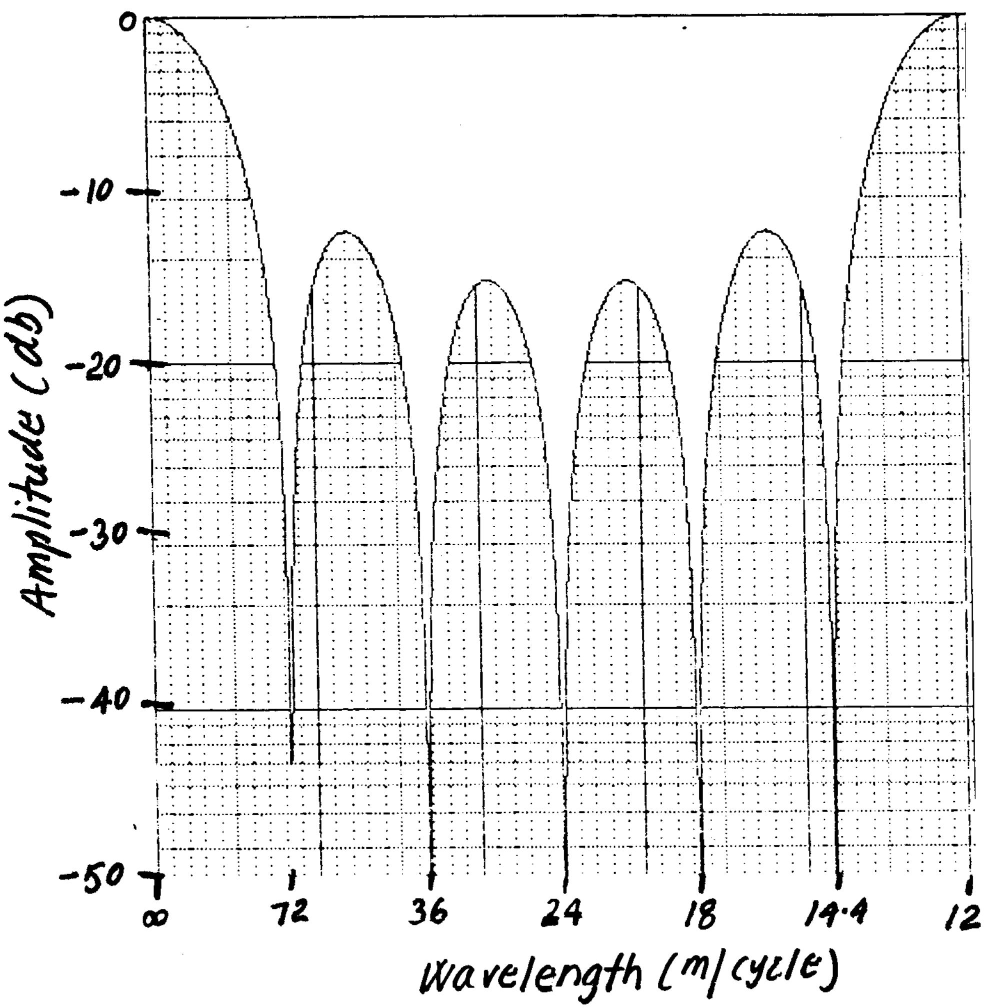

Effective group length: $L = ns = 72m$

Receiver Spacing : $s = 12m$

No. of Receivers/group: $n = 6$

Figure 80

10) Compare the required noise attenuation with the attenuation of the reject band of the array computed in step 9. Note, that the graph on Figure 34 (attenuation envelope) may also be used to estimate the attenuation of the reject band. If the average attenuation of the reject band is less than the required noise attenuation, a linearly tapered receiver array or a linear source array (or linearly tapered source array) or some combinations must be used to achieve required attenuation.

Linearly tapered receiver arrays can easily be implemented by adding additional strings. The availability of source arrays depends on the type of source used and economics. Source arrays (linear or tapered) are readily available with vibroseis or other surface sources, but may be impossible with deep hole dynamite shooting.

b) Tapered Receiver Arrays

Attenuation may be Increased by tapered receiver arrays.

It was shown by comparing Figures 58, 60, and 62 that the best response of linearly tapered arrays is the flat top array design, which provides a flat rejection band and approximately 30 db attenuation. This type of array requires the weights to be tapered in integral steps away from the centre, with repetition of weights at the centre.

The number of elements in the subarrays should be slightly different (e.g., 5 x 6 or 6 x 5 or 8 x 9 or 10 x 12, etc.) and the spacing of the elements the same in both subarrays (weights decrease in the integral steps) or the reject band will be uneven with less than 30 db attenuation as shown on Figure 66.

A symmetric configuration (6 x 6 or 9 x 9) is a triangular taper with less attenuation.

c) Combination of Linear Source and Receiver Arrays

Attenuation may be increased by the combination of linear receiver array and linear source array.

The basic rules to follow in the design of source arrays have been discussed on Figure 67:

i) The effective length of the receiver array is equal to the longest wavelength to be attenuated.

ii) The source array is the subarray with the fewer elements, with an effective length of 70 percent of the receiver array. This tends to broaden the reject band, provides flat response and 30 db attenuation in the reject band.

The six-element array in the example (response on Figure 80) achieves only an average of 13 db attenuation. The crew in this prospect had only four strings of six phones per group, therefore, a maximum of 4 x 6 array could be used. The response of the 4 x 6 array is shown on Figure 81 and it provides a 30 db attenuation in the reject band. Therefore, a tapered 4 x 6 receiver array is adequate to attenuate the coherent noise. Source array is not necessary.

2. <u>Reflected Signal Attenuation</u>

1) Compute the maximum group interval to avoid spatial aliasing of the maximum signal frequency.

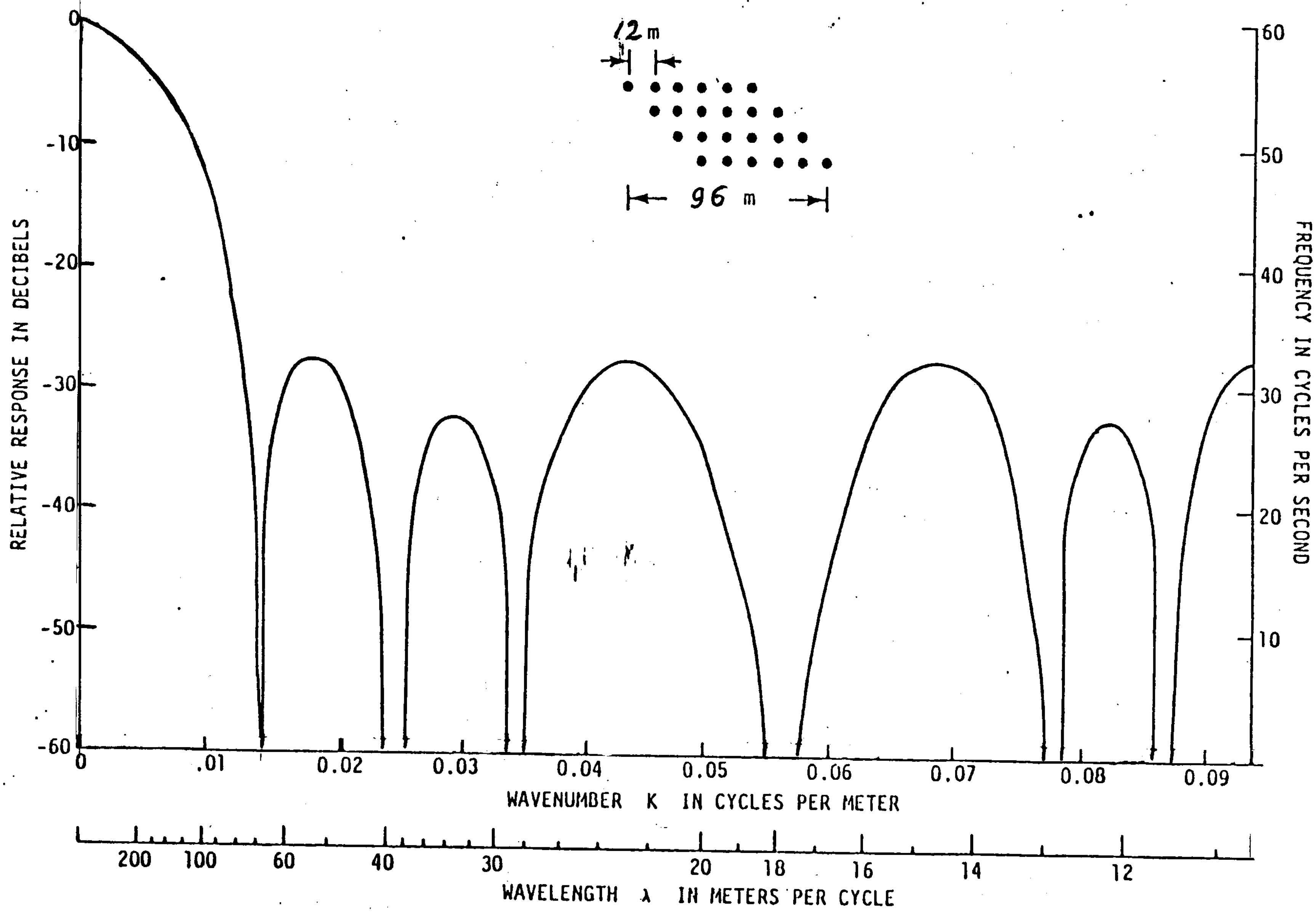

Figure 81 - Array Response of 4 x 6 Parallelogram, 12-m Geophone Spacing

The maximum group interval from equation (13).

$$\Delta xmax = \frac{Vamin}{2fmax}$$

Where:

Vamin = the minimum expected apparent velocity
fmax = maximum signal frequency

From equation (38)

$$Vamin = \bar{V}min \left[1 + \left(\frac{\cos \alpha}{\frac{xmax}{\bar{V}min \quad Tomin} + \sin \alpha} \right)^2 \right]^{\frac{1}{2}}$$

Where:

$\bar{V}$min = average velocity to shallowest horizon of interest
Tomin = reflection time to shallowest horizon of interest
xmax = maximum offset
α = dip of shallowest horizon

In the example: the maximum dip is 15°,

Tomin = 1.5 sec, xmax = 1680 m, $\bar{V}$min = 2500 m/sec,

fmax = 40 Hz.

$$Vamin = 2500 \left[1 + \left(\frac{\cos 15}{\frac{1660}{2500 \times 1.5} + \sin 15} \right)^2 \right]^{\frac{1}{2}} = 4233 \text{ m/sec}$$

$$\Delta xmax = \frac{4233}{2 \times 40} = 53 \text{ m}$$

Therefore, assuming a 48 trace split configuration the maximum group interval is 54 m and the revised maximum offset is 50 x 24 = 120 m.

2) Compute the maximum group length to pass the desired signal. The frequency corresponding to the "-6 db" attenuation is given by equation (43):

$$f(-6\ db) = 0.605 \frac{\bar{V}amin}{(ns)max}$$

Therefore, $(ns)max = 0.605 \frac{\bar{V}amin}{fmax}$

In the example:

$\bar{V}amin = 4233$ m
fmax = 40 Hz

(nsmax) = 105.8 m which is longer than the length of receiver array designed for coherent noise attenuation (70 m), therefore, the 70 m effective array length is acceptable.

Note, that in linearly tapered arrays the first notch is located at the effective group length of the longer subarray, however, the slope of the pass band will be steeper than for the longer linear subarray, therefore, equation (43) over estimates the maximum acceptable group length. $(\Delta l)_{max}$ may also be estimated from the graphs on Figures 41-48.

3) Check reflected signal attenuation due to maximum surface slope across the group for the maximum desired signal frequency.

From Figure 53:

$$\Delta E_{max} = \frac{\frac{\emptyset}{2}}{180} \cdot \frac{V}{f_{max}}$$

Where $\emptyset/2$ is computed from

$$0.5 = \frac{1}{n} \left| \frac{\sin \frac{n}{n-1} \frac{\emptyset}{2}}{\sin \frac{1}{n-1} \frac{\emptyset}{2}} \right|$$

The graph on Figure 54 may also be used to estimate "ΔE_{max}".

4) Compare maximum allowable array length to pass signal (determined in step 2) with array length computed to attenuate coherent noise. If the longest subarray length exceeds the length required to pass signal, select the array length according to which is more important:

a) To pass the signal with no more than 6 db attenuation:

Select array to pass signal and sacrifice noise attenuation.

b) To attenuate coherent noise by 30 db:

Select array length design to attenuate noise and sacrifice signal amplitude.

c) Select an average of the two array lengths (a happy medium).

5) Compute the attenuation of the maximum desired signal frequency by the CDP trace.

Using equations (46) and (47) the response of the array is computed as follows:

Equation (47) computes the amplitude response of one group of source and receiver pairs and equation (46) for a symmetric CDP configuration. This comparison is important, especially if in step 4 it is found that in order to attenuate coherent noise, the array length is excessive to pass the signal. Since the attenuation by the CDP trace is usually less than by a group at the longest offset, the array length may be increased to attenuate the undesirable coherent noise.

C. Array Design in the f-k Domain

The design procedures in the f-k domain are the same as in the time-distance domain. The only difference is that spatial frequencies (k) rather than wavelengths are used in the design equations.

The first step is to transform the wave test data into the f-k domain (an example of a wave test and its F-k representation is shown on Figure 82).

1. Coherent Noise Attenuation

Steps recommended for array design to attenuate coherent noise:

First, design a simple linear array.

1) Identify coherent noise events on the time-distance and f-k plots.

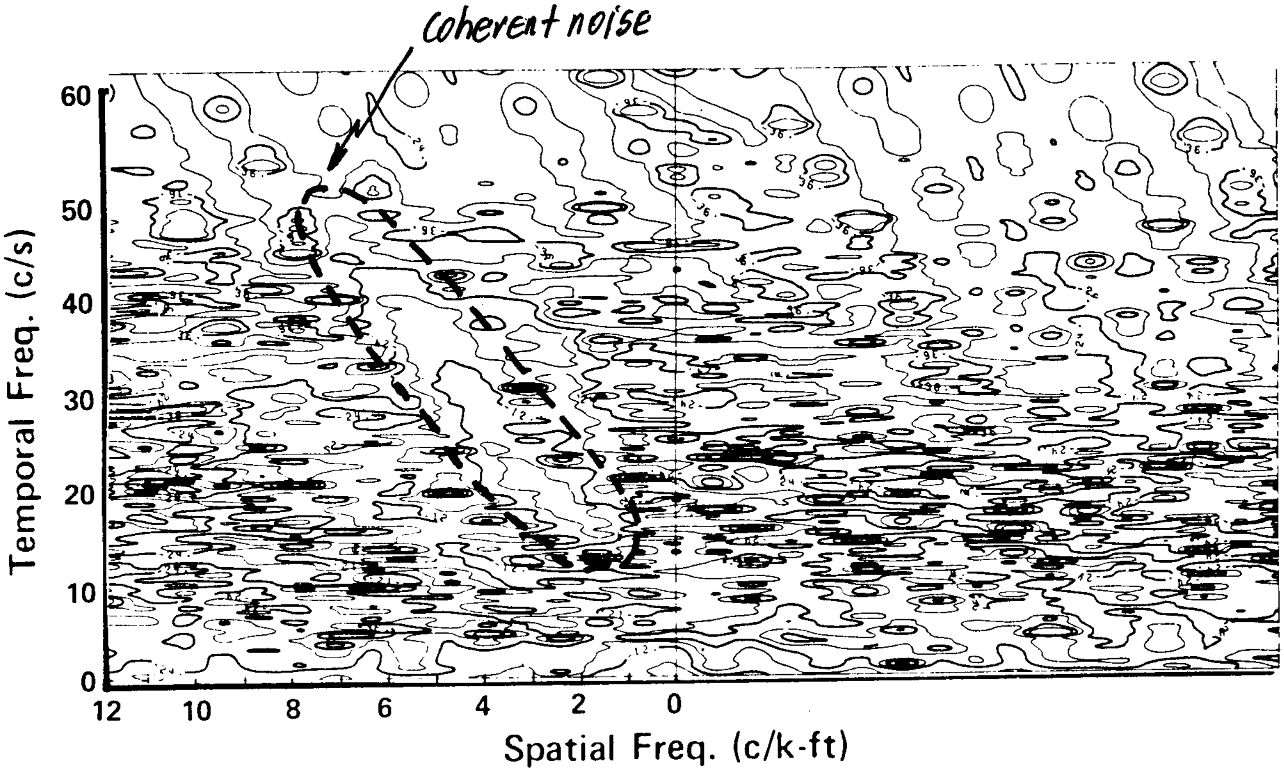

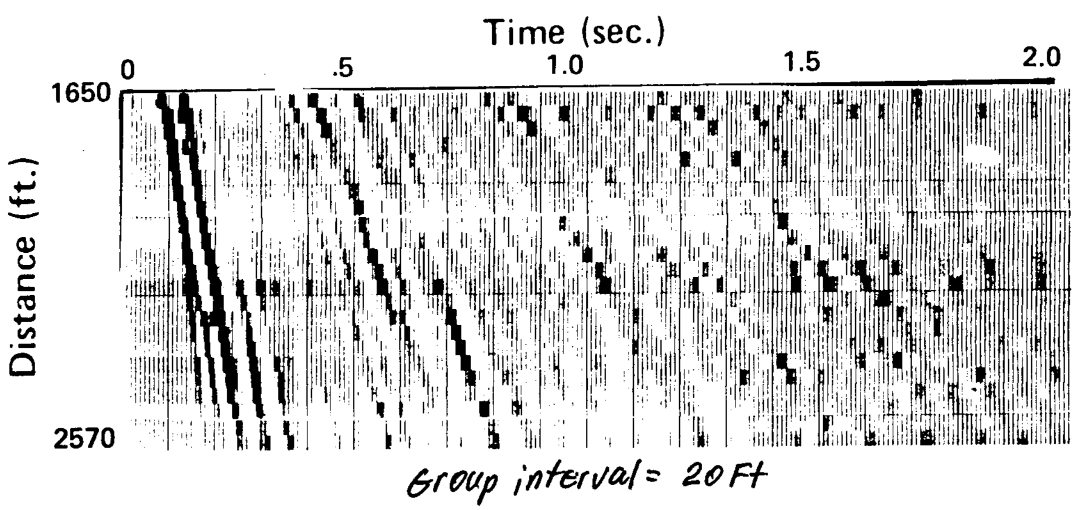

Quinn Canyon

Figure 82

2) Determine the band of spatial frequencies for the coherent noise, train that is kmax and kmin. In the example on Figure 82.

kmax = 8 cycles/kft

kmin = 1 cycle/kft

3) Place "kmin" at first notch of linear array and "kmax" at last notch.

4) Determine the number of elements in the array:

$$n = \frac{kmax + kmin}{kmin}$$

For the example:

$$n = \frac{1 + 8}{1} = 9$$

5) Determine the spacing of elements and effective array length.

$$s = \frac{1}{n\ kmin} \qquad s \cong \frac{1}{9 \times .001} = 111\ Ft$$

To accommodate the master cable available s = 120 feet and n = 9 was used.

The parameters of the receiver array:

n = 9
s = 120 ft
ns = 1080 ft

The amplitudes on the f-k plot of Figure 82 are normalized to the highest amplitude and contoured in negative db-s.

6) Determine the degree of noise attenuation needed by observing the difference in amplitudes between signal and noise. The filtered noise amplitude must be at least 12 db below signal.

7) Multiply the spatial frequency response of the array (Figure 83) and the input frequency response of the wave test (Figure 82) and transform the filtered f-k response into the time-distance domain to determine the effectiveness of spatial filter.

Figure 84 shows the filtered wave test f-k response and the filtered time-distance plot. It appears the array was effective in attenuating the coherent noise.

Amplitude Response – 9 Element Linear Array

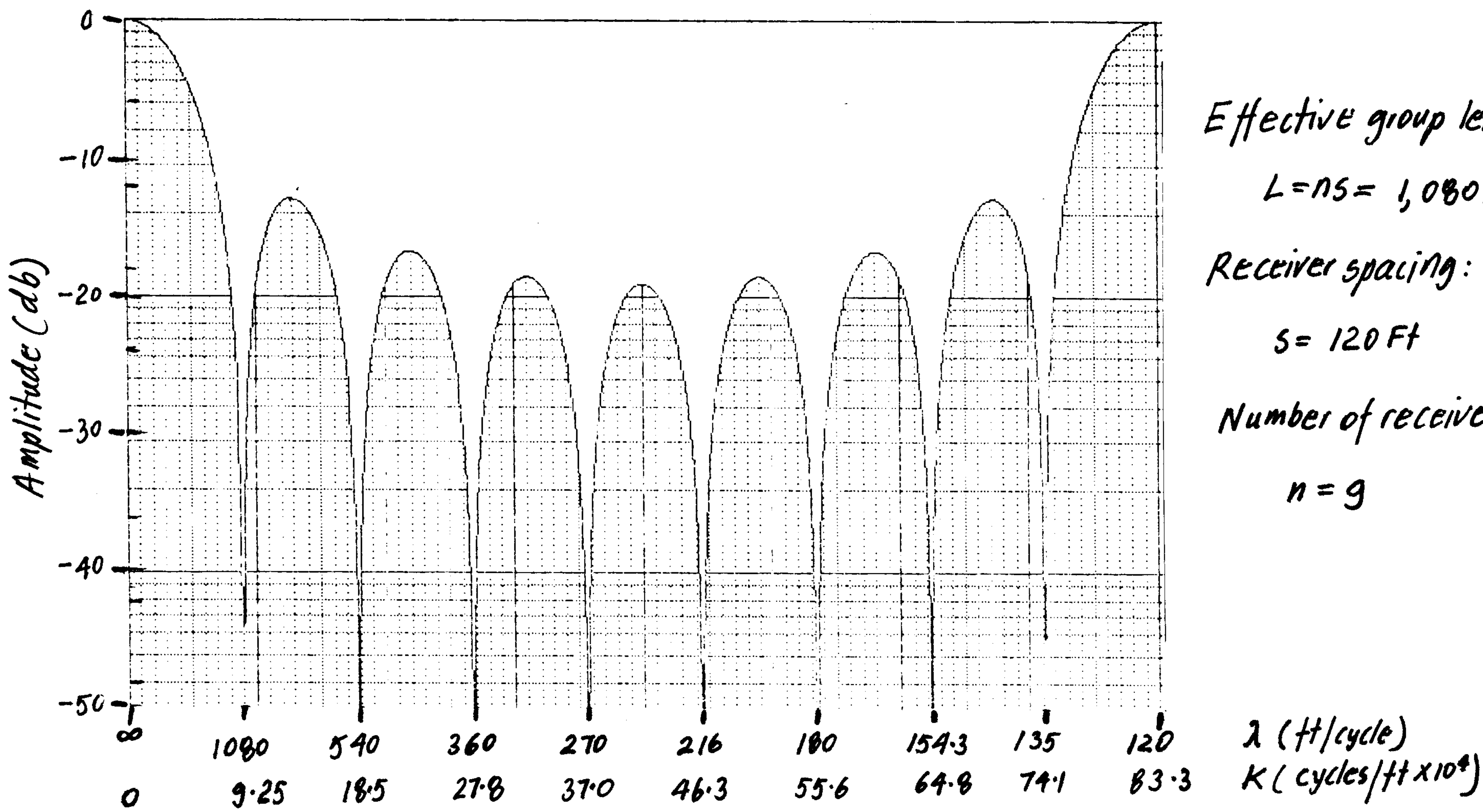

Effective group length:

$L = ns = 1{,}080$ Ft

Receiver spacing:

$s = 120$ Ft

Number of receivers

$n = 9$

Figure 83

Quinn Canyon Pattern Response Filtered (9 Seis at 120 Ft.)

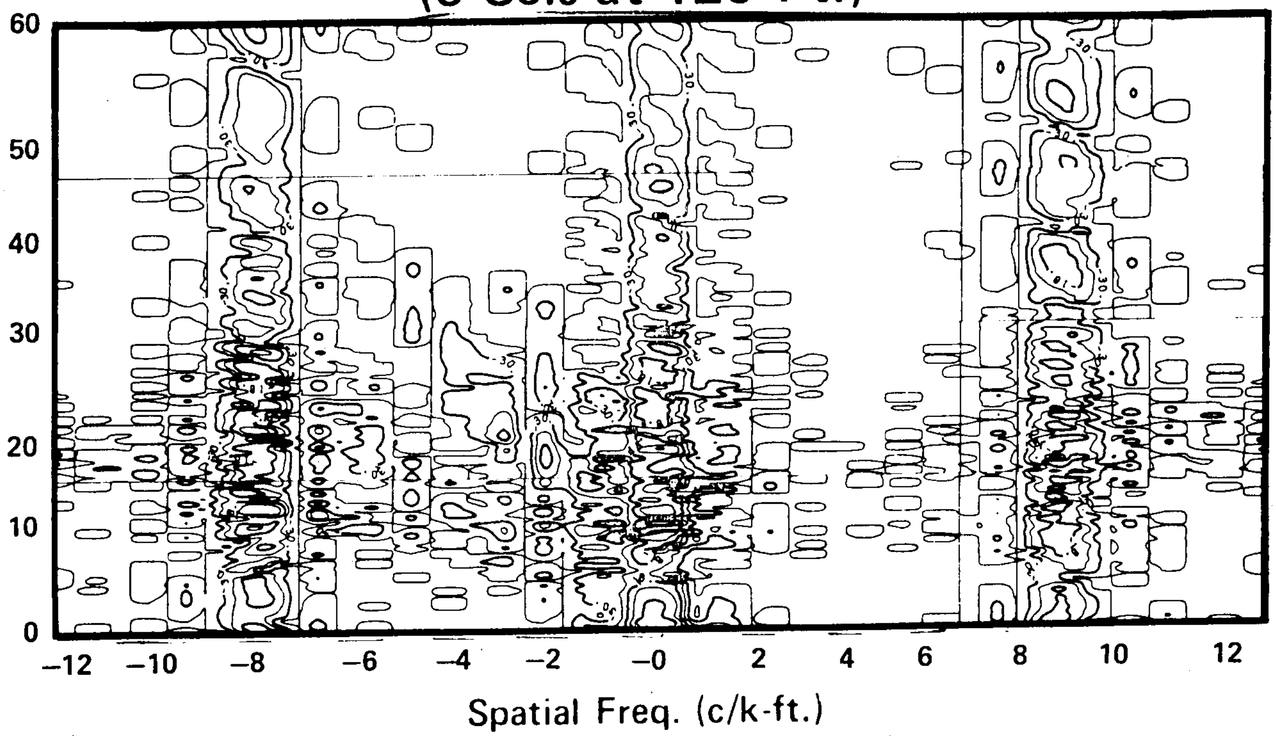

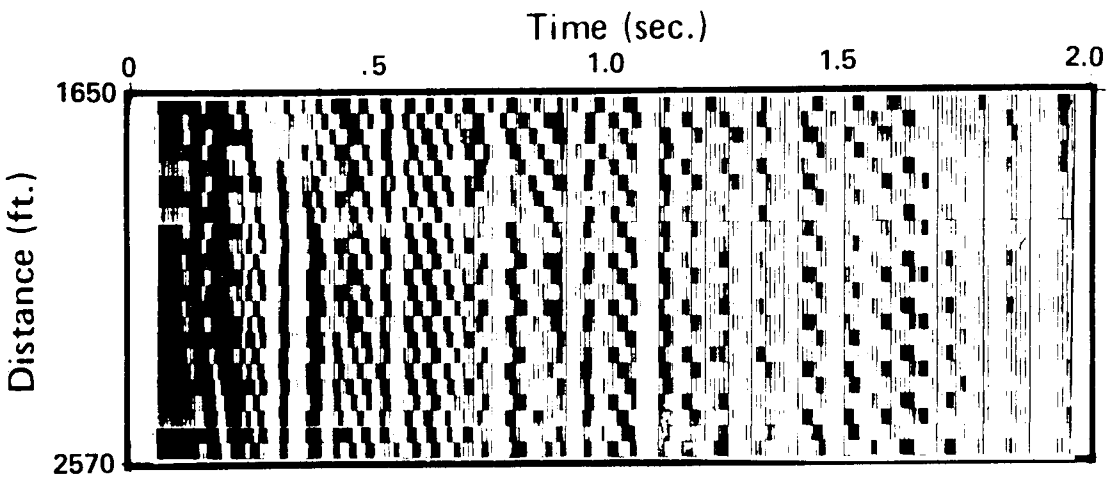

Quinn Canyon Filtered

Figure 84

If the desired attenuation is not achieved a tapered linear array must be designed as described in steps 10a and b of "Array Design in the Time-Distance Domain".

2. Reflected Signal Attenuation

To check the effect of arrays on the reflected signal, the same steps are followed as discussed in the section on array design in the time-distance domain.

The maximum group interval to avoid spatial aliasing may also be determined in the f-k domain by taking the original wave spread and rejecting traces, thus creating wave tests of increasing group interval. The data is transformed into the f-k domain and checked for wrap-around (aliasing). The largest group interval not showing aliasing is the maximum allowable group interval.

D. Complementary Field Tests for Array Design

The optimum array has been designed based on theoretical equations, which ignores the effect of element errors shown by Newman and Mahoney.

Therefore, the effectiveness of the theoretical array must be checked in the field by "Residual Wave Tests" or "Residual Wave Test Stimulation (RWAV)".

1. Residual Wave Test

A residual wave test is a wave spread that has an array built in, hence, instead of recording individual phones at each station of the original wave test, the geophone array designed is recorded. The resultant wave test shows if there is any array leakage.

Array leakage may also be checked by the regular production spread laid out with the "optimum array".

The advantage of residual wave test is that due to the close sampling, possible spatial aliasing problems are avoided and weak residual noise trains (usually higher spatial frequency) are readily recognizable. However, following this procedure two wave tests are required: a simple wave test and a residual wave test.

A better approach is the Residual Wave Test Stimulation which only requires one wave test.

2. Residual Wave Test Simulation (RWAV)

The method is describing by P. W. Johnson in Amoco Research Report No. F-81-E-24.

The program requires that the spacing of the phones be equal or less than the theoretically determined element spacing.

The computation consists of performing a weighted inter-record mix of the input traces for each output trace to simulate the desired arrays (Figure 85). The number of output traces is the same as the number of input traces and at the same trace spacing. The output is in "true amplitude". Figures 86-88 show the original wave spread and two linear array simulations. This method is highly recommended, where well designed arrays are a must. The method is expensive, requiring many shots.

Residual Wave Test Simulation.

Recorded Wave Spread

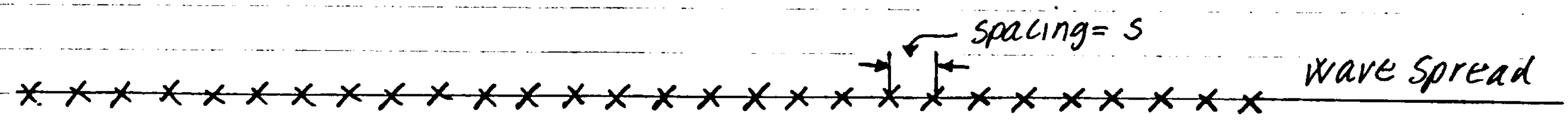

Simulated Residual Wave Spreads

Example: 6 phones/group, uniform array, group length = 5s

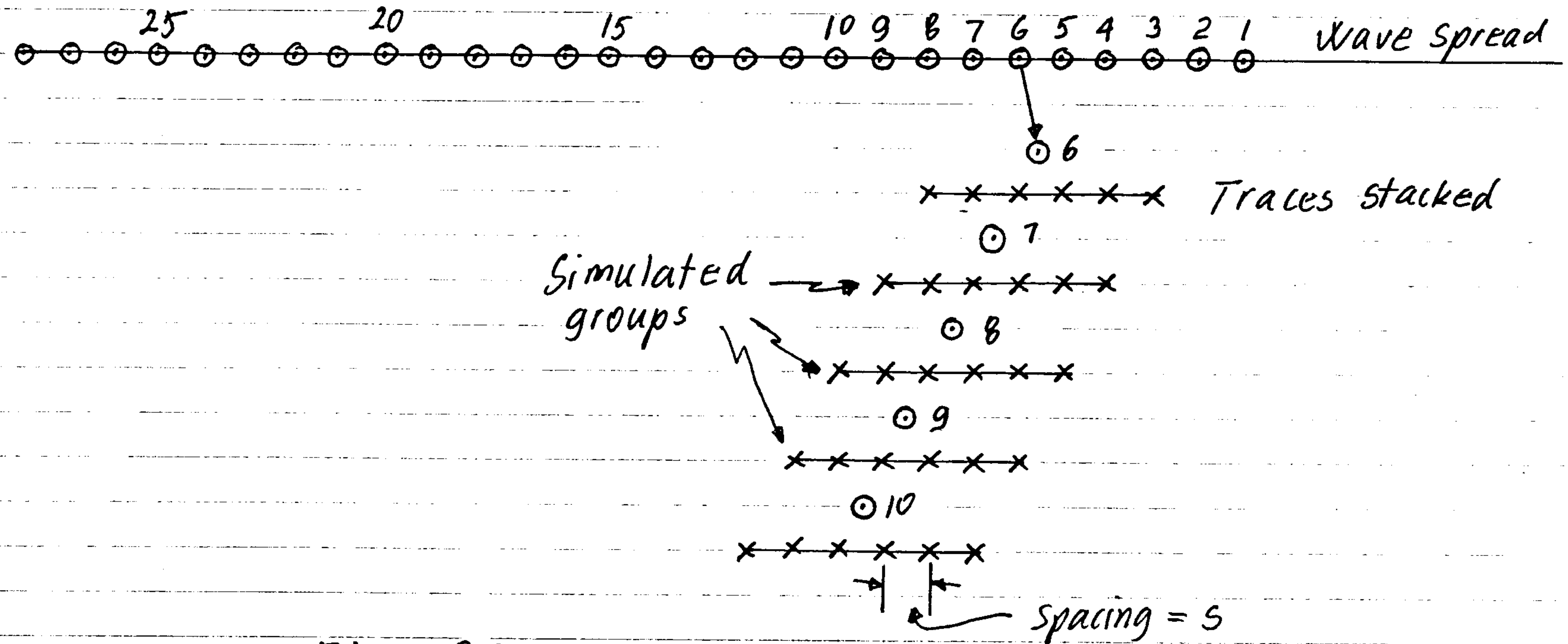

Figure 85

Residual Wave Spread Simulation
Raw Wave Spread

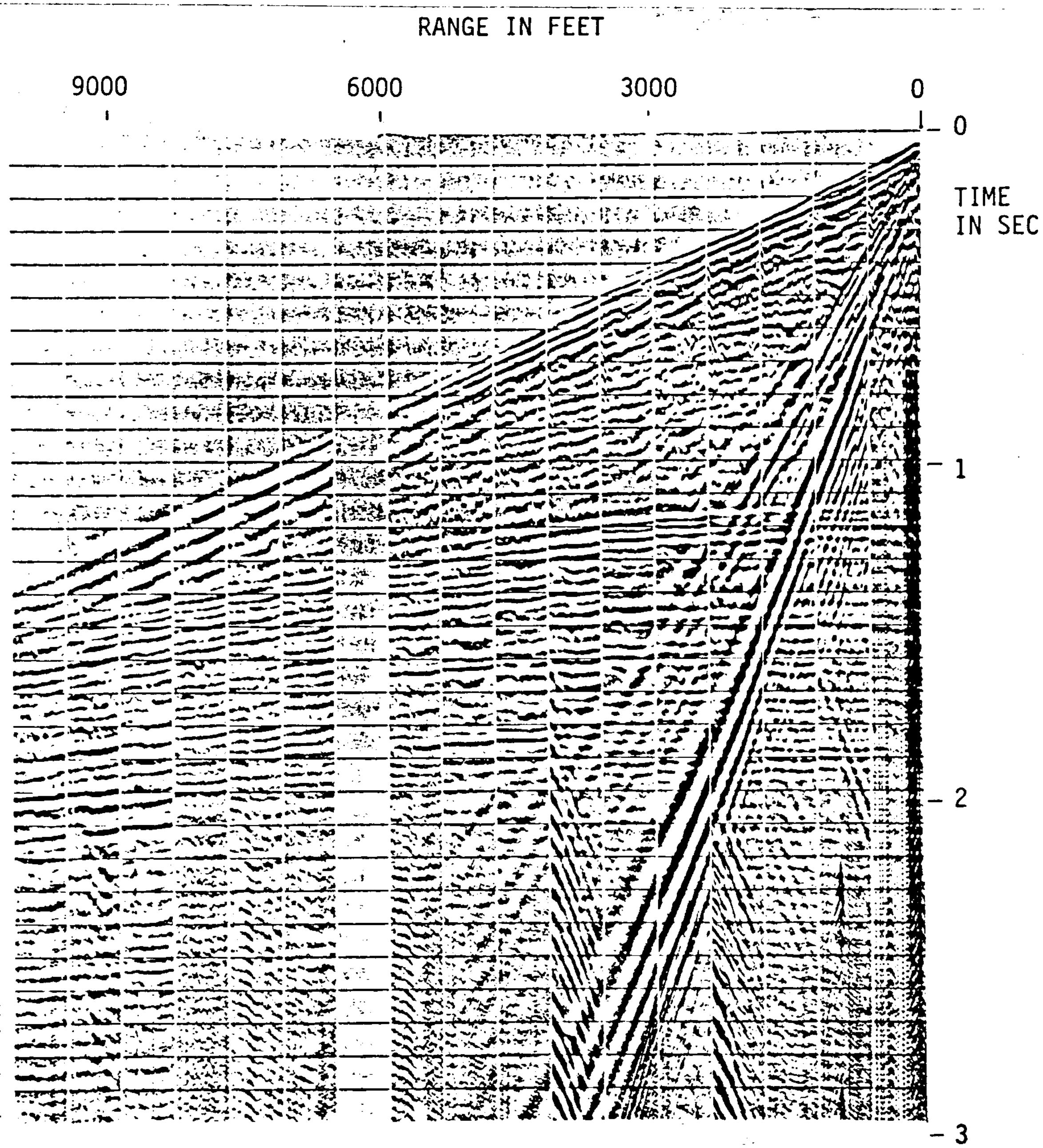

THE RAW WAVE SPREAD.

Phone spacing = 4Ft

Figure 86

Residual Wave Spread Simulation

13 element array over 48 Ft

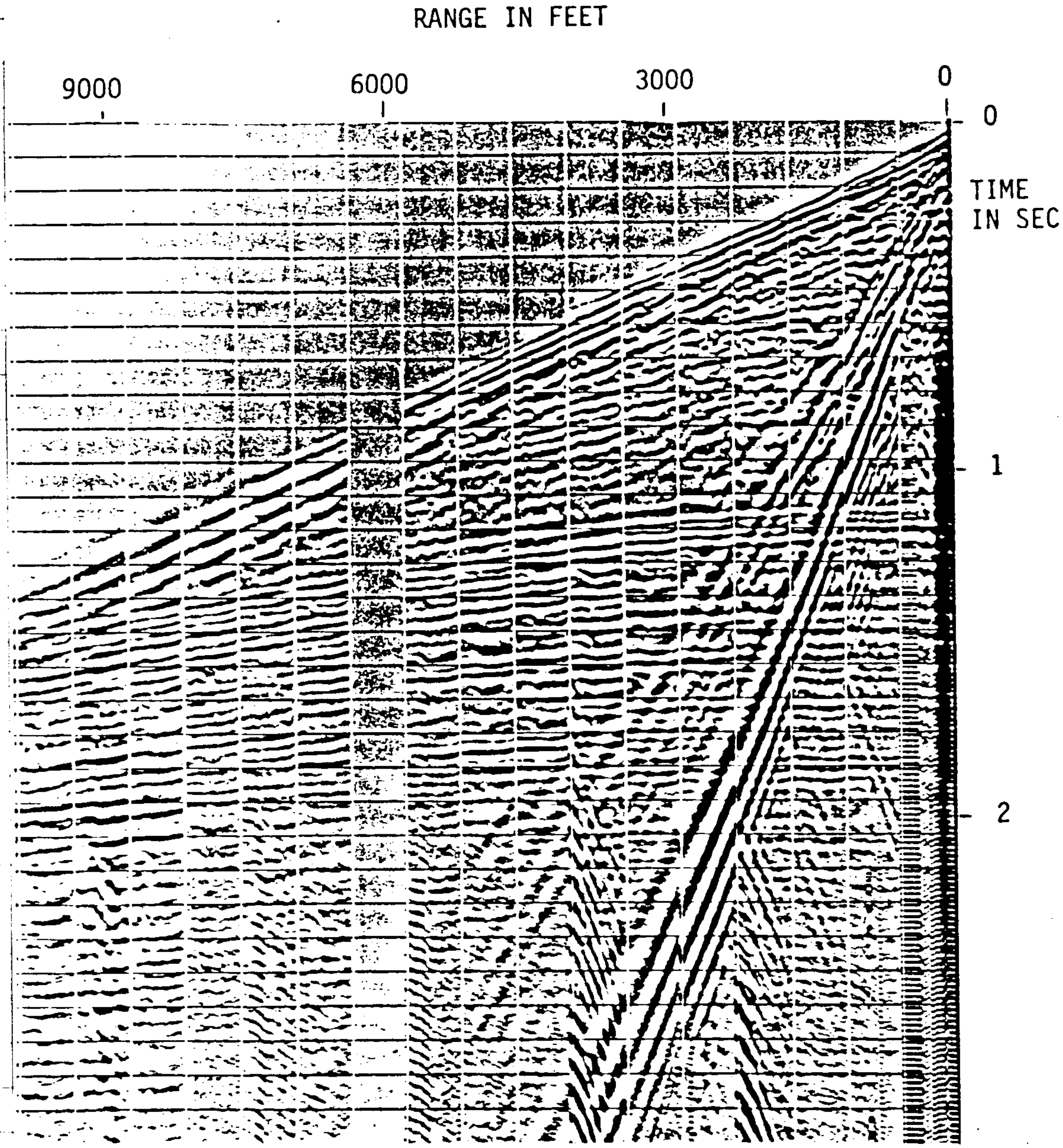

Number of elements = 13
Effective group length = 52 Ft
Element spacing = 4 Ft
Group interval = 4 Ft

SIMULATED RESIDUAL WAVE SPREAD USING 52 FOOT EFFECTIVE GROUP LENGTH.

Figure 87

Residual Wave Spread Simulation

51 element array over 200 Ft

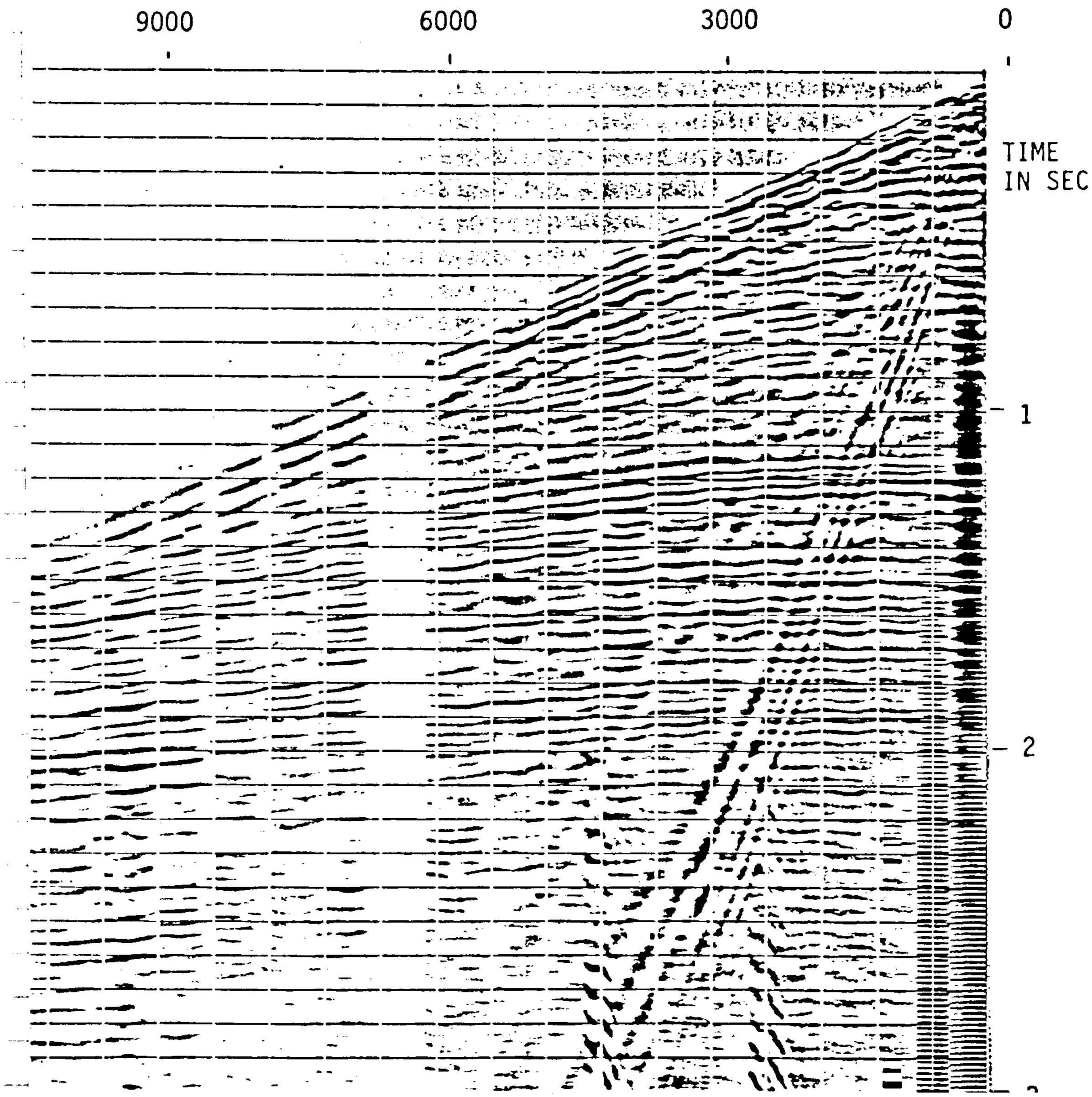

Number of elements = 51
Effective group length = 204 Ft
Element spacing = 4 Ft
Group interval = 4 Ft

SIMULATED RESIDUAL WAVE SPREAD USING 204 FOOT EFFECTIVE GROUP LENGTH.

Figure 88

3. Multifold Arrays as Spatial Filters of Noise

Multifold arrays (the CDP trace) are spatial filters similarly to source and receiver arrays.

Basic properties:

1) The number of elements is equal to the fold.

2) The spacing of elements is equal to the spacing of traces in the CDP:

$$s = \frac{(GI)(Tr)}{n}$$

Where

GI = Group interval
Tr = No. of traces recorded in spread.

3) For coherent linear noise cancellation single ender configuration must be used, since the linear noise in a split CDP trace is smeared, but not necessarily attenuated, due to the reversal of dips on the two sides of split shots.

4) Since in the CDP stacked trace the data is corrected for NMO, the effect of multifold array on the coherent noise is determined by transforming the wave test into the f-k domain and multiplying the response with the multifold array response and transforming the data back into the time-distance domain. Note, that after NMO, the linear noise is no longer linear and care must be taken in the

process of identification, especially in the f-k domain. Furthermore, due to NMO, the range of spatial frequence is also altered.

5) The multifold array may also be used to attenuate multiples.

Steps to follow in multifold array design:

a) Shoot an expanding spread. The purpose of the expanding spread is to obtain a large number of raypaths at different ranges from the same subsurface coverage. The field layout, the section layout and an example are shown on Figures 89, 90, and 91.

b) Correct the section for NMO.

c) Transform data (each side independently) into F-k domain.

d) Determine "kmax" and "kmin" for multiple.

e) Compute reject band: number of elements (fold) and spacing.

$$n = \frac{kmax + kmin}{kmin}$$

$$s = \frac{(GI)(Tr)}{n} = \frac{1}{n\ kmin}$$

$$GI = \frac{1}{kmin\ Tr}$$

f) Compute response of multifold array.

PROD/slk
88265ACC0077-p

Expanding Spread – Field Layout

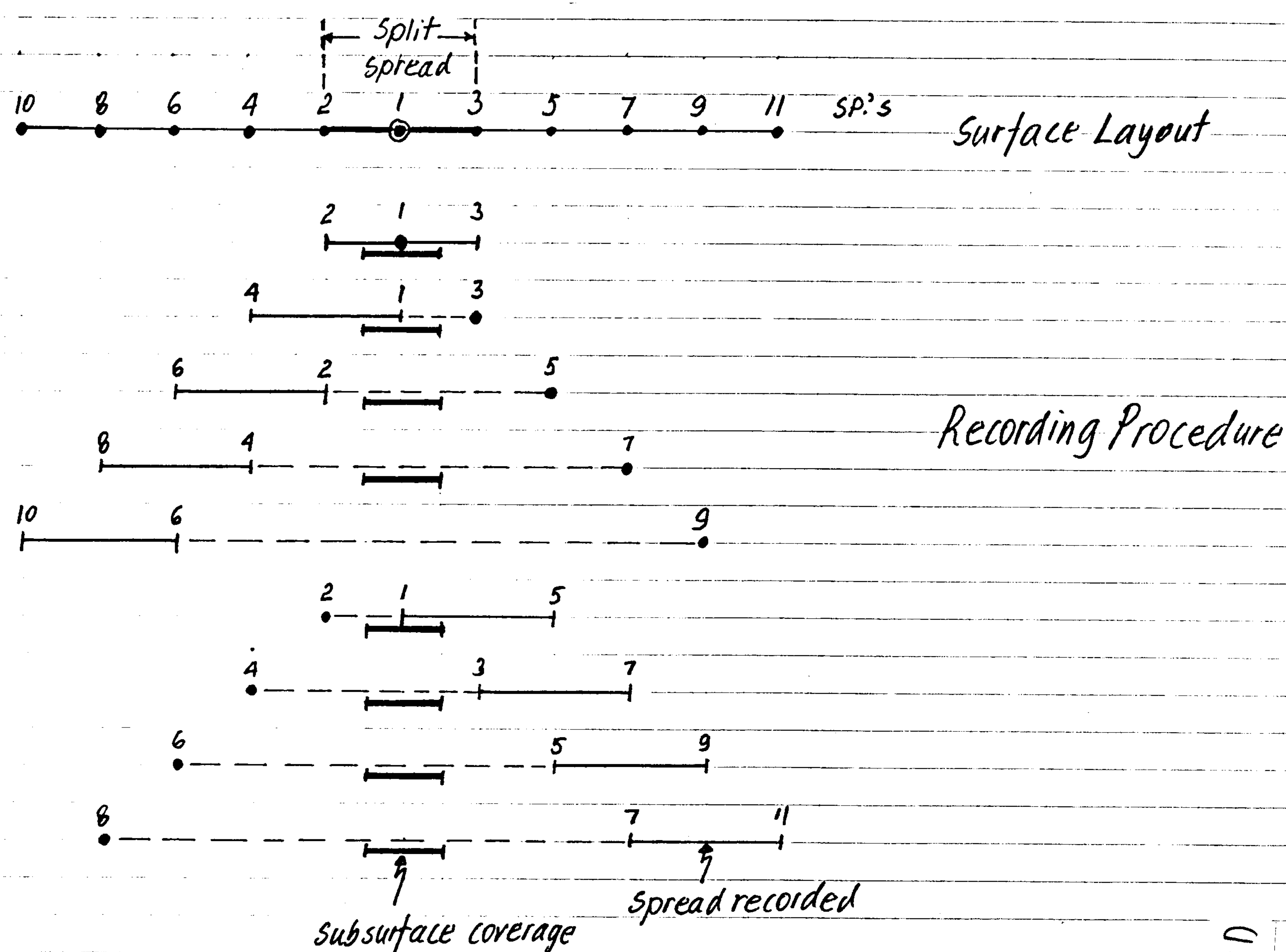

Figure 89

P.I. Display – Expanding Spread.

Field Layout on Fig 113a

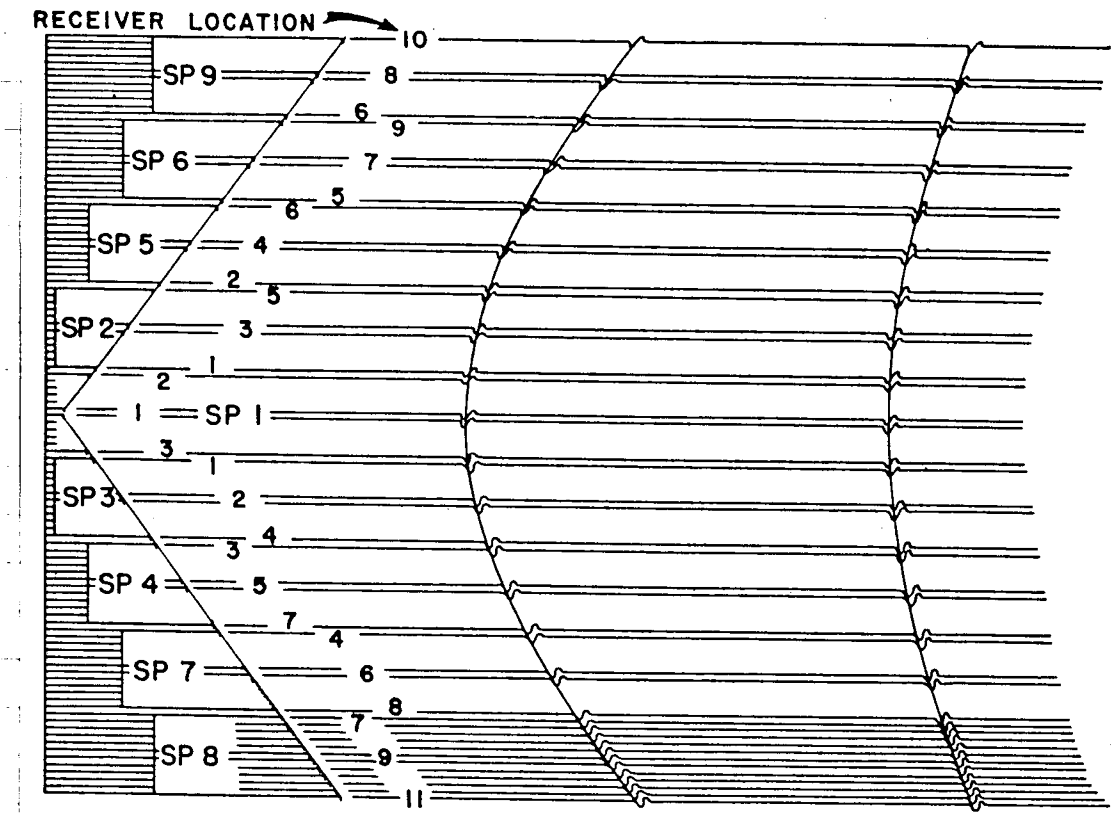

RECORD SECTION LAYOUT

Diagrammatic layout of record section displaying the first breaks and two hyperbolas from plane flat reflectors.

Figure 90

P.I. Display – Expanding spread

Good reflection quality, small amount of multiple interference

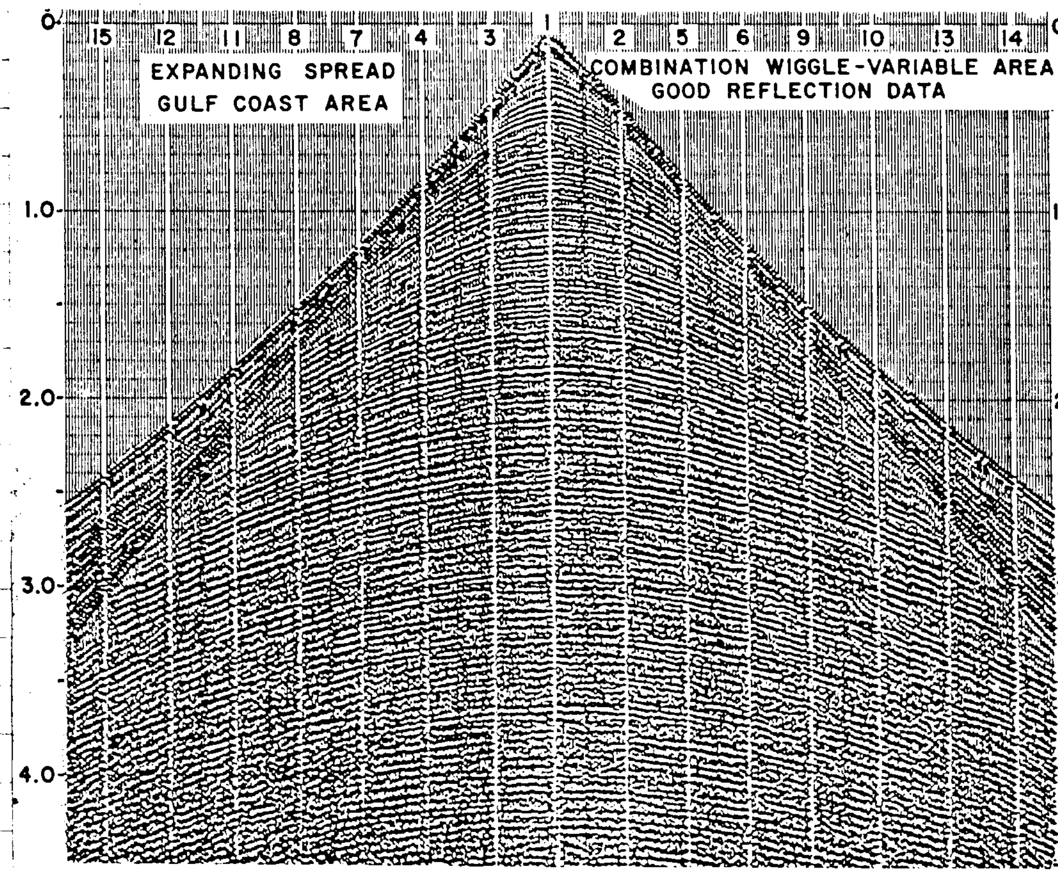

Actual expanding spread from the lower Gulf Coast area. This is a combination wiggle-variable area presentation of good reflection data between the limbs of the noise cone on this spread.

Figure 91.

Amoco Canada Petroleum Company Ltd.

Engineering Chart

Sheet No. File (198)

Appn.

Date

By

Subject: Source and Receiver Arrays Figures

Fig 1 : A short course on arrays by Norman Cooper, Amoco Canada, Fig. 1 page 62-22

Geophone Arrays – Theory and Design by Norman Cooper. Geophysical Technical Report 79-1, Amoco Canada, Figure 4, slide No CS-5340

Fig. 2 : The F-K Primer or an Empirical Introduction to the Two Dimensional Fourier Transform, By M.A. Verdeil Geophysical Technical Report No 76-6, Amoco Canada (Example 15A)

Fig 3 : The F-K Primer – Example 1

Fig. 4 : The F-K Primer – Example 2

Fig. 5 : Seismic Data Acquisition for Practicing Explorationists by Nabil A. Morgan, International Human Resources Course, 1981; page 3.36 – Fig 3.4.5

Fig. 6 : Seismic Data Acquisition by N.A. Morgan page 3.40 – Fig. 3.4.8

Fig. 7 : Seismic Data Acquisition by N.A. Morgan page 3.38 – Fig 3.4.6

Fig. 8 : Made by A. Pap

Fig. 9 : Source, Receiver and Multifold Array Design by G.M. Greve. From "Seismic Field Testing and Array Design" Amoco Production Co., 1974 Fig. 1, page 55

Fig 10 : A short Course on Arrays by N. Cooper, Fig 4, page 62-25; Also Amoco Canada Tech. Report No 79-1, Fig 9, slide CS-5335

Sheet No. (199)
File
Appn.
Date
By

Amoco Canada Petroleum Company Ltd.

Engineering Chart

Subject

Fig. 11 : A short Course on Arrays by N. Cooper, page 62-26 Fig 5. Also Amoco Tech Report No 79-1, Fig 10 slide No CS 5336

Fig 12 : A short Course on Arrays by N. Cooper, page 62-28 Fig 7, Also Amoco Canada Tech Report No 79-1, Fig. 12, slide No CS-5338

Fig. 13 : 2-D Fourier Transform and F-K Filtering by J.P. Dorrier, 1979, page 61-26, Fig. 2

Fig 14 : J. P. Dorrier, page 61-24, Fig. 1

Fig 15 : J.P. Dorrier, page 61-30, Fig 4

Fig 16 : J.P Dorrier, page 61-32, Fig 5

Fig 17 : J.P Dorrier, page 61-36 Fig 7

Fig 18 : J.P. Dorrier, page 61-38 Fig 8

Fig 19 : A Preacquisition Modelling Study for a Complex Area. by Carl. J. Regone Amoco Research Report No F81-E-26, Fig 22

Fig 20 : Trace Interpolation by Western Geophysical Fig. 2, 3a, 3b

Fig 21 : Trace Interpolation by Western Geophysical Fig. 4a, 4b

Fig 22 : Hand drawn by A. Pap, no original

Fig 22a, b : J. P. Dorrier, page 61-48 (Fig 13) & 61-49 (Fig 13A)

Form 371 5-71

Amoco Canada Petroleum Company Ltd.

Engineering Chart

Sheet No (200) of

File

Appn.

Date

By

Subject

Fig 23	:	Hand drawn by A. Pap, no original
Fig. 24	:	" " " " " "
Fig 25	:	A Preacquisition Modelling by C.J. Regone F-81-E-26, Fig 22
Fig 26	:	J.P. Dorrier, page G1- 98,99 (Fig 29A,B)
Fig 27	:	J.P Dorrier, page G1- 108,109 (Fig 32A,B)
Fig 28	:	J.P. Dorrier, page G1-112,113 (Fig 34A,B)
Fig 29	:	Field Array Design A Primer by R.S. Kallweit Houston Tech. Report No 76-6, Fig 1
Fig 30	:	Seismic Field Acquisition on Land With Buried Explosives Sources by A. Pap Page 92, Fig 34 (Original in vault)
Fig 31	:	Figure 30 modified
Fig 32	:	Hand drawn by A. Pap, no original
Fig 33	:	Source, Receiver and Multifold Array Design by G.M. Greeve. From "Seismic Field Testing and Array Design". Amoco Production Co, 1974. page 61, figure 4.
Fig. 34	:	Hand drawn by A. Pap, no original
Fig 35	:	Attenuation of the CDP Trace Due to NMO Cancellation in the Groups. Amoco Canada Tech Report No 80-1. Page 6, Fig 1

Form 371 5-71

Fig. 36 : "Frequency Attenuation of the Seismic Signal Due to Long Array Length" by A. Pap (March, 1980). Not published, Graph 1

Fig 37 : Frequency Attenuation ..... by A. Pap, Graph 2

Fig. 38 : " " " " Graph 4

Fig 39 : " " " " Graph 7

Fig 40 : " " " " Graph 10

Fig 41 : Attenuation of the CDP Trace Due to NMO..... by A. Pap. Amoco Canada Tech Report No 80-1, Plate 1

Fig 42 : Attenuation ..... Plate 2

Fig 43 : " " 3

Fig 44 : " " 4

Fig 45 : " " 5

Fig 46 : " " 6

Fig 47 : " " 7

Fig 48 : " " 9

Fig 49 : " Page 21, Fig. 6

Fig 50 : " Page 29, Fig. 8

Fig 51 : " " 30, Fig 9

Amoco Canada Petroleum Company Ltd.

Engineering Chart

Subject

Fig. 52 : Attenuation ..... Page 31, Fig 10

Fig 53 : " Page 18, Fig 5

Fig 54 : " Plate 11

Fig 55 : "Geophone Arrays – Theory and Design" by N.M. Cooper Amoco Canada Tech Report No 79-1 Fig 24, slide CS-5225
Also A Short Course on Arrays by N. Cooper page 62-39, Fig 18. Amoco Training Centre course, 1979

Fig 56 : Geophone Arrays ..... Fig 25, slide CS5219
Short Course ..... page 62-40, Fig 19

Fig 57 : " " ..... page 62-43, Fig 22

Fig 58 : " " ..... page 62-44, Fig 23

Fig 59 : " " ..... page 62-41, Fig 20

Fig 60 : " " ..... page 62-42, Fig 21

Fig 61 : " " ..... page 62-45, Fig 24

Fig 62 : " " ..... page 62-46, Fig 25

Fig 63 : Hand drawn by A. Pap, no original

Fig. 64 : Field Array Design A Primer by R.S. Kallweit Houston Tech Report No 76-6, page 15, Fig 5A

Fig 65 : Field Array Design ..... page 16, Fig. 5B

Amoco Canada Petroleum Company Ltd.

Engineering Chart

Sheet No. (203)
File
Appn.
Date
By

Subject

Fig 66 : Field Array Design .... Page 17, Fig. 5C

Fig 67 : " " " page 18

Fig 68 : Short course .... page 62-47, Fig 26

Fig 69 : " " .... page 62-48, Fig 27

Fig 70 : " " .... page 62-49, Fig 28

Fig 71 : " " .... page 62-50, Fig 29

Fig 72 : Geophone Arrays - Theory and Design by Cooper Fig. 35, slide CS-5221

Fig 73 : "Patterns with a Pinch of Salt" by Newman and Mahony. Geophysical Prospecting, Vol 21 1973, Fig 11

Fig 74 : Patterns with a Pinch of Salt, Fig 14

Fig 75 : Patterns with a Pinch of Salt, Fig 15

Fig 76 : Seismic Data Acquisition for the Practicing Explorationist by Nabil A. Morgan. An IHRDC course. Page 4.28, Fig 4.2.4A

Fig 77 : Seismic Data Acquisiton ... by Morgan Page 4.29, Fig 4.2.4B

Fig 78 : Seismic Data Acquisition .. by Morgan Page 4.41, table 4.3.1

Fig 79 : Seismic Data Acquisition .... by Morgan Page 4.43, Fig 4.3.1

Sheet No. (204)
File
Appn.
Date
By

Amoco Canada Petroleum Company Ltd.

Engineering Chart

Subject

Fig. 80 : Hand drafted by A. Pap, no original

Fig 81 : Seismic Data Acquisition .... by Morgan
Page 4.47, Fig 4.3.4

Fig 82 : Source, Receiver and Multifold Array Design
by G.M. Greeve; Fig 10, Page 70

Fig 83 : Geophones and Energy Sources as Arrays
by W.S. Hawes and D.G. Lang, 1974
A Petty-Ray Geophysical Publication
Figure 24

Fig 84 : Source, Receiver and Multifold Array Design
by G.M. Greeve; Fig 11, page 72

Fig 85 : Hand drafted by A. Pap, no original

Fig 86 : Residual Wave Spread Simulation (RWAV)
Amoco Research Report No. F81-E-24
by P.W. Johnson, Fig 3

Fig 87 : RWAV Report Fig 4

Fig 88 : RWAV Report Fig 5

Fig 89 : Hand drawn by A. Pap, no original

Fig 90 : Application of the Expanding Reflection
Spread by A.W. Musgrave; Geophysic
Vol. 27, No 6 (Dec 1962); Fig 6

Fig 91 : Application of the Expanding Spread by Musgrave
Fig 9

Form 371 5-71